Trace Amine-Associated Receptor 1: a Novel Target of Methamphetamine

By

Edmund Arthur Reese

A Dissertation

Presented to the Neuroscience Graduate Program
and the Oregon Health & Science University
School of Medicine
in partial fulfillment of
the requirements for the degree of
Doctor of Philosophy

March 2008

School of Medicine

Oregon Health & Science University

CERTIFICATE OF APPROVAL

This is to certify that the Ph.D. dissertation of

Edmund Arthur Reese

has been approved

David K. Grandy MS, PhD Mentor/Advisor

Jeffrey Karpen PhD, Chair and Member

Philip Copenhaver PhD, Member

David Farrens PhD, Member

Kim Neve PhD, Member

Robert Shapiro PhD, Member

Table of Contents

Chapter 1 Introduction and Statement of Thesis

Acknowledgements

Many people have given me support and encouragement throughout my graduate school experience in the Neuroscience Graduate Program here at Oregon Health & Science University. I would like to thank them for their help.

First of all, I would like to thank David Grandy for giving me the opportunity to work in his laboratory where I have been able to investigate interesting and relevant topics. I appreciate David's commitment to teaching graduate students and the individual mentoring he provided me in the scientific approach to investigating biological questions, his attention to experimental details, and his coaching in the area of scientific writing.

I would like to thank my thesis advisory committee; Jeffrey Karpen, Philip Copenhaver, David Farrens, David Grandy, Kim Neve, and Robert Shapiro, for their review and guidance of my research efforts. I feel fortunate to have had such a knowledgeable group of experts assembled on my behalf.

I would like to thank Ed McClesky, the former director of the Neuroscience Graduate Program and Peter Gillespie, the current director, for their support and for their role in deciding to give me the opportunity to enter the program. I appreciate Peter's wisdom and leadership in directing the program.

For all of her help I also acknowledge Liz Lawson-Weber. She has been very helpful and effective at making things happen and getting the things done that need to be done.

I would like to thank Seksiri Arttamangkul for her interest in my work, for taking time to discuss technical challenges that helped me make progress, and for her friendship.

Thank you Rachel Dresbeck for teaching me how to write and for your ability to extract clarity from confusing sentences.

I also appreciate the contribution of Pamela Shaw Ph.D., Biostatistics Research Branch, National Institute of Allergy and Infectious Diseases, Bethesda, MD, a.k.a. cousin Pam, for consulting help with statistical analysis.

Thank you to the members of the Grandy lab. Special thanks go to Jim Bunzow for his wealth of knowledge and his willingness to share it. Thank you to Katie Suchland for numerous contributions to the laboratory and especially for helping me maintain multiple tissue culture cell lines. Thank you to Tom Keck, fellow graduate student, for many technical and non-technical discussions and for your tolerance with my papers repeatedly spilling over onto your desk. To Charles Jimenez, thanks for your help with experiments and proofreading drafts of my writing and for many stimulating conversations. And thank you to Ebony Morris for assistance with cAMP assays used to generate data in chapter 3.

Thank you to Susan Amara for giving me the opportunity to explore the "messy world of molecular biology" by letting me work in her laboratory prior to entering the NGP.

To Stefanie Kaech Petri, thank you for showing me how to operate the confocal microscope and for mentoring me during my first rotation in the program.

And most of all I appreciate the love, support, sacrifices, and encouragement from my wife Sharon. I would like to dedicate this work to the memory of our parents, Tom and Eleanor Shaw, and James and Helen Reese, and to our children Eddie, Laura, and Andrew.

Abstract

Trace amine-associated receptor 1 (TAAR1) is a member of a distinct family of G-protein coupled receptors. TAAR1 is activated by endogenous trace amines (TA) such as *β*-phenylethylamine (PEA) and *para*-tyramine (*p*-TYR). Abnormal levels of TAs have been associated with mood disorders, but the physiological role of TAAR1 remains unclear. My thesis is that TAAR1 represents a novel target of amphetamine (AMPH) and methamphetamine (METH). The four studies described here were designed to test hypotheses derived from this thesis. In the first study I tested the hypothesis that AMPH and METH are agonists at several mammalian species of TAAR1. A pharmacological characterization of the activation of TAAR1 by trace amines, AMPH, and METH was carried out using an *in vitro* cAMP assay. The results show that PEA and *p*-TYR are potent agonists at TAAR1, that there is a significant difference in stereoselectivity with respect to isomers of AMPH and METH, and the stereoselectivity is species-dependent.

In the second study I explored the determinants of species-specific TAAR1 stereoselectivity. I hypothesized amino acids that differ between species in key locations of the putative ligand-binding domain for TAAR1 are responsible for the observed species-dependent stereoselectivity. Using site-directed mutagenesis, a mutation to transmembrane 6, M6.55T for the rat and T6.55M in the case of the mouse, caused a decrease of potency in the rat while increasing potency in the mouse for both the S(+) and R(-) enantiomers of AMPH and METH. A mutation in transmembrane 7, N7.39Y for the rat and Y7.39N for the mouse, reversed the species

dependent stereoselectivity of the rat and mouse TAAR1 to enantiomers of AMPH and METH.

My third study tested the hypothesis that METH and AMPH activate the wild-type human TAAR1 (hTAAR1). Using a cAMP-dependent reporter assay I demonstrated that PEA as well as both isomers of METH and AMPH activated the wild-type hTAAR1 in a dose-dependent manner at concentrations that are exceeded by users of these drugs.

The fourth study investigated the hypothesis that the human dopamine transporter (hDAT) and hTAAR1 co-localize in cells. HEK-293 cells, stably expressing hDAT fused to green fluorescent protein (hDAT-GFP), were treated with METH resulting in redistribution of hDAT-GFP from the cell surface to the cytoplasm. There was also some preliminary evidence of hTAAR1 and hDAT co-localization.

In conclusion, TAAR1 is potently activated by METH *in vitro* at concentrations less than those commonly observed in drug abusers. Preliminary evidence of DAT co-localization with hTAAR1 and METH induced internalization of DAT suggests that hTAAR1 could play a role in mediating some of METH's mental and physical effects. Therefore, I conclude that TAAR1 represents a novel target for potential anti-METH medication and for improved psychotherapeutics in some mood disorders.

List of Figures

Chapter 1

Chapter 2

Chapter 3

Chapter 4

Chapter 5

Chapter 6

List of Tables

List of Abbreviations

AADC	aromatic amino acid decarboxylase
ADHD	Attention Deficit Hyperactivity Disorder
AMPH	amphetamine
AP-2	adaptor protein 2
β_2AR	beta 2 adrenergic receptor
CaMK	Ca^{2+} calmodulin-dependent kinase
cAMP	cyclic adenosine monophosphate
CBP	CREB binding protein
CHO	Chinese hamster ovary
CNS	central nervous system
CRE	cAMP response element
CREB	CRE binding protein
CRELuc	CRE Luciferase
DA	dopamine
DAG	diacylglycerol
DAT	dopamine transporter
DMEM	Dulbecco's modified Eagle's medium
DAR	dopamine receptor
EA	enzyme acceptor
EC_{50}	concentration of an agonist required to produce half of the saturated maximum response
ED	enzyme donor

EFC	enzyme fragment complementation
ER	endoplasmic reticulum
EV	empty vector
GABA	gamma-aminobutyric acid
GFP	green fluorescent protein
GPCR	G protein-coupled receptor
HA-tagged	hemagglutinin epitope YPYDVPDYA from the influenza virus
hDAT	human DAT
HEK	human embryonic kidney
hβ_2AR	human β_2AR
5HT	serotonin, 5-hydroxytryptamine
hTAAR1	human TAAR 1
IBMX	3-isobutyl-1-methyl-xanthine
IP_3	inositol 1,4,5-trisphosphate
kb	kilo base pair
KRH	Krebs-Ringer-Hepes
LSD	lysergic acid diethylamide
M	molarity
MAO	monoamine oxidase
MAP	mitogen-activate protein
MDMA	3,4-methylenedioxymethamphetamine
METH	methamphetamine
mTAAR1	mouse TAAR1
mTM6	mouse TAAR1 with TM6 mutation T6.55M (T268M)

mTM7	mouse TAAR1 with TM7 mutation Y7.39N (Y287N)
mWT	mouse WT
NE	norepinephrine
NET	plasma membrane norepinephrine transporter
NHERF	Na+/H+ exchanger regulatory factor
NMDA	N-methyl D-aspartate
OCT	octopamine
8-OH-DPAT	8-hydroxy-2-(di-n-propylamino)tertraline
PEA	β-phenylethylamine
PEA_{max}	maximum cAMP produced in response to PEA
PIP_2	phosphatidylinositol 4,5-bisphosphate
PKA	protein kinase A
PKC	protein kinase C
PLC	phospholipase C
PMA	phorbol 12-myristate 13-acetate
POHA	para-hydroxyamphetamine
rTAAR1	rat TAAR1
rhTAAR1	rhesus monkey TAAR1
rTM6	rat TAAR1 with TM6 mutation M6.55T (M268T)
rTM7	rat TAAR1 with TM7 mutation N7.39Y (N287Y)
rWT	rat wild type
SEM	standard error of the mean
SERT	plasma membrane serotonin transporter
TA	trace amine

TAAR	trace amine-associated receptor
TM	transmembrane domain
TRP	tryptamine
TYR	para-tyramine
T1AM	3 - iodothyronamine
VMAT	vesicular monoamine transporter
WT	wild type

Chapter 1 Introduction

Overview of Trace Amines and TAAR1

For more than thirty years trace amines (TAs) have been known to exist in mammalian brains (Durden et al., 1973; Philips et al., 1974a; Philips et al., 1974b; Saavedra et al., 1974b). Their role in the central nervous system (CNS) however, remained uncertain due to the lack of evidence for an endogenous receptor. This changed with the discovery of the trace amine-associated receptors (TAAR)s, a distinct family of G protein-coupled receptors (GPCRs) that were cloned in 2001 (Borowsky et al., 2001; Bunzow et al., 2001). A recent review provides a comprehensive survey of TAs and TAARs and includes an extensive list of references to provide the interested reader access to the literature in the field (Grandy, 2007). TAAR1, one member of this large family, is widely expressed in mammalian brains. It is found in the substantia nigra, nucleus accumbens, ventral tegmental area, dorsal raphe nucleus, and amygdala, regions associated with monoaminergic neurons (Borowsky et al., 2001; Miller et al., 2005; Lindemann et al., 2007; Xie et al., 2007).

Trace amines, and more recently the TAARs, have been implicated in drug abuse (Bunzow et al., 2001; Branchek and Blackburn, 2003), as well as mood disorders such as depression (Sandler et al., 1979; Sabelli et al., 1996), bipolar disorder (Abou Jamra et al., 2005; Pae et al., 2008) and schizophrenia (Vladimirov et al., 2007).

Statement of Thesis

The central thesis of this dissertation is that the human TAAR1 (hTAAR1) also represents a novel site of methamphetamine (METH) action. This idea grew out of

previous findings that METH activates the rat TAAR1 expressed *in vitro* (Bunzow et al., 2001). The goal of my work was to ascertain whether such activation was also a characteristic of the human and mouse TAAR1. To test this thesis, I hypothesized that the concentration of METH required to activate human TAAR1 *in vitro* would be less than the blood levels of the drug achieved in human METH addicts (Chapter 2); that key amino acids determine the species-dependent TAAR1 stereoselectivity for the enantiomers of amphetamine (AMPH) and METH (Chapter 3); that METH directly activates hTAAR1 *in vitro* (Chapter 4); that METH causes internalization of surface human dopamine transporter (hDAT) by virtue of its co-interaction with hTAAR1 (Chapter 5).

The remainder of this chapter summarizes relevant evidence and the rationale for the approaches used to address each specific hypothesis. This is followed by general background information pertaining to the TAARs, the use of site-directed mutagenesis in the study of GPCRs, the known mechanisms by which METH elicits its effects, and the association of TAARs with mood disorders.

Chapter 2: TAAR1 displays species-dependent stereoselectivity for amphetamines

In the 2001 paper by Bunzow et al. it is shown that rat TAAR1 (rTAAR1) responds to trace amines and to AMPH and METH with EC_{50}s and efficacies that are enantiomer-dependent. This observation laid the foundation for the hypothesis that mouse and human TAAR1s will respond to METH and AMPH in the same manner *in vitro* with an isomeric preference for both compounds, and with the same isomeric

preference reflected in the behavioral preference for the S(+) isomer as reported previously by others (Angrist et al., 1971; Segal, 1975).

My experimental approach to testing this hypothesis was to characterize the concentration-dependent accumulation of cyclic adenosine monophosphate (cAMP) in human embryonic kidney (HEK) cells stably expressing rat TAAR1, mouse TAAR1, or a genetically engineered rat-human chimeric TAAR1 *in vitro*.

The rationale for this experimental approach was to expand the investigation of this receptor using techniques that had already been successfully demonstrated and was based on the assumption that TAAR1 of each species would display the same preference for the isomers of AMPH, METH, and related compounds. The justification for characterizing mouse TAAR1 in addition to the human receptor is the mouse is often used as an experimental animal model in laboratory studies. Since mice completely lacking a particular gene product can be engineered, they provide a powerful resource for understanding novel receptors *in vivo*. Preliminary evidence suggested unexpectedly dramatic stereoselective differences in cAMP accumulation that was species-dependent. This generated additional interest in determining whether wild type human TAAR1 also displays a stereoselective preference for the enantiomers of AMPH and METH. We wanted to know if there was a stereoselective preference for AMPH isomers and congeners such as METH and their metabolite *para*-hydroxy amphetamine (POHA).

Chapter 3: METH activation of TAAR1 and determination of selectivity by site-specific mutagenesis

After the first study revealed a species-dependent stereoselectivity for amphetamines, the goal of my next study (Chapter 3) was to test the hypothesis that each species' TAAR1 preference for isomers of AMPH and its congeners depends on key amino acid residues that differ across species in key sites in the receptor's putative ligand binding domain. We wanted to know what amino acids of the TAAR1 transmembrane domains were involved in ligand binding. Furthermore, we wanted to know which amino acids accounted for the difference in stereoselectivity profiles displayed by the rat and the mouse as described in Chapter 2 and why the response of the human chimera TAAR1 was more similar to the response of the mouse than that of the rat.

My experimental approach was to use site-directed mutagenesis to develop stably expressing cell lines with single amino acid substitutions at suspected key sites and to generate concentration-response curves for cell lines expressing rat or mouse wild type or mutant receptors. The choice of candidate sites for mutagenesis was made by examining amino acid sequence alignments of putative TMs of the TAAR1 receptors that correspond to known ligand binding sites for the human beta 2 adrenergic receptor ($h\beta_2AR$). Residues that differed between the species at these sites were identified.

My rationale for the site-directed mutagenesis approach was based on successful results from prior studies of the β_2AR by other laboratories that indicated that transmembrane (TM) domains TM3, TM5, TM6, and TM7 are involved in binding

catecholamines. Also, the existence of conserved residues in all seven TM domains in the β_2AR and the TAAR1 sequences was taken into consideration.

A proof of concept for this approach was to mutate the aspartate D3.32 in TM3 of the TAAR1 receptor to an alanine with the expectation of knocking down the cAMP response. Here the GPCR sequence numbering uses the system of Ballesteros and Weinstein where the first character is the single letter code for an amino acid, the first number represents the TM, and the second number positions the residue with 50 representing the most conserved residue (Ballesteros, 1995). The conserved aspartate, D3.32, is thought to be crucial for monoamine ligand binding due to the ionic interaction of the positively charged amino group of the ligand and the carboxylate side chain of the aspartate residue of the receptor.

Site-directed mutagenesis involving TM6 and TM7 was expected to reverse the TAAR1 receptor stereoselectivity since the proposed sites to be mutated have been shown to be exposed in the binding pocket of other receptors such as the βARs and the dopamine receptor 1 (DAR1). My rationale was that the proposed mutation site is at a position that directly interacts with the ligands of these receptors. The polar groups of agonists are thought to interact with residues of the receptor that have polar side chains (Kristiansen, 2004). In hβ_2AR the asparagine in TM6, N6.55 (N293), interacts with the β-OH group of norepinephrine (Wieland et al., 1996; Swaminath et al., 2004). Even though AMPH and METH do not have a *β*-OH group, at the corresponding site in TAAR1s the residue for the rat, M6.55 (M268), differs from the residue for the mouse, T6.55 (T268). The mouse residue and the aligned residue, T6.55 (T271), in the human sequence are the same.

In TM7 of the hβ_2AR there is an asparagine, N7.39 (N312), that is conserved in all the βARs (Suryanarayana and Kobilka, 1993; Kristiansen, 2004). My rationale for selecting the aligned residue in TAAR1 that aligns with this asparagine was based on site-directed mutagenesis studies at this site that showed this asparagine is involved in binding aryloxyalkylamines, compounds with an ether oxygen that separates a phenol ring from an alkylamine side chain. This residue is responsible for species differences in the binding of aryloxyalkylamines (Guan et al., 1992; Suryanarayana and Kobilka, 1993). Examination of the sequence alignments for TM7 revealed that the corresponding rat TAAR1 residue N7.39 (N287) is the same as the asparagine in the hβ_2AR but the mouse TAAR1 residue Y7.39 (Y287) is different. The approach was to swap these residues in the rodent TAAR1s to see if the rat TAAR1 with just this TM7 mutation would mimic the mouse response and if the response for the mouse TAAR1 with just this TM7 mutation would resemble that for the rat wild type TAAR1.

A computer-generated model showing the putative seven transmembrane domains of the rat TAAR1 as alpha helices is shown (Figure 1). Amino acid sites that were mutated in TM3, TM6, and TM7 are shown as space filled (Figure 2). This model was described recently (Tan et al., 2008) and is based on the TAAR1 sequence superimposed on the recently published β_2AR crystal structure (Rosenbaum et al., 2007) .

Figure 1. A model of rat TAAR1. Amino acid sequences of the putative 7 TM domains were aligned with the β_2AR crystal structure. The model was created by Eli Groban in Matthew Jacobson's laboratory at the University of California at San Francisco (Tan et al., 2008) and was rendered using Pymol software (DeLano, W.L. The PyMOL Molecular Graphics System (2002) DeLano Scientific, Palo Alto, CA, USA).

Figure 1.

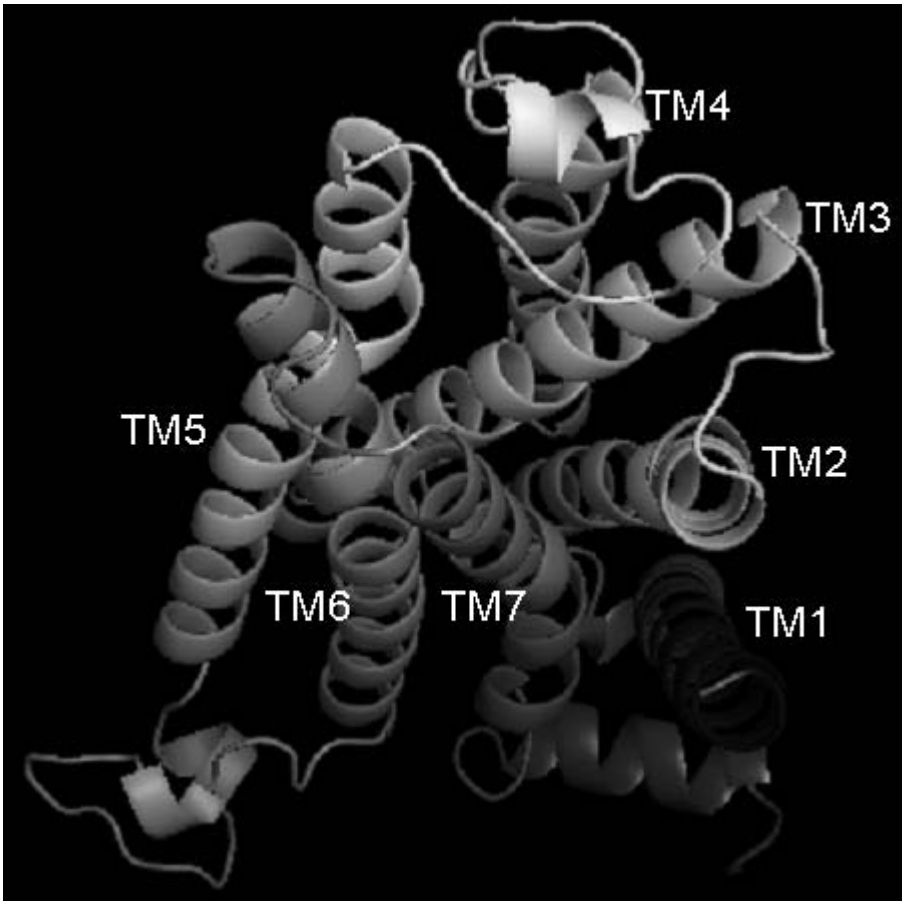

Figure 2. A model depicting rat TAAR1 7TM domains and amino acid residues that were mutated. Residues targeted for mutation are shown as space filled. The model was created by Eli Groban in Matthew Jacobson's laboratory at the University of California at San Francisco (Tan et al., 2008) and was rendered using Pymol software (DeLano, W.L. The PyMOL Molecular Graphics System (2002) DeLano Scientific, Palo Alto, CA, USA).

Figure 2.

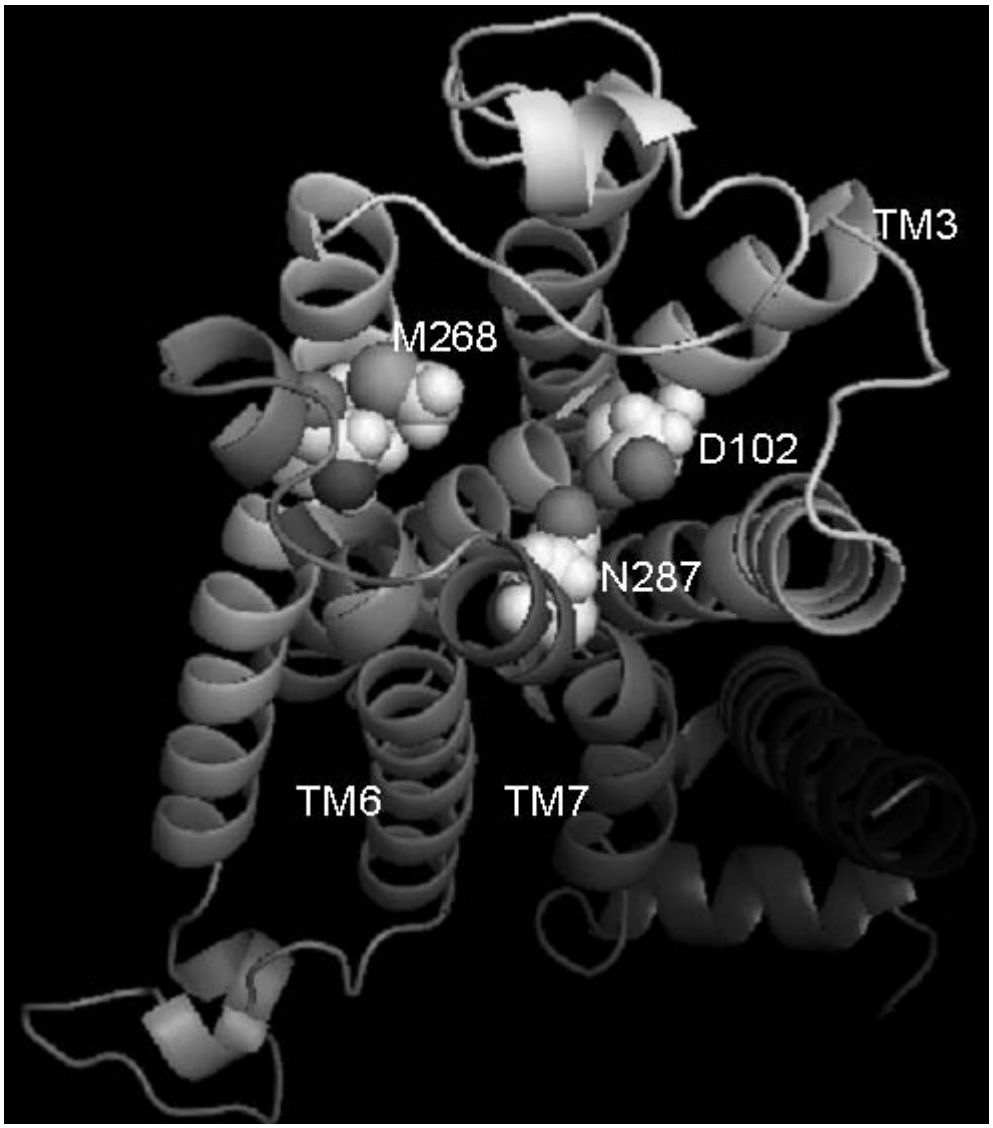

Chapter 4: hTAAR1 activation by METH demonstrated by a CRE reporter assay

In addition to characterizing wild type rat and mouse TAAR1 my original study (Reese et al., 2007) included a human-rat chimera. This artificial construct was needed due to difficulty stably expressing the wild type human sequence. Although the chimera couples to cAMP production it remained to be demonstrated that it accurately represents the wild type human receptor. The chimera consists of the human sequence for all the TM domains and all the connecting loops, with the exception of intracellular loop 3, and the N- and C-termini that are rat (Lindemann et al., 2005). I wanted to know if the wild type human TAAR1 receptor (hTAAR1) is activated by methamphetamine since the rat, mouse, and human-rat chimera receptors are activated by it (Bunzow et al., 2001; Reese et al., 2007). The Miller laboratory reported that methamphetamine activates the rhesus monkey TAAR1 (rhTAAR1) (Xie et al., 2007), a protein that is 97% homologous with the hTAAR1 sequence (Miller et al., 2005).

The experimental approach was to transiently express wild type hTAAR1 along with a luciferase reporter gene with a CRE-driven promoter in HEK293 cells. These transfected cells were then treated with TAAR1 agonists, and chemiluminescence due to CRE-driven luciferase expression was quantified. The rationale for taking this approach was that we had experienced difficulty stably expressing hTAAR1 in any cell line and that a cAMP-dependent, CRE-promoter driven reporter would be a down stream indicator of induced cAMP accumulation. Furthermore, it was expected that the CRELuc reporter gene would respond proportionately to cAMP levels that should be proportional to concentrations of applied agonists.

Chapter 5: DAT TAAR1 co-localization

An excellent and thorough review by David Sulzer et al. on the mechanisms of neurotransmitter release by AMPH and related compounds such as METH was recently published (Sulzer et al., 2005). A report documenting dopamine transporter enhancement of the rhesus monkey TAAR1-coupled cAMP production in response to trace amines, monoamine neurotransmitters and amphetamines by Xie et al. suggests a functional interaction between the monoamine transporters and TAAR1 (Xie et al., 2007). If TAAR1 is a modulator of DAT then the proteins are likely to be in close proximity, at least during the time they interact. I wanted to know if co-expressed hTAAR1 and hDAT would co-localize. In addition I wanted to determine whether treatment with AMPH or METH would cause the independent or coincident relocation of DAT and TAAR1.

My experimental approach was to use immunofluorescence microscopy to document the cellular location of wild type hTAAR1 and hDAT in HEK293 cells. I established a stably expressing HEK293 cell line for this study using a previously engineered plasmid designed to express hDAT protein fused to Green Fluorescent Protein (hDAT-GFP). The approach further included the transient co-transfection of these cells with a wild type hTAAR1 construct. The rationale for this approach was to utilize confocal microscopy to detect the green hDAT-GFP construct and immunoreactivity associated with hTAAR1 protein labeled with a second antibody, Fab-Cy3, that fluoresces red. Upon merging these separate green and red images, if areas of yellow resulted then this could be interpreted as evidence of co-localization of the two proteins.

Background - Trace Amine-Associated Receptors (TAARs)

TAARs are GPCRs that make up a phylogenetically distinct family of receptors separate from other related biogenic amine receptor families such as the 5HT family (Borowsky et al., 2001) (Lindemann et al., 2005). Until 2001, the existence of receptors for TAs in mammals had been suspected but none had been identified. In 2001 Borowsky et al. reported the cloning of a family of receptors, two of which bind to, and are activated by, trace amines. A short time later Bunzow et al. reported the characterization of a rat TAAR1 (rTAAR1) they had independently discovered (Bunzow et al., 2001). Agonist stimulated, heterologously expressed rTAAR1 couples to the activation of cAMP production *in vitro* by the trace amines β-phenylethylamine (PEA), *para*- tyramine (*p*-TYR), tryptamine (TRP), and octopamine (OCT), as well as psychostimulants including AMPH, METH, 3,4-methylenedioxymethamphetamine (MDMA), and lysergic acid diethylamide (LSD) (Bunzow et al., 2001; Wainscott et al., 2006).

The rat TAAR1 is activated to a lesser degree, by the neurotransmitters dopamine (DA) and norepinephrine (NE). Possible endogenous ligands for hTAAR1 include *p*-TYR, PEA, OCT and DA while for hTAAR4 *p*-TYR and PEA are the likely candidates. It has also been shown that 3-iodothyronamine (T1AM), a natural derivative of the thyroid hormone thyroxine and discovered in the Grandy laboratory, is a full and potent TAAR1 agonist *in vitro* with profound physiological effects *in vivo* (Scanlan et al., 2004). These observations led Grandy and Scanlan to speculate that TAAR1 plays a role in metabolism and mood.

TAARs have been found in every species examined including the rat, mouse, guinea pig, human, chimpanzee, rhesus monkey, and zebrafish (Grandy, 2007). Lindemann et al. determined that there are three subfamilies of TAARs: TAAR1-4, TAAR5, and TAAR6-9, based on phylogenetic considerations and consensus sequences thought to constitute the ligand binding pocket (Kratochwil et al., 2005; Lindemann et al., 2005). There are different numbers of functional genes in each species. The rat genome contains 19 TAARs, of which 17 are predicted to be functional and two are likely to be pseudogenes. The mouse has 15 functional and one pseudogene. Both the human and chimp genomes contain nine TAARs but it appears humans express six functional TAAR subtypes compared to three in the chimp (Lindemann et al., 2005).

A pseudogene is a gene that does not code for a functional protein. The most common causes of non-functionality in pseudogenes are the insertion of a stop codon or frameshifts due to the insertion or deletion of nucleotide bases that prevent translation of a functional protein. For example, the human TAAR4 is a pseudogene because it contains a stop codon following the sequence that codes for transmembrane 3 as well as two single nucleotide insertions between TM5 and TM6 that alter the reading frame. Only three of the chimpanzee TAAR genes contain intact open reading frames.

Homologies for TAAR1 are fairly high for the mammalian species. The human and rat TAAR1 have a 79% sequence identity, human and mouse, 76%, mouse and rat, 87%, and the human and chimp are 99%. The sequence homology between the rhesus monkey and the human TAAR1 is 97%.

All the TAARs except for TAAR2 are coded by a single-exon gene of about 1 kilobase-pair (kb) length. In each species the TAARs all map to a compact region of a single chromosome. The human TAARs span about 109kb and are located on chromosome 6q23.1.

In vitro TAAR1 immunoreactivity appears to be primarily localized in the cytoplasm of neurons (Borowsky et al., 2001) and cells heterologously expressing the receptor (Bunzow et al., 2001). Most GPCRs appear to traffic primarily to the cell surface. Interestingly, a recent study in rats found a predominantly intracellular distribution of the 5-HT(2A) immnoreactivity with 80 to 90% cytoplasmic distribution and 10 – 20% expression in the cell membrane (Cornea-Hebert et al., 2002).

The topic of comparing the activity of PEA-occupied TAAR1 receptors to that of other GPCRs was raised by my thesis advisory committee. This question was not addressed in these studies and a review of the TAAR1 literature also found no comparison of TAAR1 activity with other receptor types. In their 2001 report, Bunzow et al. reported that DA but not PEA, *p*-TYR, or AMPH induces a response in HEK293 cells transfected with the hD1 receptor. However, they did not report the cAMP levels so no direct comparison can be made.

Site-directed mutagenesis of GPCRs

GPCRs represent important targets for pharmaceutical therapeutics since over 25% of all approved drugs target this class of receptor (Hopkins and Groom, 2002). Ligand binding research has been aided by the publication of a low resolution crystal structure of rhodopsin which identifies features including seven transmembrane alpha

helices connected by three external and three intracellular loops and with N-terminal and C-terminal tails (Palczewski et al., 2000). Recently, the crystal structure for the hβ_2AR was determined which has a high degree of similarity to the rhodopsin structure (Rasmussen et al., 2007).

The β_2AR receptor has been extensively studied using site-directed mutagenesis to determine ligand binding sites (Strader et al., 1989; Suryanarayana and Kobilka, 1993; Wieland et al., 1996). These studies have led to the identification of important amino acids with side chains associated with binding to aminergic ligands. One of these sites is D3.32 (D113), which is conserved across all aminergic GPCRs (Ballesteros, 1995). This aspartate is involved in hydrogen bonding with the amine group of the ligands.

GPCR endocytosis and membrane trafficking

GPCRs can become desensitized following sustained stimulation. Phosphorylation of GPCRs by protein kinase A (PKA) as well as GPCR kinases (GRKS) causes decoupling of the receptor from the G protein subunits and promotes binding of β-arrestin to the GPCR. β-arrestin in turn recruits clathrin and the clathrin adaptor protein 2 (AP-2) complexes that lead to endocytosis in clathrin-coated vesicles. Endocytosed GPCRs may be either recycled to the plasma membrane or targeted to lysosomes for degradation. Recycling of the β_2AR is dependent on a C-terminal amino acid sequence and a Na+/H+ exchanger regulatory factor (NHERF) protein that interacts with the recycling sequence (Hanyaloglu and von Zastrow, 2008).

A less familiar function of GPCRs is the involvement of sequence motifs in receptor protein trafficking and cellular localization. A retention motif, RXR(R) present in the C-terminal tail of the gamma-aminobutyric acid (GABA) $_B$ receptor, led to the finding that $GABA_B$ receptor is a heterodimer (Marshall et al., 1999). Dimerization in the ER of the two GPCRs, $GABA_{B1a}$ and $GABA_{B2}$, masks the retention motif which allows release of the dimer from the ER and trafficking to the cell surface. Reading about this retention motif led me to search the literature for export motifs. Two ER exit motifs in the C-terminus are FXXXFXXXF (Bermak et al., 2001) and $F(X)_6LL$ (Duvernay et al., 2004). The later motif is present in the β_2AR and $GABA_{B1}$. Both of these exit motifs are present on the dopamine D1 and D2 receptors. A close inspection of TAAR1 TM7 and adjacent C-terminal sequences revealed modified ER exit motifs that may account, in part, for the observation that these receptors appear to remain stuck in the cytoplasm. In Chapter 5 I present my experimental results and discuss possible interpretations including co-localization of hTAAR1 with hDAT and the effects of amphetamine treatments on the localization of both proteins.

Trace Amines, noncatecholic biogenic amines: monoamine catabolites or neuromodulators?

Trace amines (TA), also referred to in the the early literature as noncatecholic phenylethylamines, are endogenous compounds that occur in the central and peripheral nervous systems of mammals and invertebrates (Saavedra et al., 1974a; Boulton, 1976; Roeder, 1999). TAs contain the core chemical structure of the biogenic amine neurotransmitters (figure 3).

Figure 3. Chemical structure of trace amines and monoamine neurotransmitters.

Figure 3.

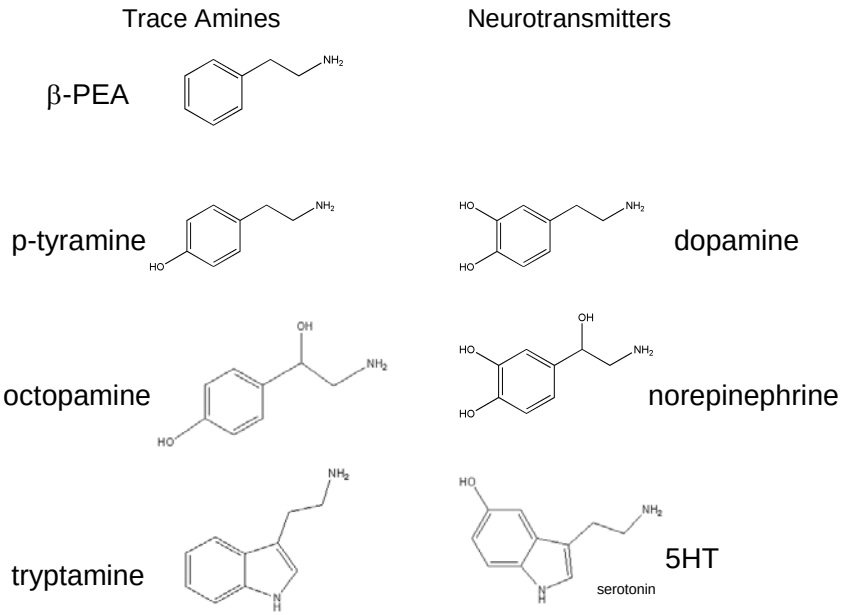
Trace Amines
Neurotransmitters
β-PEA
p-tyramine
dopamine
octopamine
norepinephrine
tryptamine
5HT
serotonin

TAs are produced from their precursor amino acids. PEA is synthesized directly by decarboxylation of the amino acid L-phenylalanine by the enzyme aromatic acid decarboxylase (AADC) as shown in Figure 4 (Young et al., 1982; Berry, 2004). Tryptamine is similarly produced from the amino acid tryptophan. In contrast, the TA octopamine (OCT) is synthesized from *p*-TYR by the sequentioal addition of a beta hydroxyl group. Synephrine is produced from OCT by methylation of the primary amine. OCT has been shown to function as a bona fide neurotransmitter in invertebrates (Roeder, 1999; Grohmann et al., 2003) but their function in mammals is unclear (see below). They may be involved in antidepressant effects (Sabelli et al., 1996).

TA content in rat brain is about two orders of magnitude lower than levels of the classical monoamine neurotransmitters DA, NE, and serotonin (5HT) (Durden and Davis, 1993; Berry, 2004). Since the TAs have a similar structure to these neurotransmitters they were once thought to be by-products of catecholamine biosynthesis (Premont et al., 2001). Although the TAs are chemically and structurally close relatives of DA, NE, and 5HT, these classic monoamine neurotransmitters are much less potent than the TAs or amphetamine-like psychostimulants with respect to stimulating TAAR1 heterologously expressed *in vitro*.

Figure 4. Biosynthesis of Trace Amines from Amino Acid Precursors.

Figure 4.

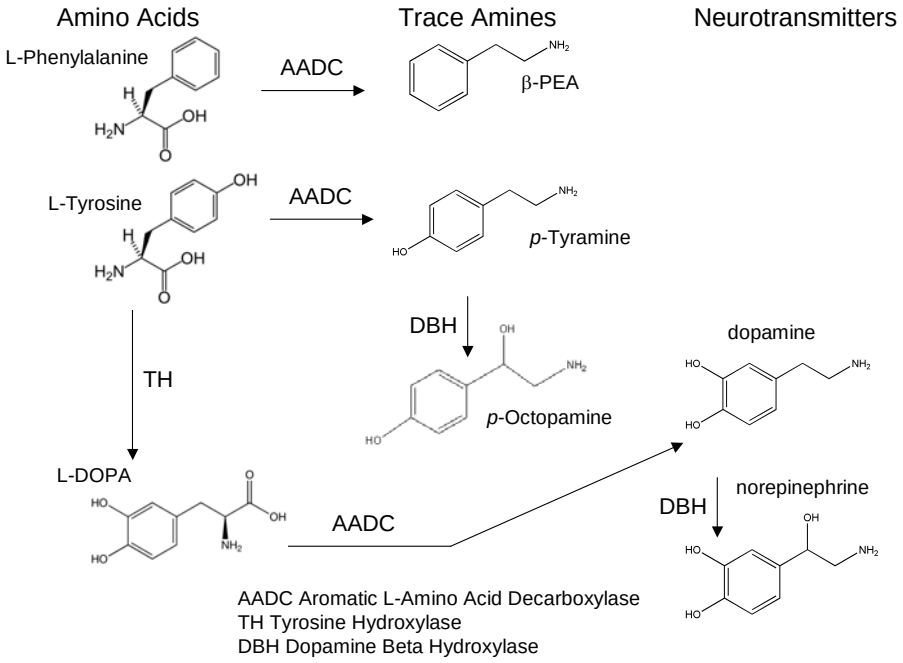
Amino Acids
Trace Amines
Neurotransmitters
L-Phenylalanine
AADC
β-PEA
L-Tyrosine
AADC
p-Tyramine
DBH
dopamine
TH
p-Octopamine
L-DOPA
AADC
DBH
norepinephrine
AADC Aromatic L-Amino Acid Decarboxylase
TH Tyrosine Hydroxylase
DBH Dopamine Beta Hydroxylase

Amine metabolism occurs primarily by monoamine oxidases A and B (MAO-A, MAO-B). PEA is selectively acted upon by MAO-B while NE and 5-HT are substrates for MAO-A and DA is a substrate at both (Yang and Neff, 1974). Levels of TAs are increased subsequent to the inhibition of MAO or in knockout mice lacking MAO (Holschneider et al., 2001).

It has been proposed that the TAs may serve as endogenous antidepressant agents (Sabelli et al., 1996) contributing to alertness and behavioral activity. Others have suggested their dysregulation might contribute to the etiology of depression and mania. PEA closely resembles AMPH and in animals does produce AMPH-like effects by inducing the neuronal release of DA in the midbrain (Sandler and Reynolds, 1976; Baud et al., 1985; Janssen et al., 1999; Ballesteros et al., 2001). The TAs PEA and *p*-TYR are considered to be "amphetamine-like substances" since they both can increase extracellular levels of DA by an exchange mechanism mediated by the dopamine transporter (DAT) (see below) (Geracitano et al., 2006). However, it requires much less AMPH to produce behavioral effects similar to those due to high doses of PEA and *p*-TYR. The basis for this discrepancy has been shown to be the alpha methyl group, characteristic of the AMPHs, that renders these compounds poor MAO substrates (Sabelli, 2002)

Drugs of abuse: METH and AMPH, and known mechanisms of action

Normal controls given AMPH can develop psychotic behavior indistinguishable from that of paranoid schizophrenics (Griffith et al., 1972). METH and AMPH elicit their effects by causing the release of DA, NE, and 5HT from neurons into midbrain

and cortical synapses. There are three pathways by which AMPH and METH are known to stimulate the release of DA: reverse transport via the dopamine transporter, reverse transport via the vesicular monoamine transporter (VMAT), and competitive inhibition of MAO-A and MAO-B. These routes to increased DA tone are indirect. At the dopamine transporter AMPH acts is a substrate that is more preferentially bound than DA thus inhibiting DA reuptake. AMPH is transported into the cell and reverses the direction of neurotransmitter transport, causing DA to flow from the cytoplasmic side of the cell (Rutledge, 1970; Parker and Cubeddu, 1988; Schmitz et al., 2001). This mechanism is referred to as "accelerated exchange diffusion" but the exact details at the molecular level are not yet fully understood (Liang and Rutledge, 1982). Another effect of AMPH on DAT is to promote its cellular internalization (Kahlig et al., 2004).

AMPH also acts at synaptic vesicles that store DA and NE causing these molecules to leak into the cytoplasm (Sulzer et al., 1995). The proposed mechanism for this redistribution is thought to be the collapse of the proton gradient that maintains the concentration of neurotransmitters in the vesicles (Smith and Davis, 1977).

Finally, AMPH is known to inhibit MAO-A and MAO-B resulting in decreased breakdown of the catecholamine neurotransmitters and hence higher cytoplasmic concentrations (Leitz and Stefano, 1971).

Association of TAARs with mood disorders

Recent studies have reported an association of the human TAAR6 gene with susceptibility to schizophrenia and bipolar disorder (Duan et al., 2004; Abou Jamra et

al., 2005; Pae et al., 2008) . This association is somewhat controversial because another study involving a Swedish population found no association between TAAR6 and bipolar disorder (Venken et al., 2005). This discrepancy may be due to genetic isolation in the populations sampled.

Initial mRNA evidence in the human CNS indicates that TAAR1 message is detectabe in the amygdala and in trace amounts in the dorsal root ganglia, hippocampus, hypothalamus, and the pituitary (Borowsky et al., 2001). More recent work involving rhesus monkey brain has provided evidence that TAAR1 mRNA and protein are expressed in the substantia nigra, nucleus accumbens, raphe nucleus, locus coeruleus, and amygdala (Xie et al., 2007).

TAs and TAARs may be involved in the etiology of some depression (Davis and Boulton, 1994) attention deficit hyperactivity disorder (ADHD) (Seeman and Madras, 1998; Kusaga, 2002; Kusaga et al., 2002), migraine headaches (Merikangas et al., 1995; Millichap and Yee, 2003), bipolar disorder (Pae et al., 2008), and Parkinsons Disease (Zhou et al., 1997; Zhou et al., 2001). Decreased levels of PEA in the brain have been proposed to be a contributing factor to the development and maintenance of depression (Sabelli and Mosnaim, 1974). In some early studies it was reported that urinary excretion of PEA is lower for depressed patients compared to control subjects. Interestingly, elevated urinary excretion of PEA was reported in schizophrenics (Shirkande et al., 1995). Urinary PEA and plasma levels of *p*-TYR were lower in children with ADHD compared to a control group (Baker et al., 1991). Plasma levels of TYR, OCT, and synephrine were higher in subjects with headaches compared to controls (D'Andrea et al., 2004). Plasma PEA concentrations in

Parkinson's Disease patients were significantly lower compared to those of a control group (Zhou et al., 2001).

Stereoselectivity of Methamphetamine and Amphetamine

AMPH and METH exist as two stereoisomers and at both the behavioral and molecular levels a preference for one over the other is seen in animal and human subjects. In humans S(+) amphetamine is the more potent psychostimulant with greater abuse potential than R(-) amphetamine (Bunney et al., 1975; Cho AK, 1994). In separate human studies involving depressed patients and normal subjects S(+)AMPH is more than twice as effective in producing activation and antidepressant effects (Van Kammen and Murphy, 1975; Smith and Davis, 1977). Studies in rat caudate synaptosomes as well as in cell lines heterologously expressing DAT show that the S(+) isomers of METH and AMPH are more potent than the R(-) isomers at inhibiting neurotransmitter uptake by DAT (Giros et al., 1994; Eshleman et al., 1999; Rothman et al., 2001).

A recently published study reported the pharmacokinetics of AMPH and METH stereoisomers in humans (Mendelson et al., 2006). They found following intravenously applied S(+) or R(-)AMPH the mean plasma concentration vs. time for S(+) AMPH is greater than for R(-)AMPH. However, for METH's two enantiomers there was no significant difference in the drug concentration over time.

If TAAR1 is indeed an important site of action for AMPH and METH we predict the stereoselectivity of TAAR1 to match the behavioral and molecular stereospecificity of amphetamines. My results presented in Chapters 2 and 4

demonstrate that hTAAR1 does in fact display a preference for the S(+)enantiomer of AMPH and METH.

In summary, my data supports the interpretation that hTAAR1 is likely to be activated by AMPH-like substances *in vivo* and may play a vital role in the development and maintenance of psychostimulant drug use. In addition TARR1 may contribute to the etiology of some psychiatric disorders. This likelihood is underscored given that the receptor is potently activated by AMPH and METH, it appears to be located in regions of the brain thought to be involved in these disorders, and that TAs produce amphetamine-like effects on DAT. Therefore, taken together, these observations suggest that TAAR1 is a promising target for developing novel anit-METH agents and potentially for novel therapeutics to improve treatments for some mental disorders.

Chapter 2

Trace Amine-Associated Receptor 1 Displays Species-Dependent Stereoselectivity for Isomers of Methamphetamine, Amphetamine and *para*-Hydroxyamphetamine

E.A. Reese[1]; J.R. Bunzow[1]; S. Arttamangkul[1,2]; M.S. Sonders[3]; D.K. Grandy[1]

[1] *Dept. of Physiology & Pharmacology Oregon Health & Science Univ., Portland, OR, USA , (EAR, JRB, DKG)*

[2] *Vollum Institute, Oregon Health & Science Univ., Portland, OR, USA (SA)*

[3] *Center for Molecular Recognition, Columbia Univ., New York, NY, USA (MSS)*

Published in: Journal of Pharmacology and Experimental Therapeutics **321**:178-186. January, 2007

Abstract

The synthetic amines methamphetamine (METH), amphetamine (AMPH), and their metabolite *para*-hydroxyamphetamine (POHA) are chemically and structurally related to the catecholamine neurotransmitters and a small group of endogenous biogenic amines collectively referred to as the trace amines (TAs). Recently it was reported that METH, AMPH, POHA, and the TAs *para*-tyramine (TYR) and *β*-phenylethylamine (PEA) ~~concentration-dependently~~ stimulate cAMP production ~~at rat trace amine-associated receptor 1 (rTAAR1) heterologously expressed~~ in human embryonic kidney (HEK-293) cells expressing rat Trace Amine-Associated Receptor 1 (rTAAR1). The discovery that METH and AMPH activate the rTAAR1 motivated us to study the effect of these drugs on the mouse TAAR1 (mTAAR1) and a human-rat chimera (h-rChTAAR1). Furthermore, since S(+) isomers of METH and AMPH are reported to be more potent and efficacious *in vivo* than R(-), we determined the enantiomeric selectivity ~~for these drugs at~~ of all three species of TAAR1. In response to METH, AMPH, or POHA exposure~~,~~ the accumulation of cAMP by HEK-293 cells ~~that~~ stably ~~heterologously~~ express~~inged~~ different species of TAAR1 was concentration- and isomer-dependent. EC_{50}s for S(+)-–METH were 0.89 μM, 0.92 μM, and 4.44 μM for rTAAR1, mTAAR1, and h-rChTAAR1, respectively. PEA was a potent and full agonist at each species of TAAR1 while TYR was a full agonist for the rodent TAAR1s but was a partial agonist at h-rChTAAR1. Interestingly, both isomers of METH were full agonists at mTAAR1 and h-rChTAAR1 while both were partial agonists at rTAAR1. Taken together these *in vitro* results suggest ~~indicate~~ that, *in vi~~tr~~vo*, ~~r~~TAAR1 ~~1, mTAAR1, and h-rChTAAR1 are c~~stereoselectively ~~activated by~~

~~METH, AMPH, and POHA suggesting TAARs~~ ould ~~represent~~ be a novel~~ther~~ mediator of ~~system through which~~ these drugs' effects ~~are mediated~~.

Introduction

Methamphetamine (METH) and its congener amphetamine (AMPH) are potent psychostimulants that can lead to abuse and often to addiction. METH, AMPH, and the monoamine neurotransmitters dopamine (DA) and norepinephrine (NE) share a similar chemical structure with the endogenous trace amines (TAs) *β*-phenylethylamine (PEA) and *para*-tyramine (TYR). In invertebrates the ~~trace amines~~ TAs octopamine (OCT) and TYR are *bona fide* neurotransmitters that act to modulate metabolism and skeletal muscles (Axelrod and Saavedra, 1977; Roeder, 2005) but the role of ~~trace amines~~ TAs in mammalian physiology is unclear. Some evidence suggests that decreased levels of TYR, OCT, and PEA are found in patients with clinical depression and elevated levels of PEA exist in patients with schizophrenia (Sandler et al., 1979; Davis and Boulton, 1994).

In the early 1930's AMPH was marketed as both a decongestant and a bronchial dilator. However, its ability to promote wakefulness and vigilance was utilized to treat narcolepsy (Prinzmetal, 1935). Soon thereafter a study demonstrated that administration of Benzedrine (racemic *dl*-AMPH) could improve the academic performance of children with behavior disorders (Bradley, 1937). This laid the foundation for the use of psychostimulants in the treatment of attention-deficit hyperactivity disorder (ADHD). Clinically both AMPH and METH (Anglin et al., 2000) have been used as anorectic agents for controlling obesity.

The few medically recognized therapeutic benefits of METH or AMPH consumption are derived from low dose exposure over time. In contrast, rapidly administered high doses of either drug produce short-lived feelings of intense elation or euphoria, stimulated libido, enhanced self-confidence, heightened motivation, and increased initiative resulting in a significant potential for abuse. Due to the development of tolerance, long-term users of METH and AMPH can eventually resort to taking gram quantities per day (Derlet et al., 1989). Due to the high bioavailability and low protein binding characteristics of METH and AMPH (Drummer, 2001) peak free drug in human blood can reach high micromolar to low millimolar concentrations (Logan et al., 1998) often resulting in death from hyperthermia or stroke. Other adverse health consequences include violent mood swings, aggressive behavior, anxiety, confusion, psychotic ideation, paranoia, delusions, hallucinations, and convulsions. In rodents a single high dose of METH or AMPH is reported to cause neurotoxic effects on DA and serotonin (5HT) producing neurons (Metzger et al., 2000; Jeng, 2006). Presently there is no known antidote for METH or AMPH overdose or pharmacotherapy for dependence.

Currently the molecular mechanisms by which METH and AMPH are thought to alter the distribution of DA, NE, and 5HT levels in the central nervous system (CNS) include interfering with reuptake by monoamine transporters ~~reuptake~~, vesicular storage, and inhibition of deamination by monoamine oxidase (MAO) (Sulzer et al., 2005; Partilla et al., 2006).

Discovery of the novel rat G protein-coupled receptor (GPCR) (Borowsky et al., 2001; Bunzow et al., 2001), now referred to as rat Trace Amine-Associated Receptor

1 (rTAAR1) (Lindemann et al., 2005), and the demonstration that it is functionally activated by PEA and TYR led Bunzow et al. (Bunzow et al., 2001) to test synthetic amines structurally related to PEA and TYR, such as METH, AMPH, and their metabolite *para*-hydroxyamphetamine (POHA), and METH*para*-hydroxyamphetamine (POHA). Human embryonic kidney (HEK) cells stably expressing rTAAR1 and exposed to AMPH or METH responded by elevating their cAMP content in a concentration-dependent and saturable manner. EC_{50}, the effective concentration of an agonist that produces half the maximum effect, is often used as a measure of potency. Although the R(-) and S(+) enantiomers of AMPH have approximately equivalent potencies with respect to stimulating cAMP production (EC_{50}s in the 300-800 nM range) in HEK-293 cells expressing rTAAR1, R(-)-AMPH is 30% less efficacious. (Bunzow et al., 2001).

Forensic pharmacokinetic data for METH and AMPH indicate that human METH abusers addicts taking grams of drug per day can achieve and survive steady state blood levels exceeding 10 several mg/L (e.g. 2 mg/L = 13 μM;) (Baselt, 2002; Peters et al., 2003). Here we report lower concentrations evoke responses of HEK-293 cells heterologously expressing recombinant rat, mouse, or the chimeric human TAAR1 (see Methods) to the stereoisomers of METH, AMPH, and POHAMETH. Moreover, we used the *in vitro* functional assay of cAMP accumulation to establish the steroselectivity of these drugs for all three species of TAAR1 from each species for these compounds in terms of potency and efficacy. While there is as yet no publication documenting *in vivo* TAAR1 activation, the results of this study unequivocally demonstrate that amphetamines are sufficiently potent to activate

TAAR1s *in vitro* and raise the possibility that TAAR1 may be activated in chronic abusers of amphetamines.

Methods

Cloning and Plasmids for rat, mouse, and human chimeric TAAR1

Cloning of the rat TAAR1 was described previously (Bunzow et al., 2001). Due to difficulties associated with stably expressing the wild-type human TAAR1 in a cell line, modifications were made to the hTAAR1 sequence (Lindemann et al., 2005) that replaced short, selected regions with rat TAAR1 sequences. Briefly, stretches of nucleotide sequence coding for the N-terminus (residues 1-20), C-terminus (residues 305-340), and third intracellular loop (residues 204-258) of the human TAAR1 were replaced with the corresponding rat sequences while retaining all of the transmembrane domains from the human TAAR1. In addition, the hemaglutinin virus sequence immediately followed by an M1 FLAG epitope was added to the N-terminus of this chimeric sequence as previously described (Lindemann et al., 2005). The human-rat TAAR1 chimera (h-rChTAAR1) expression vector was constructed by inserting the chimeric TAAR1 coding sequence into the expression vector pcDNA3.1/V5/His-TOPO Invitrogen (Carlsbad, CA). The resulting chimera was then stably expressed in HEK-293 cells. A line of HEK-293 cells stably expressing the human-rat chimera receptor was established by picking colonies from cells grown under G418 sulfate (geneticin), Gibco-Invitrogen (Grand Island, NY) selection.

Plasmids containing the TAAR1 genes for the wild-type rat or mouse were constructed using the same expression vector. The mouse and human TAAR1 were cloned from genomic DNA. The receptor sequences are reported in Acc. No. AY702315 and AF380186 for rTAAR1; Acc. No. AF380187 for mTAAR1; and Acc. No. AF200627 and AF380185 for hTAAR1. As a control for endogenous receptor expression and possible expression vector-specific effects the response of G418 (Ggeneticin)-resistant HEK-293 cells harboring the empty expression vector to each drug treatment was monitored in parallel with receptor-expressing cells. Cells stably expressing just the empty vector produced no cAMP accumulation in response to any drug treatments above the endogenous background level.

Tissue culture and cAMP binding assay

Stably-transfected HEK-293 cells were grown and maintained in Dulbecco's Modified Eagle Medium (DMEM) GIBCO-Invitrogen (Grand Island, NY) plus 10% fetal bovine serum media at 37^{o}C with 5.1% CO_2. Cells were grown to approximately 80% confluence, rinsed, and harvested in Krebs-Ringer-HEPES buffer (KRH) which consisted of freshly mixed NaCl (140mM), KCl (5mM), $CaCl_2$ (2mM), $MgSO_4$ (1.2mM), KH_2PO_4 (1.2mM) glucose (6mM) HEPES (25mM) at pH7.4. Cells were pre-treated with 200 μM 3-isobutyl-1-methyl-xanthine (IBMX), an inhibitor of phosphodiesterase. KRH buffer (200 μL) to which was added 4μL of drug compound at 100x final concentration or forskolin at 10μM was then combined with 200 μL of the IBMX-treated cell suspension. Cells were incubated for 1 hr at 37^{o}C in a water bath, then lysed by adding 400 μL of 0.5 mM Na acetate, briefly vortexed, and incubated at 100^{o}C for 20 minutes. Cell lysate debris was pelleted by centrifugation

and 200 μL of supernatant were transferred to labeled tubes. To each sample was added 200 μL of ice cold Tris ethylenediaminetetraacetic acid (EDTA) followed by 100 μL of [^{3}H] cAMP and 100 μL of DPC's (Diagnostic Products Corp., Los Angeles, CA) cAMP binding protein. After brief mixing, tubes were incubated at 0^{o}C for at least 90 minutes when 500 μL of freshly prepared charcoal dextran was then added to all tubes. These tubes were vortexed and incubated for 10 minutes at 0^{o}C, centrifuged for another 10 minutes at 4^{o}C, and then 800 μl of supernatant from each tube was added to vials containing ScintiSafe 30% liquid scintillation fluid (Fisher Scientific, Fair Lawn, NJ), shaken and counted for 5 minutes. Data were normalized according to protein content which was determined using a Bradford Protein Assay reagent (Bio-Rad Laboratories, Inc. Hercules, CA). Concentration response values were calculated using Excel (Microsoft, Redmond, WA). Non-linear sigmoidal concentration-response curves were fitted to the data and plotted and EC_{50} values were calculated using Prism software (GraphPad, San Diego, CA).

PEA, TYR, or the S(+)- or R(-)-enantiomers of AMPH, POHA, or METH were applied to HEK-293 cells stably expressing rTAAR1 and the induced cAMP level was measured. Identical experiments were conducted using the mouse TAAR1 (mTAAR1) and the human-rat TAAR1 chimera (h-rChTAAR1). For any given experiment all cells were harvested from the same tissue culture and the reactions were carried out employing the same freshly made KRH buffer for all drugs used in a given experiment. Experiments were repeated n times (n = 3 to 8). The average and standard error of the mean (SEM) of the induced cAMP production by test compounds were normalized to the maximum level produced in response to PEA in

the same experiment. At each concentration of applied drug the average and SEM of cAMP accumulation from n experiments was calculated. These average and SEM values from multiple experiments were plotted as a function of the concentration of the drug applied and a non-linear sigmoidal curve was fit to the averages using GraphPad PRISM software. While the Hill coefficient was allowed to be variable rather than fixed, the fitted coefficients did not differ significantly from 1. The goodness of fit, as measured by R^2, was typically 0.98 to 0.99 or greater.

Flow Cytometry

HEK-293 cells heterologously and stably expressing the rTAAR1, mTAAR1, h-rChTAAR1, or empty expression vector, were grown to 80% confluence and then harvested by gentle scraping from the plate in Krebs Ringer physiological buffer (KRH). The cells were washed twice in KRH buffer and then pre-hybridized in KRH buffer plus 1% BSA for 30 min at 37 ^{o}C. The cells were then exposed to different dilutions of the anti-FLAG M1 monoclonal antibody that had been conjugated to the fluorescent dye Alexa 488 (0.2 ug/ml) for 1 hour at 4^{o}C. The cells were then washed three times and re-suspended in KRH + 1% BSA. Propidium iodide was added to stain dead cells which were then gated out when analysed on a Becton-Dickinson Flow Cytometer. The live cell fraction was analyzed and the geometric mean of fluorescence intensity for 10,000 cells, adjusted for controls, was then used to quantify the relative number of receptors expressed on the TAAR cell surface.

Drug Compounds

The S(+)- and R(-)-POHA-HBr were kindly provided by the National Institute on Drug Abuse Drug Supply System (Bethesda, MD). The S(+)- and R(-)-AMPH-sulfate and the S(+)- and R(-)-METH-HCl and all other compounds were purchased from (Sigma-Aldrich Corp. St. Louis, MO). While S and R refer to the absolute configurations of the enantiomers, (+) and (-) respectively denote the clockwise (dextro, *d*) and counterclockwise (levo, *l*) rotation of polarized light through a solution of the compound. Drugs were dissolved in water, diluted to 100x final concentration, stored at -20^{O}C, and prior to each experiment thawed and vortexed.

Statistical analysis

Calculated values of cAMP production were performed using Excel (Microsoft Corp. Redmond, WA) based on standard curves generated from known concentrations of cAMP supplied with the kit purchased from DPC (Diagnostic Products Corp., Los Angeles, CA) and processed according to the manufacturer's instructions. Absolute values of cAMP accumulation per mg of protein for each experiment were also normalized to the maximum level of cAMP produced in response to PEA for that experiment. The means and the standard error of the mean (SEM) for each concentration of all the applied agonists were calculated using Excel. Tables of cAMP mean and SEM values and concentrations of applied agonists were copied into the PRISM4 graphics and statistics software program (GraphPad Software Inc., San Diego, CA). The means and SEMs were graphed using PRISM and sigmoidal curves were generated that fit the data. EC_{50} values and 95% confidence levels were calculated. Differences between two treatments were tested for significance using

the two-tailed t-test. Differences between three treatments were tested by ANOVA with a Tukey's post test for significance. Differences were considered significant when * $p < 0.05$, ** $p < 0.01$, and *** $p < 0.001$.

Results

The synthetic psychostimulants METH and AMPH ~~and METH~~ share the phenylethylamine structure with the TAs PEA, TYR, and OCT, as well as with the catecholamine neurotransmitters DA, NE, and epinephrine (Fig. 1). The alpha carbon of ~~AMPH~~ METH and ~~METH~~ AMPH is methylated thus making possible the existence of two stereoisomers.

Consistent with the observation of Bunzow et al. (Bunzow et al., 2001), G418-resistant HEK-293 cells transfected with the empty expression vector did not produce cAMP above background levels when treated with PEA, TYR, AMPH, METH or POHA (data not shown). However, exposing cells stably expressing recombinant rTAAR1 to PEA or TYR over a range of concentrations, from 3.3 nM to 1 mM, resulted in concentration-dependent increases in cAMP accumulation that saturated between 10^{-5}M to 10^{-3}M. PEA and TYR also concentration-dependently stimulated cAMP accumulation in cells stably expressing recombinant mTAAR1 or h-rChTAAR1 (Table 1). Plotted together, the concentration-response curves for PEA of all three species of TAAR1 overlap with EC_{50} values between 0.4 μM - 0.6 μM; Fig. 2A and Table 1). In contrast, each species of TAAR1 displayed a unique TYR concentration-response profile (Fig. 2B; Table 1). TYR was as efficacious (~99%

PEA_{max}) but more potent (EC_{50} = 80 nM) than PEA (EC_{50} = 380 nM) in stimulating cAMP accumulation by cells stably expressing rTAAR1 (Fig. 2B; Table 2). In cells expressing either the mouse or chimeric TAAR1 TYR was able to achieve ~90% of PEA's maximal effect (Fig. 2B; Table 2) with EC_{50}s that were 690 nM and 2.26 μM, respectively (Table 1).

Although some reports show normalization of concentration-response data to forskolin, a direct stimulator of adenylyl cyclase, we chose to normalize all subsequent drug-response data to PEA's maximum effect (PEA_{max}) since it acts as a full and equipotent agonist at all three species of heterologously expressed TAAR1s, stimulating cAMP accumulation concentration-dependently and in a saturable manner.

Many GPCRs, such as opioid receptors, display stereoselectivity for their cognate ligands. Furthermore, some of the behavioral literature indicates that the S(+) -isomer of AMPH is more potent and efficacious than the R(-) in eliciting locomotor activation in rodents (Angrist et al., 1971) and in producing activation and antidepressant effects in humans (Smith and Davis, 1977). Consequently, it was of interest to determine whether the different species of TAAR1 display preferences for either isomer of METH, AMPH, or POHA.

In agreement with Bunzow et al. (Bunzow et al., 2001) the EC_{50} of the R(-) isomer of AMPH appeared to be slightly lower, and statistically different (p=0.0152) than the EC_{50} of the S(+) isomer at stimulating cAMP in cells stably expressing rTAAR1 (Table 1). However, relative to PEA the S(+)-AMPH isomer was a full agonist while the R(-) AMPH was a 30% less efficacious partial agonist (Fig. 3A; Table 2). When

HEK-293 cells stably expressing mTAAR1 were exposed to AMPH both isomers were found to be nearly full agonists (~895% PEA_{max}; Table 2) but displayed an order of magnitude difference in potencies ($p<0.0001$) as measured by EC_{50}: S(+)-AMPH displayed an average EC_{50} of 210 nM compared to 4.96 μM for R(-)-AMPH (Fig. 3B; Table 1). In cells stably expressing the h-rChTAAR S(+)-AMPH was not only significantly more potent than R(-)-AMPH (EC_{50}=1.12 μM vs. 3.09 μM with $p<0.0001$) with respect to stimulating the accumulation of cAMP (Fig. 3C; Table 1) but it was also a full agonist (Table 2).

An identical analysis was performed using the S(+) and R(-)- isomers of METH. When either S(+)-METH or R(-)-METH was applied to cells in culture expressing the recombinant rTAAR1 both isomers concentration-dependently stimulated cAMP production until a maximum accumulation was reached at drug concentrations of 10^{-4} M and higher (Fig. 3D). Both isomers of METH had similar EC_{50}s (~890 nM to 1.19uM; Table 1) but different efficacies with S(+)-METH appearing more efficacious than R(-)-METH (~86% PEA_{max} vs. ~75% but with a non-significant p-value of 0.1191). Plotting the cAMP accumulation data collected from mTAAR1-expressing cells following treatment with either S(+)- or R(-)-METH (Fig. 3E) revealed that, as with AMPH, the S(+) and R(-) isomers were equally efficacious full agonists achieving ~92% and 91% of PEA_{max}, respectively (Table 2) but that the S(+) isomer was significantly more potent (EC_{50} of S(+)-METH = 920 nM vs. 2.44 μM for R(-)-METH, $p<0.0001$, Table 1). When the cAMP accumulation following incubation with a range of METH concentrations was determined and plotted for cells stably expressing the h-rCh TAAR1, both S(+)-METH and (R-)-METH were full agonists

with S(+)-METH about twice as potent as its R(-)-enantiomer (Fig. 3F) with an EC_{50} value 4.44 μM compared to 9.83 μM (p=0.002, Table 1). Of the compounds evaluated in this study, both isomers of METH and PEA appeared to be the most efficacious in terms of activating h-rChTAAR1, (Table 2).

The *para*-hydroxylated form of AMPH (POHA), also known as 4-hydroxyamphetamine, is a major metabolite of both AMPH and METH (Law and Moody, 2000; Kanamori et al., 2005). Produced by the cytochrome P_{450} detoxification system, POHA is reported to have biological effects of its own (Kaminskas et al., 2002). Following up on the observation reported by Bunzow et al. (Bunzow et al., 2001) that a racemic mix of POHA concentration-dependently stimulates cAMP production in cells expressing rTAAR1, the present study examined the ability of each isomer to stimulate cAMP accumulation in each of the three TAAR1-expressing cell lines. Over the concentration range examined, unfortunately limited due to unavailability of both POHA enantiomers, rTAAR1-expressing HEK-293 cells responded to both isoforms (Fig. 3G), however, R(-)-POHA displayed a higher, but not significant (p=0.1105), potency than S(+)-POHA (EC_{50} of 60 nM vs. 190 nM; Table 1). In spite of R(-)-POHA's greater potency the S(+) enantiomer stimulated ~20% more cAMP accumulation than PEA (119% vs. 100%, Table 2) and almost 30% more of an effect than R(-)-POHA (p = 0.0251; Table 2). Although cells expressing mTAAR1 also responded concentration-dependently to both isomers of POHA with an increase in cAMP accumulation (Fig. 3H), S(+)-POHA, with an EC_{50} value of 280 nM (Table 1), appeared to be over an order of magnitude more potent than the R(-)isomer. Since the effect of R(-)-POHA did not saturate at the highest

drug concentration attainable, an approximate EC_{50} value of 5.65 μM was calculated (Table 1). By comparison, the response of cells expressing the h-rChTAAR1 revealed both isomers of POHA to be weak agonists (Fig. 3I) and S(+)-POHA appeared to be more potent than R(-)-POHA.

To facilitate the visualization of all 3 species of receptor in terms of their stereoselectivity, the data presented in Fig. 3 was re-plotted so that the accumulation of cAMP could be easily viewed as a function of isomer and species of TAAR1 (Fig. 4). From this representation of the data several observations can be made. First, in general the 3 receptors responded in similar ways to the S(+)- and R(-)-isomers of all compounds tested with the exception of POHA (Fig. 4C & F). Over the limited range of POHA concentrations evaluated, each species of TAAR1 responded in a unique and characteristic way. Cells that expressed either of the rodent TAAR1s responded to low nM concentrations ($EC_{50\ rTAAR1}$=190 nM; $EC_{50\ mTAAR1}$=280 nM) of POHA's S(+)-isomer. This isomer also exhibited full agonism at rTAAR1 (~119% PEA_{max}) compared to mTAAR1 (~87% PEA_{max}), as previously noted (Fig.3G and Fig. 4C). In contrast, cells expressing the h-rChTAAR1 only responded at much higher concentrations of S(+)-POHA. Interestingly, cells expressing mTAAR1 appeared relatively insensitive to R(-)-POHA responding in a manner similar to cells harboring h-rChTAAR1. In contrast cells expressing rTAAR1 responded to R(-)-POHA by achieving ~91% PEA_{max} with the lowest EC_{50} of any compound studied ($EC_{50\ rTAAR1}$=60 nM).

This display of the data also revealed that the S(+)-AMPH (Fig. 4A) appeared more potent in stimulating cAMP accumulation in HEK-293 cells expressing

mTAAR1 ($EC_{50\ mTAAR1}$=210 nM) than either rTAAR1- ($EC_{50\ rTAAR1}$=810 nm) or h-rChTAAR1-expressing cells ($EC_{50\ h\text{-}rChTAAR1}$=1.12 μM) but appeared less efficacious (~89% PEA_{max}) in producing cAMP than in cells expressing rTAAR1 (~105% PEA_{max}). Cells expressing either rodent TAAR1 also appeared more sensitive to the stimulating effects of (+)-METH (Fig. 4B; avg. $EC_{50\ rodentTAAR1}$= ~905 nM) than cells expressing the h-rChTAAR1 ($EC_{50h\text{-}rChTAAR1}$=4.44 μM). Interestingly, while R(-)-AMPH (Fig. 4D) appeared significantly more potent in stimulating rTAAR1-expressing HEK-293 cells than cells expressing either mTAAR1 or h-rChTAAR1 (EC_{50}=290 nM vs. 4.96 μM and 3.09 μM, respectively), the difference in efficacy appeared less (~68% of PEA_{max}) compared to h-rChTAAR1 (~78% PEA_{max}) or mTAAR1 (~91% PEA_{max}). R(-)-METH (Fig. 4E) was least potent at h-rTAAR1 (EC_{50}=9.83 μM) compared to either rodent TAAR1 ($EC_{50\ mTAAR1}$=2.44 μM vs. $EC_{50\ rTAAR1}$= 1.19 uM) but was a full agonist and as efficacious in stimulating h-rChTAAR1 (~91% PEA_{max}) as mTAAR1 (~91% PEA_{max}) compared to rTAAR1 (~75% PEA_{max}).

Since it has been shown that the level of receptor and G-protein expression can influence potency and efficacy, a saturation-binding assay would have been useful to experimentally determine the total number of receptors per mg of protein per cell line. Unfortunately, a viable binding assay is not currently available due to the lack of a labeled ligand with high affinity for the TAAR1 receptor and low non-specific binding. Consequently, the relative amounts of cell surface TAAR1 ~~receptor~~ protein expression ~~levels~~ in the three different cell lines were estimated by flow cytometry. Fluorescence measurements were taken of samples containing ~~samples containing~~

HEK-293 cells that expressed vector alone or epitope-tagged and fluorescent anti-FLAG M1 antibody-labeled mTAAR1, rTAAR1, or h-rChTAAR1. Analysis of the fluorescence corresponding to rmTAAR1 and mrTAAR1 normalized to the fluorescence of h-rChh-rChTAAR1, which had the least number of receptors, gave relative cell surface receptor expression levels of approximately 2.8 : 1.25: 1, 125% and 284% (data not shown).

Since surface receptor densities and possibly G-protein densities may be different for cell lines expressing different species of the TAAR1, the above comparisons need to be considered cautiously.

Figures and figure legends

Figure 1. Chemical structures of the trace amines β-phenylethylamine, *para*-tyramine, and octopamine as well as amphetamine compounds S(+)- and R(-)-Amphetamine, S(+)- and R(-)-*para*-OH-Amphetamine, and S(+)- and R(-)-Methamphetamine and the neurotransmitters dopamine, norepinephrine, and epinephrine.

Figure 1

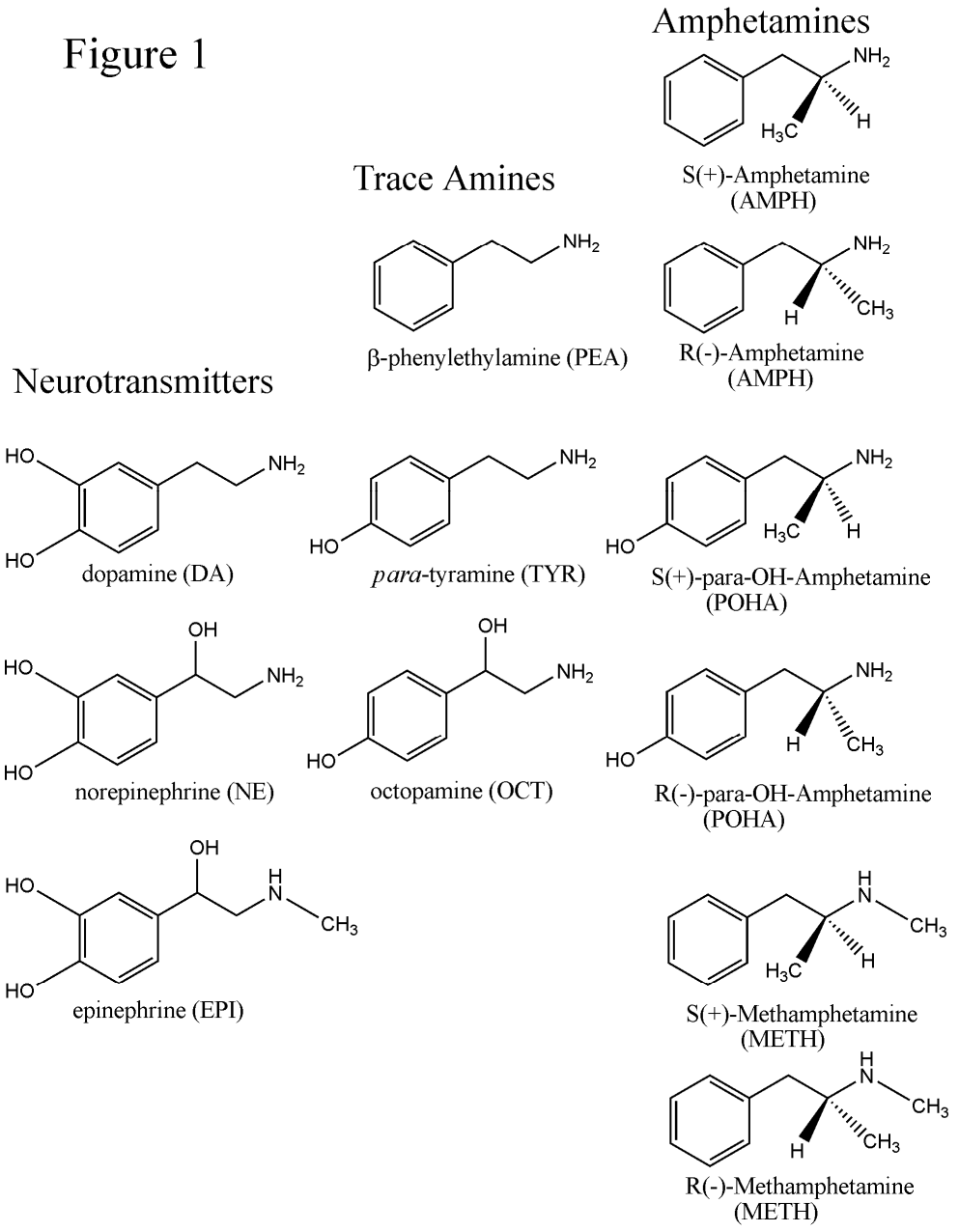
Amphetamines
S(+)-Amphetamine (AMPH)
Trace Amines
β-phenylethylamine (PEA)
R(-)-Amphetamine (AMPH)
Neurotransmitters
dopamine (DA)
para-tyramine (TYR)
S(+)-para-OH-Amphetamine (POHA)
norepinephrine (NE)
octopamine (OCT)
R(-)-para-OH-Amphetamine (POHA)
epinephrine (EPI)
S(+)-Methamphetamine (METH)
R(-)-Methamphetamine (METH)

Figure 2. Normalized cAMP response to PEA. Data shown are the increases of cAMP production in response to drug treatments compared with the baseline response to treatment by vehicle alone. Data are the percentage of the response at each concentration normalized to the maximum level of cAMP induced by PEA. (A) superimposed concentration-dependent responses of rat(●), mouse(▲), and human-rat chimera TAAR1 (■) to PEA. (B) concentration-response curves for rat(●), mouse(▲), and human-rat chimera TAAR1 (■) expressing HEK-293 cells for stimulation by TYR. Concentrations of applied drug compounds along the X-axis are given in units of log M where M is molarity. Cells stably expressing the empty expression vector and selected by G418 produced no cAMP accumulation in response to drug treatments beyond the endogenous background level.

Figure 2.

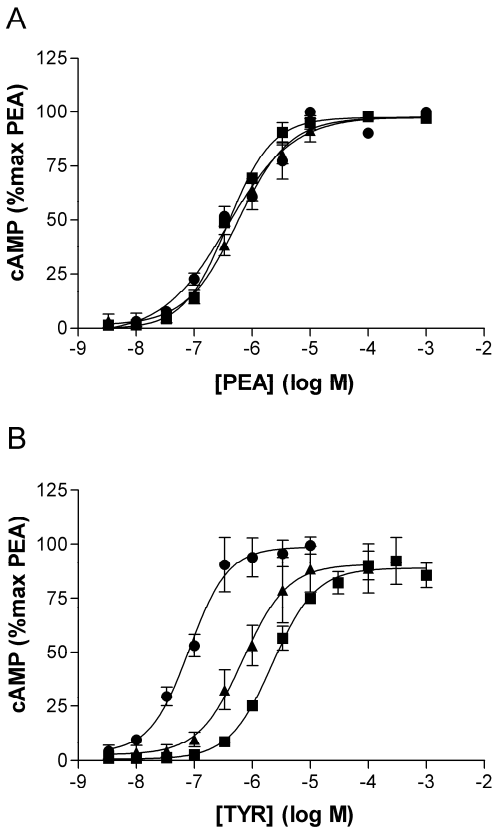
A
cAMP (%max PEA)
125
100
75
50
25
0
-9
-8
-7
-6
-5
-4
-3
-2
[PEA] (log M)
B
cAMP (%max PEA)
125
100
75
50
25
0
-9
-8
-7
-6
-5
-4
-3
-2
[TYR] (log M)

Figure 3. Concentration-dependent stimulation of cAMP accumulation in response to both isomers of AMPH or METH, or POHA in HEK-293 cells stably expressing recombinant rat-, mouse-, or the human-rat chimera h-rCh-TAAR1. cAMP response of HEK-293 cells stably expressing (A) rTAAR1 treated by S(+)-AMPH (●) and R(-)-AMPH (O), (B) mTAAR1 treated by S(+)-AMPH (▲) and R(-)-AMPH (△), (C) h-rChTAAR1 treated by S(+)-AMPH (■) and R(-)-AMPH (□), (D) rTAAR1 treated by S(+)-METH (●) and R(-)-METH (O), (E) mTAAR1 treated by S(+)-METH (▲) and R(-)- METH(△), (F) h-rChTAAR1 treated by S(+)-METH (■) and R(-)-METH (□), (G) rTAAR1 treated by S(+)-POHA (●) and R(-)-POHA (O), (H) mTAAR1 treated by S(+)-POHA (▲) and R(-)-POHA (△), and (I) h-rChTAAR1 treated by S(+)-POHA (■) and R(-)-POHA (□). Data are presented as a percentage of the maximal cAMP produced in response to PEA. Data shown are the mean ± S.E.M. from at least three experiments performed in duplicate. Concentrations of applied drug compounds along the X-axis are given in units of log M where M is molarity. Statistical significance is indicated as * $p < 0.05$; ** $p < 0.01$; and *** $p < 0.001$. Cells stably expressing the empty expression vector and selected by G418 produced no cAMP accumulation in response to drug treatments beyond the endogenous background level.

Figure 3.

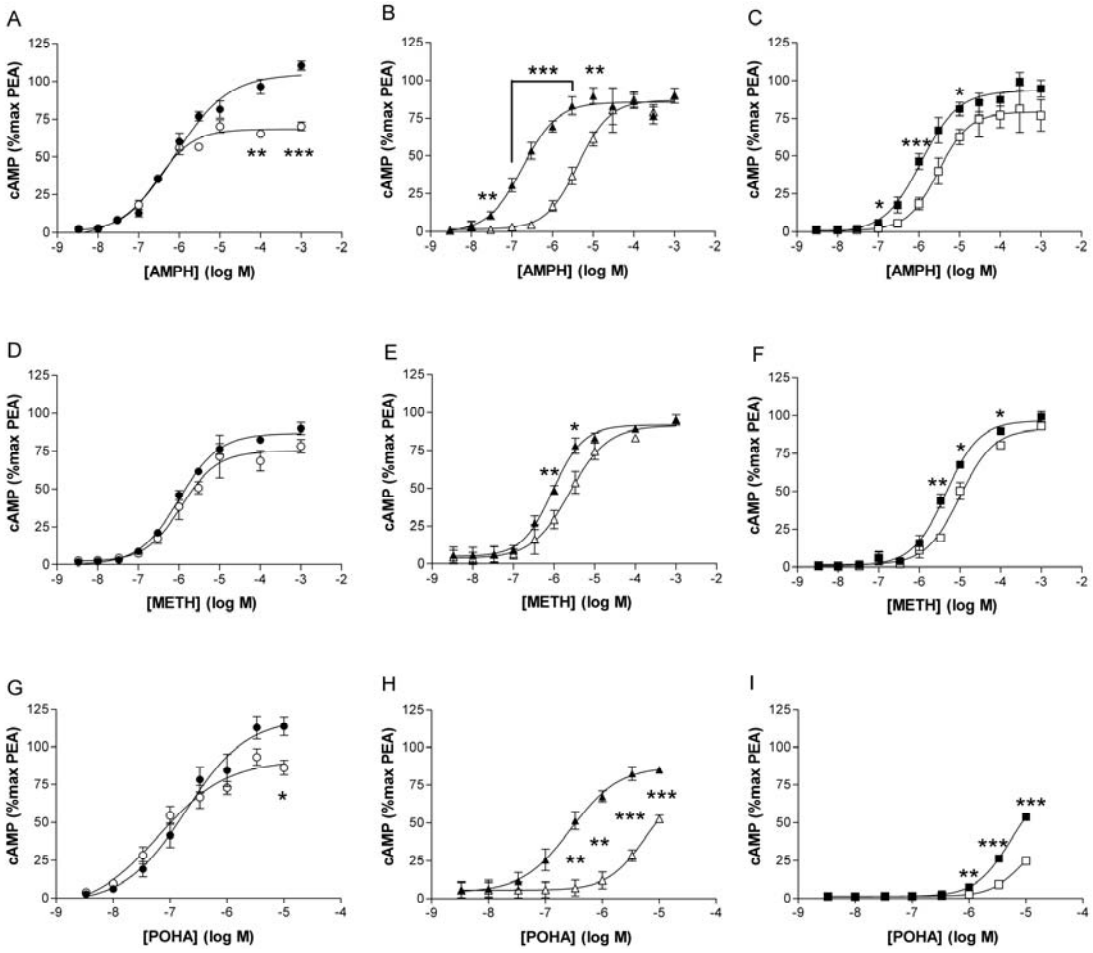

Figure 4. Species-dependent comparison of the concentration-response cAMP accumulation in HEK-293 cells stably expressing recombinant r-, m-, and h-rCh-TAAR1 in response to isomers of AMPH, METH, and POHA. Response in rat- (●), mouse- (▲) and human-rat chimera- (■) expressing TAAR1 cells to (A) S(+)- a.k.a. *d*-AMPH, (B) S(+)--METH, and (C) S(+)--POHA. Response in rat- (O), mouse- (△) and human-rat chimera- (□) expressing TAAR1 cells (D) to R(-) a.k.a. *l*-AMPH, (E) R(-)--METH, and (F) R(-)--POHA. Data are presented as a percentage of the maximal cAMP produced in response to PEA. Data shown are the mean ± S.E.M. from at least three experiments performed in duplicate. Concentrations of applied drug compounds along the X-axis are given in units of log M where M is molarity. Statistical significance is indicated as * $p < 0.05$; ** $p < 0.01$; and *** $p < 0.001$. Cells stably expressing the empty expression vector and selected by G418 produced no cAMP accumulation in response to drug treatments beyond the endogenous background level.

Figure 4.

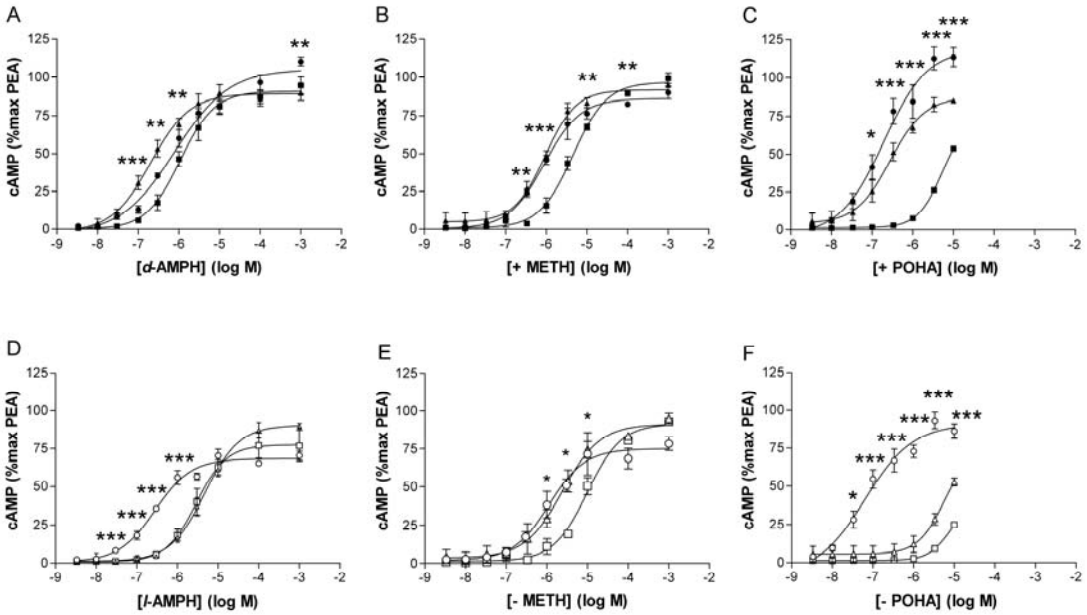
A
B
C
D
E
F
cAMP (%max PEA)
[d-AMPH] (log M)
[+ METH] (log M)
[+ POHA] (log M)
[l-AMPH] (log M)
[- METH] (log M)
[- POHA] (log M)

Table 1. Rank order of average EC_{50} [a] values for cAMP accumulation in HEK-293 cells stably expressing rTAAR1, mTAAR1, or the h-rChTAAR1 and exposed to the indicated compounds.

[a] ~~The~~ EC_{50} is calculated from concentration-response curves and is the concentration of the applied compound that results in a response equal to half of the maximum response.

[b] Statistical significance of the difference in EC_{50} values between two isomers is indicated by the *p*-value calculated from a two-tailed t-test. *p*-values relate to the comparison of EC_{50} values for enantiomeric pairs.

Table 1.

	Rat			**Mouse**			**human-rat chimera**		
Treatment	EC_{50}(95%CI)	p[b]	Rank	EC_{50}(95%CI)	p	Rank	EC_{50}(95%CI)	p	Rank
	(μM)	value	order	(μM)	value	order	(μM)	value	order
PEA	0.38(.18,.82)		5	0.56(.47,.67)		3	0.38(.31,.49)		1
TYR	0.08(.06,.12)		2	0.69(.54,.88)		4	2.26(1.86,2.50)		3
S(+)AMPH	0.81(.41,1.64)	0.0152	6	0.21(.16,.28)	<0.0001	1	1.12(.85,1.48)	<0.0001	2
R(-)AMPH	0.29(.18,.49)		4	4.96(4.32,5.69)		7	3.09(2.82,3.37)		4
S(+)METH	0.89(.69,1.14)	0.2347	7	0.92(.73,1.16)	0.0001	5	4.44(3.47,5.69)	0.002	5
R(-)METH	1.19(.72,1.96)		8	2.44(1.77,3.36)		6	9.83(6.60,14.62)		8
S(+)POHA	0.19(.08,.43)	0.1105	3	0.28(.22,.35)	na	2	>5.42 not sat	na	6
R(-)POHA	0.06(.02,.26)		1	>5.65 not sat		8	>8.54 not sat		7

Table 2. Efficacy-[a,b] of trace amines and isomers of amphetamine, methamphetamine, and *para*-hydroxy amphetamine.

[a,b]-Efficacy is the maximum level of cAMP produced as a percentage of the maximum response to PEA (PEA_{max}). Table entries are calculated best-fit values of the top of the nonlinear sigmoidal curve used to model the concentration-response data. Statistical significance of the difference in efficacy between two isomers is indicated by the *p*-value calculated from a two-tailed t-test.

[b]*p*-values relate to the comparison of values for enantiomeric pairs. Statistical significance is indicated as * $p < 0.05$; ** $p < 0.01$; and *** $p < 0.001$.

Table 2.

	Rat		**Mouse**		**human-rat chimera**	
Treatment	%PEA$_{max}$ (95% CI)	*p*-value[b]	%PEA$_{max}$ (95% CI)	*p*-value	%PEA$_{max}$ (95% CI)	*p*-value
PEA	97.88 (86.54,109.2)		97.29 (94.23,100.4)		97.44 (93.51,101.4)	
TYR	98.71 (91.11,106.3)		90.67 (85.28,96.07)		87.88 (84.89,90.87)	
S(+)AMPH	105.5 (93.57,117.3)	0.0001	89.35 (85.92,92.78)	0.9890	90.95 (85.92,95.98)	0.2937
R(-)AMPH	68.36 (62.8,73.93)	***	90.58 (87.68,93.47)		77.72 (76.11,79.34)	
S(+)METH	86.20 (81.99,90.41)	0.1191	91.76 (87.48,96.03)	0.9751	96.71 (91.16,102.3)	0.2034
R(-)METH	75.05 (67.83,82.27)		91.33 (85.42,97.23)		91.55 (83.25,99.84)	
S(+)POHA	119 (94.12,143.8)	0.0251	87.42 (81.93,92.90)	na	76.01 not sat	na
R(-)POHA	91.04 (70.73,111.3)	*	74.79 not sat		43.20 not sat	

Discussion

Here we have characterized the potency and efficacy of AMPH, METH, and POHA to stimulate the accumulation of cAMP in HEK-293 cells stably expressing recombinant TAAR1 sequences cloned from mouse and human sources, in addition to the previously described rTAAR1 (Bunzow et al., 2001). The chimeric receptor (h-rChTAAR1) was engineered to overcome difficulties associated with stable *in vitro* expression of functional human TAAR1.

In this study we normalized cAMP results to the maximum cAMP level produced in response to PEA, a convention also adopted by Wainscott et al. (Wainscott et al., 2006), since PEA is a full agonist for each species of TAAR1. The normalized concentration-response curves for PEA for each species were virtually coincident across all the applied concentrations.

However,

~~—~~r~~R~~eceptor density and G-protein abundance ~~density~~ can both affect apparent agonist potency and efficacy in an *in vitro* assay (Kenakin and Morgan, 1989). Using a mathematical model it was shown that increasing concentrations of receptors cause an increase in both potency and efficacy (Kenakin and Morgan, 1989). Consequently, caution should ~~needs to~~ be observed whenever ~~interpreting~~ comparing results from ~~comparisons obtained from~~ two or more cell lines heterologously expressing different species of GPCR~~receptor~~, that in all probability have different receptor densities, as in the present study where flow cytometry revealed that the rTAAR1-expressing HEK-293 cells expressed on average two to three times as many receptors on their surface as either the mTAAR1 or h-rChTAAR1. . ~~In this study~~

~~we normalized cAMP results to the maximum cAMP level produced in response to PEA, a convention also adopted by Wainscott et al. (Wainscott et al., 2006), since PEA is a full agonist for each species of TAAR1. The normalized concentration-response curves for PEA for each species were virtually coincident across all the applied concentrations.~~

With the above caveat in mind our results demonstrated a species-specific response to the compounds tested. The TAs PEA and TYR concentration-dependently stimulated each species of TAAR1 stably and heterologously expressed in HEK-293 cells (Fig. 2). In cells expressing the h-rChTAAR1 chimera, ~~the most sensitive compound was~~ PEA had the lowest rank order of potency and was a full agonist, which ~~finding~~ suggests that ~~PEA~~ it could be an endogenous ~~ligand for~~ TAAR1 ligand in humans.

More than 30 years ago it was shown that an animal's physiological and behavioral responses to S(+) isomers of AMPH and METH are more potent and efficacious than their optical antipodes at inducing motor hyperactivity (Angrist et al., 1971; Segal, 1975). Although both isomers were full agonists at mTAAR1 and h-rChTAAR1 (Table 2) the potencies ~~potency~~ of the S(+) isomers of METH and AMPH were significantly greater than the potencies~~y~~ of the R(-)-isomers (Table 1). In cells expressing rTAAR1 both enantiomers of METH were ~~more~~ approximately equipotent but only partial agonists ~~in stimulating cAMP accumulation~~ (Fig. 3).

The stereoselectivity of mTAAR1 was especially apparent for the isomers of POHA. S(+)-POHA was apparently the more ~~apparently~~ potent of the two isomers

(Fig. 3H) given that the— R(-)POHA response did not reach a saturated maximumsaturate. For rTAAR1 expressing cells, the R(-)-isomers of AMPH and POHA showed significantly (p=0.0001 and 0.025 respectively) lower efficacy than than the S(+) forms in terms of stimulating cAMP accumulation (Fig. 3A, 3G). At the concentrations tested tThe h-rChTAAR1 was less responsive to POHA than either of the rodent receptors.

The physiological and behavioral effects of AMPH and METH are generally accepted to be mediated by their actions as substrates for the dopamine, norepinephrine, and vesicular monoamine transporters. The main mechanism for the termination of monoamine neurotransmitter signaling is by reuptake of DA, NE, and 5HT via the pre-synaptic plasma membrane transporters DAT, NET, and SERT. Once in the cytoplasm these neurotransmitters are either sequestered for reuse in storage vesicles via the vesicular monoamine transporter (VMAT2) or are inactivated by deamination by monoamine oxidase (MAO). This reuptake process is interfered with by compounds such as AMPH and METH that act as "substrate-type releasers" (Rothman and Baumann, 2006), which promote neurotransmitter release from synaptic storage vesicles into the cytoplasm and by reversing the direction of neurotransmitter flow through the transporter (Partilla et al., 2006).

Pharmacological data characterizing the inhibition of monoamine uptake and increased neurotransmitter release by various AMPHs was reported recently (Rothman et al., 2001). The EC_{50} of (+)--AMPH to release DA via DAT iwas 25nM, with K_i^{uptake} values in rat synaptosomes for this neurotransmitter of 34nM at the DAT,

concentrations approximately 20-3100 fold lower than the EC_{50} values we calculated for eliciting an *in vitro* functional response from rTAAR1 (0.8 υMμM).

Chronic psychostimulant METH abusers can typically consume gram quantities of AMPH or METH drug per day (Kramer et al., 1967).

—Given its high bioavailability, low protein binding, and long half life, plasma concentrations of both drugs can reach into the high micromolar range (Baselt, 2002; Peters et al., 2003). Although tThe extracellular free concentration of METH around relevant human dopaminergic synapses presumably involved in producing desirable CNS effects is not known with certainty,relevant concentration for human CNS effects, the extracellular free concentration of AMPH or METH in the vicinity of dopaminergic synapses, is not known. iIn rats, however, rats the METH serum levels are typically one tenth what is found in brain concentration of METH in the brain is about an order of magnitude greater than in serum (Riviere et al., 2000).

If the *in vivo* response for TAAR1 to amphetamines is similar to our *in vitro* pharmacological data then for plasma concentrations of AMPH and Forensic evidence indicates that METH that cause intoxication in experienced METH users can typically achieve peak blood concentrations of 100 μM (Baselt, 2002; Peters et al., 2003).,- Both isomers of METH were full agonists of h-rChTAAR1 over a range of EC_{50}s from 3.5 to ~15υMμM, concentrations that can be often exceeded in the blood of human METH addicts (Derlet et al., 1989). If TAAR1s, whether expressed in the CNS or periphery, are exposed to such concentrations it is possible TAAR1 receptors they could become functionally activated.

The existence of receptors specific for TAs has revived interest in the possibility that the TAAR gene family could contribute importantly to human mental health, including an individual's response to the psychostimulants METH and AMPH. However, in spite of considerable evidence collected over the years that is consistent with the involvement of TAs in the etiology of several adverse human health conditions including hypertension (Borowsky et al., 2001), migraine headache (D'Andrea G, 2006) schizophrenia (Yoshimoto et al., 1987), ADHD (Madras et al., 2005), depression (Carter et al., 1980), bipolar disorder (Abou Jamra et al., 2005) and stress (Paulos and Tessel, 1982), the biological functions of TAs in vertebrates have been difficult to demonstrate with any certainty. This is due in large measure to the difficulties associated with routinely achieving heterologous stable expression of functionally coupled members of this receptor family in tissue culture. A recent report using transient expression claims to have overcome this impediment (Liberles and Buck, 2006) and suggests that several members of the mTAAR receptor family, but not TAAR1, are expressed in mouse nasal epithelia where they respond to volatile amines present in mouse urine that may serve as social cues. Studies involving TAAR1 knockout mice could aid efforts to identify physiological and behavioral effects of METH and AMPH that are TAAR1-mediated.

The EC_{50} values calculated for the compounds examined in the present study (Table 1) are similar to those reported elsewhere (Bunzow et al., 2001; Lindemann et al., 2005; Miller et al., 2005; Lewin, 2006; Wainscott et al., 2006). For cells expressing rodent TAAR1s ~~rTAAR1,~~ both TYR and PEA were potent and full agonists ~~the AMPH metabolite R(-)POHA had the highest potencies of the~~

~~compounds tested,~~ supporting the interpretation that either one ~~TYR is~~ could be an ~~potentially an~~ endogenous TAAR1 ligand ~~in rats~~.

The present study also revealed that different chemical and structural features of AMPH, METH, and POHA are important depending on the species of TAAR1. The *para*-hydroxyl group on the benzene ring is a functional group that is important for activating rTAAR1 since compounds that contain it, TYR and POHA, displayed the highest potency and efficacy of the compounds tested (Table 1, Table 2). For POHA, rTAAR1 had a strong concentration-response to both isomers, while for h-rChTAAR1 both isomers were weak stimulants, results similar to recent findings by Wainscott et al. who reported higher potency for para-substituted compounds at rTAAR1 compared to the hTAAR1 (Wainscott et al., 2006). At mTAAR1 the orientation of the ligand's α-methyl group emerged as the most important structural feature of AMPH, METH, and POHA with respect to potency but was of no consequence in terms of efficacy. Future investigations involving site-directed mutagenesis of the putative ligand binding pockets of these receptors should help clarify the structural basis for their stereoselectivites.

In summary, we have established that AMPH, METH, and POHA can be potent and efficacious agonists of TAAR1s heterologously expressed *in vitro* and that they display concentration-dependent and species-dependent stereospecific pharmacological profiles. Given that the ~~eir~~ EC_{50}s for METH and AMPH activation ~~at~~ of the h-rChTAAR1 *in vitro* are well below the~~ir~~ concentrations frequently found in addicts, we suggest that TAAR1 might be a potential mediator of some of the effects of AMPH and METH in humans, including hyperthermia and stroke. In

addition~~Consequently~~, the possibility should be explored that genetic variants in hTAAR1, or other TAAR genes, may be important to several conditions thought to involve TAs including ADHD, depression, mania, psychosis, and addiction. If TAAR1 is confirmed as a target of ~~amphetamines~~ METH and AMPH *in vivo* then developing ~~understanding its interactions with~~ novel TAAR1-selective agonists and antagonists ~~compounds~~ could ultimately lead to successful pharmacotherapies for METH and AMPH addiction and overdose as well as contribute to a better understanding of the etiology of several mental disorders.

Chapter 3

Methamphetamine Activation of Rat and Mouse Species of TAAR1: Determination of Stereoselectivity by Site-Directed Mutagenesis

Manuscript in Preparation

Abstract

Methamphetamine and amphetamine are abused psychostimulants that potently activate the TAAR1 receptor *in vitro*. In an effort to reveal the ligand and receptor molecular basis for the species-dependent stereo-selective activation of TAAR1 by amphetamine and methamphetamine, I investigated *in vitro* cAMP production mediated by the mouse and rat TAAR1 in response to both isomers of methamphetamine and amphetamine using site-directed mutagenesis. Molecular modeling and mutagenesis results for the β_2AR that previously had identified amino acid residues responsible for specific interactions with agonists and antagonists were used to select TAAR1 residues to be mutated. Concentration response curves of cAMP produced in response to amphetamine and methamphetamine were generated for mutant and wild type receptors of rat and mouse TAAR1 stably expressed in HEK293 cells. The concentration-response curves and the EC_{50} for PEA, S(+) and R(-)AMPH, and S(+) and R(-)METH were all shifted to the right for the rat TM6 mutation, M6.55T, compared to the rWT TAAR1 curves. In contrast, for the mouse TM6 mutation, T6.55M, the concentration-response curves and the EC_{50}s for these compounds were all shifted to the left compared to the mWT TAAR1 curves. The rat trans-membrane domain 7 (TM7) mutant, N7.39Y (N287Y), had an order of magnitude lower EC_{50} for the S(+) isomer of amphetamine compared to the R(-) isomer, similar to the responses to these isomers by the mouse wild type receptor. The mouse TM7 mutant, Y7.39N (Y287N), had an EC_{50} for the R(-) isomer of amphetamine less than or equal to that for the S(+) isomer which was similar to the responses of the rat wild type receptor. Activation of cAMP by methamphetamine and amphetamine mediated by the mutant rat and mouse TAAR1 receptors

demonstrated that a single amino acid difference in TM7 was responsible for the reversed stereo-selectivity for the two species.

Introduction

The S(+)isomers of amphetamine and methamphetamine that are responsible for the greater *in vivo* psychostimulant effects in humans and increased locomotor effects in other mammals are the same isomers that more potently activate cAMP responses *in vitro* by the trace amine-associated receptor 1 (TAAR1). These *in vitro* responses are species-dependent.

Prior pharmacological studies of the TAAR1 receptor revealed a species dependent stereoselectivity to S(+) isomers of amphetamine (Wainscott et al., 2006) and methamphetamine (Reese et al., 2007) but the physicochemical properties of the receptor and the receptor-ligand interaction responsible for this stereoselectivity are unknown.

Trace amines (TAs) are endogenous monoamines found in mammalian CNS and include *p*-tyramine (TYR), *β*-phenylethylamine (PEA), tryptamine (TRP), and octopamine (OCT). Due to their structural similarity to monoamine neurotransmitters, the TAs were once thought to be metabolic derivatives of the neurotransmitters dopamine, norepinephrine, and serotonin. Concentrations of trace amines in the brain are about 1000 times lower than that of these neurotransmitters. In 2001, a family of GPCR receptors, some members of which are activated by trace amines, was discovered independently by two groups (Borowsky et al., 2001; Bunzow et al., 2001). TAAR1, a member of that family, mediates an increase in cAMP

accumulation in cells heterologously expressing the receptors in response to the application of trace amines.

TAAR1 is found in regions of the brain associated with monoaminergic neurons such as the substantia nigra, nucleus accumbens, ventral tegmental area, dorsal raphe nucleus, and amygdala (Borowsky et al., 2001; Lindemann et al., 2007; Xie et al., 2007). Trace amine receptors were found in the mouse epithelial tissue which suggested a possible role as odorant sensors for members of the family of receptors other than TAAR1 (Liberles and Buck, 2006). One hypothesis for their function is that they act as neuromodulators by increasing the sensitivity of monoamine neurotransmitter signaling (Berry, 2004; Xie et al., 2007).

Rat-, mouse-, and a human chimera-TAAR1 have been stably expressed but in our experience the TAAR1 location is mainly in the cytoplasm. A recent report described the establishment of stable cell lines expressing the wild type (WT) human- as well as rat- TAAR1 (Wainscott et al., 2006).

For small biogenic amine neurotransmitters such as dopamine and norepinephrine the ligand binds to the receptor in a ligand-binding pocket that is formed in the TM domain region beneath the surface of the plasma membrane. An example of this is the binding of norepinephrine to the well-studied β_2AR (Strader et al., 1987; Swaminath et al., 2004).

An example of stereoselectivity by GPCRs is 8-hydroxy-2-(di-n-propylamino) tetrain (8-OH-DPAT), a 5HT1A agonist (Dabrowska and Brylinski, 2006). The R isomer acts as a full and potent agonist at 5-HT1A receptors but the S isomer acts as a partial agonist, while both have similar binding affinities. In this study I investigated

what TAAR1 amino acid residues are responsible for the species-dependent stereoselectivity of AMPH and METH using site-directed mutagenesis.

To characterize cAMP production, the trace amine PEA and both enantiomers of amphetamine and methamphetamine were applied in a range of concentrations to mouse and rat TAAR1 receptors stably expressed in HEK293 cells. TAAR1 mutants to TM6 and TM7 residues thought to play a role in ligand-receptor binding were also stably expressed in HEK293 cells and characterized for cAMP production in response to PEA, AMPH and METH.

Studies of the β_2AR have shown that catecholamine ligand binding occurs in the plasma membrane region of the transmembrane domains in a pocket involving TM3, TM5, TM6, and TM7 of the receptor (Suryanarayana and Kobilka, 1993; Freddolino et al., 2004) .

The aspartate D3.32 (D102) in TM3 of the rat and mouse TAAR1 is conserved in biogenic and trace amine receptors. Site-directed mutagenesis of the β_2AR showed that this conserved residue, aspartate D3.32 (D113) in the β_2AR, electrostatically attracts the amine group of agonists and antagonists (Swaminath et al., 2005).

In this study I used the same site-directed mutagensis approach to replace the conserved TM3 aspartate with an alanine in both the rat- and mouse-TAAR1 which resulted in a knockdown in the cAMP response to known agonists.

It was also shown for the β_2AR that N6.55 (N293) on TM6 is involved in hydrogen bonding to the β-OH of epinephrine (Freddolino et al., 2004). Inspection of the TAAR1 sequences aligned to the β_2AR revealed a species-specific difference of amino acids at the site that aligns with the β_2AR N6.55 (N293). The rat sequence

contains a methionine while the mouse and human TAAR1 sequences contain a threonine at that location. This TM6 location was targeted for mutation since the wild type mouse and human chimera TAAR1 responses to the enantiomers of amphetamine are similar while both the mouse and human responses are different from the rat response.

Another site that is conserved in βARs and $5HT_{1A}$ receptors is N7.39 (N312) in TM7 of the β2AR. This site was identified in site-directed mutagenesis studies as a major determinant for species differences in binding aryloxalkylamines (Suryanarayana and Kobilka, 1993). The observation that the mouse and rat have different residues at this site prompted the mutation of TM7 of the mouse- and rat-TAAR1. The mouse mutation Y7.39N (Y287N) gave the rat residue and the rat mutation was N7.39Y (N287Y) which resulted in the mouse residue at that site of the rat TM7 sequence. For the wild type receptors the S(+)AMPH had an order of magnitude lower EC_{50} at the mTAAR1 compared to the R(-)AMPH while for the rTAAR1 both isomers were nearly equipotent. These results are similar to the previously reported results for the wild type receptors (Reese et al., 2007). Here the mouse TAAR1 with TM7 mutation Y7.39N (Y287N) displayed the stereoselectivity of the wild type rTAAR1 to isomers of AMPH. Correspondingly, the rat TAAR1 with TM7 mutation N7.39Y (N287Y) displayed the characteristics of the wild type mTAAR1 in response to isomers of AMPH. Thus, the stereoselectivity of the rat and mouse TAAR1 in response to isomers of AMPH was reversed for a single amino acid mutation to TM7. The response curves for rTM7 for both S(+) and R(-) METH were not shifted compared to the curves for the rWT TAAR1 (figure 7c, 7e). But for the

mouse TAAR1, both the S(+) and R(-)METH concentration-response curves for mTM7 were shifted to the right compared to the mWT curves (figure 7d, 7f). The EC_{50}s for the S(+) and R(-)METH concentration-response curves for mTM7 were virtually the same (figure 7b), while for rTM7 the EC_{50} for S(+)METH was less than for R(-)METH (figure 7a).

Methods and Materials

Site-directed Mutagenesis

Mutations to the TM3, TM6, and TM7 domains of the rat and mouse TAAR1 were generated using the QuikChange Site-Directed Mutagenesis Kit from Strategene following the manufacturer's instructions. Primers for each mutant were designed and purchased from Invitrogen. Guidelines used for designing primers are as follows. Both the forward and reverse primers contained the desired mutation and anneal to the same sequence on opposite strands of the plasmid. Primers were between 25 and 45 bases in length. The melting temperature of the primers was greater than or equal to 78^{o}C. The desired mutations were in the middle of the primer with about 10 to 15 bases of correct sequence on both sides of the mutation. The primers had a minimum GC content of 40% and terminated in one or more C or G bases. The following rat and mouse primers were used. The highlighted base was different from the wild type.

rat TM3 Asp to Ala on rTAAR1 rD3.32A
Forward primer 5' CTT CAC ACC AGC ACT GCT ATC ATG CTG AGC TCG 3'
Reverse primer 5' CGA GCT CAG CAT GAT AGC AGT GCT GGT GTG AAG 3'

mouse TM3 Asp to Ala on mTAAR1 mD3.32A
Forward primer 5' CAC ACC AGC ACC GCT ATC ATG CTG AGC TCC GCC 3'
Reverse primer 5' GGC GGA GCT CAG CAT GAT AGC GGT GCT GGT GTG 3'

rat TM6 TAAR1 Met268Thr on rTAAR1 rM6.55T
Forward primer 5’ CCG TTC TTT TTC TGC ACG GTC CTG GAC CC 3’
Reverse primer 5’ GG GTC CAG GAC CGT GCA GAA AAA GAA CGG 3’

mouse Thr268Met on TM6 mT6.55M
Forward primer 5’ CCG TTC TTT CTC TGC ATG GTC CTG GAC CCT TTC C 3’
Reverse primer5’ G GAA AGG GTC CAG GAC CAT GCA GAG AAA GAA CGG 3’

rat TM7 rTAAR1 N7.39Y AAT to TAT rN7.39Y
forward primer 5’ AAT GAC ACA CTG TAT TGG TTC GGG TAC 3’
reverse primer 5’ GTA CCC GAA CCA ATA CAG TGT GTC ATT 3’
mouse TM7 mTAAR1 Y7.39N TAT to AAT mY7.39N
forward primer 5’AAT BAC GCA CTG AAT TGG TTT GGG TAC 3’
reverse primer 5’ GTA CCC AAA CCA ATT CAG TGC GTC ATT 3’

A PCR reaction was run for each mutant using the appropriate forward and reverse primers containing the desired mutation, dsDNA of the vector plasmid containing the wild type TAAR1, and Pfu Turbo DNA polymerase according to instructions supplied in the Stratagene mutagenesis kit. Both plasmid strands were replicated by the PfuTurbo polymerase. Following the PCR cycles, the product was treated with Dpn1, an endonuclease used to digest the methylated and non-mutated parental DNA template, which left only the synthesized, mutated DNA.

The vector DNA with the designed mutation was transformed into XL1-Blue supercompetent cells supplied with the kit following the manufacturers directions. Transformed supercompetent cells were then spread onto warmed agar plates containing ampicillin and incubated overnight at 37^{o}C.

Isolated colonies were picked from the agar plate and incubated in separate tubes with LB Amp broth at 37^{o}C with shaking for about 18 hours to grow up enough cells with the mutated TAAR1 in order to isolate and prepare DNA. This was repeated two

or three times for each mutant in order to increase the chances of obtaining a successful mutation.

After the overnight growup of the colonies, DNA was prepared using the Invitrogen PureLink Quick Plasmid Miniprep Kit. The quality of the eluted DNA was analyzed by measuring the optical density using the NanoDrop ND-1000 spectrophotometer. Restriction enzymes Hind3 and Xba1 were used to digest 400 to 500 ng of DNA in an overnight incubation at 37C. These restriction enzymes cut the dsDNA at the sites where the TAAR1 gene was inserted into the expression vector pcDNA3.1/V5/His-TOPO (Invitrogen, Carlsbad, CA). The digested DNA was run on a 1% agarose gel with ethidium bromide to inspect for bands in a darkroom under ultraviolet light. The plasmid is about 6.5kb and the TAAR1 gene is about 1.5kb. If a 1.5kb band was present then the DNA was sequenced. DNA was submitted to a core facility for sequencing using the T7 forward primer and the BGH reverse primer and 25ng of the DNA. After the sequences were determined they were checked to see if both the forward and reverse primer sequences gave the expected mutation. Once the correct mutation sequence was confirmed, HEK293 wild type cells were transfected with the mutated DNA.

Transfection of HEK 293 WT cells with mutated plasmids

Stably transfected HEK293 cells with mutated DNA plasmids were established using the Fugene transfection reagent according to the manufacturers instructions. Briefly, using a 2:1 volume to weight ratio, for each well of cells that were transfected, 4 ul of Fugene transfection reagent was added directly into 100ul of

Optimem and 2ug of DNA was added. The solution was mixed by a gentle vortex for 1 second then incubated at room temperature for 15 minutes. The transfection solution was applied to HEK293 cells in 12 well plates and incubated overnight. After 16 to 18 hours the medium was changed to include G418 for selection since the plasmids with the TAAR1 inserts also had the Neomycin resistance gene. The cells were split 100:1 and grown in 10cm dishes with complete Dulbecco's modified Eagle's Meduim (DMEM) (Invitrogen), 10% fetal bovine serum, 1%Penstrep, plus 0.8% G418 and incubated 8 to 10 days until individual colonies grew that were visible without magnification. Cells were then picked from the center of individual colonies and plated into individual wells in a 24 well plate. This was repeated 6 times for each 10cm dish. The 24 well plates were incubated 3 to 5 days until cells covered the bottom of the well. These were then re-plated to tissue culture plates with larger wells such as a 6 well plate. These were incubated to expand the cells. Each well of the 6-well plate with cells was then expanded into a 10cm dish. These separate cell lines were maintained and used for evaluation assays to pick clones that gave a response to the HitHunter cAMP assay described below. Evaluation assays were tested for cAMP response, which was normalized to the maximal PEA response. No other methods were used to assess relative levels of receptor expression.

Tissue Culture and cAMP Binding Assay

Stably transfected HEK-293 cells expressing the wild type mouse and rat TAAR1 as well as the mutations to TM3, TM6, and TM7 for both species were grown and maintained as described previously (Reese et al. 2007). Briefly cells were grown to

approximately 80% confluence, rinsed and harvested in Krebs-Ringer-HEPES (KRH) buffer. Cells were re-suspended in KRH using 50ml conical tubes and pretreated for 20 minutes at 37 ^{o}C with 200μM IBMX, a phosphodiesterase inhibitor in order to prevent the breakdown of cAMP.

The IBMX pretreated cells were gently mixed to be homogenously distributed and 200ul were added to 100ul of pre-warmed KRH containing 3ul of drug that was added at 100x final concentration. Drugs that were applied included PEA, both isomers of amphetamine and both isomers of methamphetamine. Cells and drugs were mixed gently then incubated for 1 hour at 37^{o}C in a water bath. Cells were then lysed by treatment with 100ul of 0.5mM sodium acetate and incubated for 20 minutes at 100 ^{o}C. Cell lysate debris was pelleted by centrifugation and 200ul of supernatant were transferred to labeled microfuge tubes. Samples were typically frozen at this step to allow completion of the assay on another day using the DiscoveRx HitHunter CyclicAMP XS EFC Chemiluminescent Detection kit (Amersham Bioxcience, UK).

This assay is based on complementation of the β-galactosidase enzyme to hydrolyze detectible chemiluminescent substrates. The functional βGal enzyme is made from combined fragments, a technique referred to as enzyme fragment complementation (EFC). Removal of 50 amino acid residues from the amino terminus of βGal produces an inactive enzyme called the enzyme acceptors (EA) (Olson and Eglen, 2007). The missing amino terminal residues are supplied separately and are referred to as the enzyme donors or (ED). When the EA and ED fragments are combined the catalytic activity of the enzyme is restored. The ED peptide is conjugated to cAMP. Thawed cell supernatant from the concentration response

protocol described above were transferred into wells of a white, 96-well Optiplate. A cAMP antibody was added to the thawed cell supernatant, mixed on a plate shaker, and incubated in the dark for 1hr at room temperature. The enzyme donor conjugated to cAMP, ED, was added to the wells, shaken, and incubated for an hour. If there was no cAMP produced in response to very low concentrations of agonists, then the ED-cAMP reacts with the cAMP antibody. As a result the ED is not able to interact with the EA due to steric hindrance and no substrate is hydrolyzed and no chemiluminescence is generated. If cAMP was produced in response to applied agonists then free cAMP from the cell lysate binds to the cAMP antibody competing with the ED-cAMP conjugate. More ED-cAMP is therefore available to complement the EA, thus forming an active enzyme that cleaves a galactoside moiety from the substrate Galacton-Star (Bronstein et al., 1989).

After the addition of a solution containing the EA portion of the enzyme, Galacton Star chemiluminescent substrate and Emerald II luminescent enhancer, the plates were again shaken for 2 minutes on a Titer Plate Shaker at speed setting 3, then covered and incubated in the dark at room temperature overnight for 15 hours. The plates were then read for chemiluminescence on the Fusion Universal Microplate Analyzer (Packard BioScience Company, Meriden, Connecticut).

Data was adjusted for background. Background levels for cells treated with no drug were subtracted from readings and the data at each concentration of applied drug was normalized to PEA with the maximum level of PEA response representing 100%. These calculations were done with Excel (Microsoft, Redmond Wal). Data values were copied into Prism (Graph Pad Software Inc., San Diego, CA.). Non-linear

sigmoidal curves were fitted to the data, EC50 values were calculated, and concentration-response curves were plotted.

The drugs PEA, or the S-(+) or R-(-) enantiomers of AMPH or METH were applied to cells expressing the wild type rat and mouse TAAR1. Identical experiments were separately conducted using the mutants to TM3, TM6, and TM7 transmembrane domains to both the rat and mouse TAAR1s. For any given experiment, all cells were harvested from the same tissue culture and the reactions were carried out using the same preparation of Krebs-Ringer-Hepes (KRH) buffer for all drugs. Experiments were repeated a minimum of three times.

Drug Compounds

The S(+) and R(-)-amphetamine sulfate and the S-(+)- and R-(-)-methamphetamine were purchased from Sigma-Aldrich (St. Louis, MO.). Drugs were dissolved in water and diluted to 100x final concentration and were stored at –20 ^{o}C. Before each experiment, the drugs were thawed and vortexed.

Statistical Analysis

Data analysis was performed with Excel spreadsheets and the Prism statistical analysis program. After experiments were repeated 3 or more times, the normalized cAMP induced luminescence response data from each experiment was entered into Excel and the average and SEM for each concentration for each drug was calculated. These calculations were copied into Prism to be analyzed using a non-linear sigmoidal curve fit with the Hill coefficient unrestrained rather than fixed. EC_{50} values with 95% confidence levels were calculated by the software.

Differences between treatments were tested for significance using the two-tailed t test. Comparisons made between responses to a drug applied to a given mutant and the wild type TAAR1 were also tested using the two-tailed t test. Differences were considered significant when *, $p<0.05$; **, $p<0.01$; and ***, $p<0.0001$.

Results

Sequence alignment of the rat, mouse, and human TAAR1 receptors to the human β_2 adrenergic receptor ($h\beta_2AR$) is shown in Figure 1. The TM3 aspartate D3.32 (D113) in the $h\beta_2AR$ is conserved across across biogenic amine receptors including the TAARs. The asparagine N6.55 (N293) in TM6 was found to be involved in ligand binding to the β–OH of norepinephrine (Swaminath et al., 2005). The site corresponding to the $h\beta_2AR$ N6.55 (N293) in the rat TAAR1 receptor has a methionine at this site, M6.55 (M268), while the mouse TAAR1 has a threonine, T6.55 (T268), at this location.

The $h\beta_2AR$ TM7 has an asparagine at N7.39 (N312), a site reported to be involved in high affinity binding of aryloxyalkylamines (compounds with an ether oxygen atom that links an amino side chain to an aromatic ring) in the β_2AR as well as the 5-HT_{1a} receptors (Guan et al., 1992; Suryanarayana and Kobilka, 1993). Again, the mouse and rat receptors have different amino acids at this site. The rat TAAR1 has a N7.39 (N287) while the mouse sequence has a Y7.39 (Y287) at this site.

The conserved aspartate in TM3 is D3.32 (D102) for both the rat and mouse TAAR1s. The mutation of this aspartate to an alanine, D3.32A (D102A), for the rat and mouse TAAR1 resulted in levels of cAMP that did not vary significantly over the

background level across the entire concentration range of the applied drugs (data not shown).

cAMP response to PEA

The cAMP response to PEA for the wild type rat and mouse TAAR1 receptors showed a higher potency for the rat WT (rWT) with an EC_{50} of 40nM compared to the mouse WT (mWT) receptor which had an EC_{50} of 189nM (Table 1, Figure 2a). The mutations to the rat TAAR1 transmembranes six and seven, M6.55T (M268T) (rTM6) and N7.39Y (N287Y) (rTM7) each caused a shift of the concentration response curve to the right compared to the rWT (Figure 3a, 3c). For the mouse transmembrane six mutation, T6.55M (T268M) (mTM6), and the mouse TM seven mutation, Y7.39N (Y287N) (mTM7), each shifted the concentration-response curves to the left compared to the mWT curve (Figure 3b,3d) which made them similar to the rWT response to PEA.

Both the TM6 and the TM7 mutations caused the response of the mutant rat (mouse) TAAR1 to PEA to resemble the response of the wild type mouse (rat) TAAR1. The difference in the EC_{50} values of the rWT and mWT TAAR1 vs. PEA was unexpected because the results from chapter 2 (chapter 2 Figure 2a) showed an overlapping response for the two species. The difference is possibly due to sensitivity differences between the assays used in the two studies. The Hit Hunter assay was adopted for this study because the vendor for the [^{3}H]cAMP assay employed in the first study discontinued supplying the reagents used in their kit.

Species-dependent stereoselectivity of rat vs. mouse

The results for the rWT and mWT TAAR1 cAMP response to S(+) and R(-) AMPH are shown in Figure 2b and 2c. These results were acquired using a cAMP assay as described in the methods sections. The results are similar to the results of chapter 2. Both studies showed the S(+)AMPH EC_{50} at the WT mTAAR1 was about an order of magnitude lower than for R(-) AMPH (Table 1). The amphetamine concentration-response results for rWT TAAR1 for the two studies were also similar since both had EC_{50}s for the S(+) and R(-) enantiomers of AMPH that were nearly equal. For both the rat and mouse wild type TAAR1 receptors, the rank-order of potency for the compounds tested were the same as in the prior study.

The results for the cAMP response to S(+) and R(-) METH at the rWT and mWT TAAR1 are shown in Figure 2d and 2e. These results are also similar to the results from Chapter 2 (Chapter 2, Figure 3d and 3e). The S(+) isomer of METH had a slightly lower EC_{50} and a slightly higher efficacy compared to R(-) METH for the rWT TAAR1. The mWT TAAR1 concentration-response curves to the enantiomers of METH are like the responses to AMPH since both isomers are equally efficatious while the S(+) isomer has a lower EC_{50}.

For the rat TM6 mutant the 214nM value for the EC_{50} of R(-)AMPH was actually less than the 677nM EC_{50} for the S(+) isomer and the difference was statistically significant (Table 1). In contrast, the mouse TM6 mutant EC_{50} for the S(+)AMPH, 4nM, was over an order of magnitude less than the 121nM EC_{50} for R(-)AMPH. The relative position of the response curves to AMPH for the TM6 mutants for the rat and mouse (Figure 4a, 4b) were the same as for the wild types (Figure 2b, 2c) while the

EC_{50}s for both S(+) and R(-)AMPH for the mouse TM6 were shifted significantly to the left compared to the mWT (Figures 4d, 4f and Table 1).

For the rat TM6 mutant the EC_{50} of R(-)METH, 1109nM, was less than the EC_{50} for S(+)METH, 2044nM, but the difference was not statistically significant (Table 1). For rat TAAR1 the EC_{50}s for the S(+) and R(-) isomers of METH at the rTM6 were about 15 fold and 5 fold higher, respectively, than for the EC_{50}s for rWT (Table 1). For the mouse TM6 the EC_{50}s for S(+) and R(-)METH were reduced by about 15 fold and 7 fold, respectively, compared to the EC_{50}s for the mWT TAAR1 (Table 1). Thus, the concentration-response curves for the TM6 mutants treated with methamphetamine (Figure 5) displayed the same relative position as the amphetamine response curves (Figure 4) for both rat and mouse.

TM7 mutations

The 14nM EC_{50} of S(+)AMPH for the rat TM7 mutant was significantly less than the EC_{50} of 170nM for the R(-) isomer (Figure 6a, Table 1). In contrast, the mouse TM7 mutant EC_{50} of 104nM for the R(-)AMPH was significantly ($p<0.001$) less than the 219nM EC_{50} of S(+)AMPH (Figure 6b and Table 1). Comparison of Figures 6a and 6b to Figures 2b and 2c clearly shows a reversal of the species-dependent stereoselectivity that was demonstrated by the wild type receptors.

For S(+)AMPH the rat TM7 mutant response was shifted to the left compared to the WT response while for R(-)AMPH the response was shifted significantly to the right (Figure 6c, 6e, and Table 1). Opposite shifts were seen in a comparison of the cAMP response for the mWT and mTM7 mutant to the enantiomers of amphetamine

(Figure 6d, 6f and Figure 2b,2c). The mTM7 concentration-response curve was shifted to the right compared to the mWT for S(+)AMPH while the mTM7 response for R(-)AMPH was significantly shifted to the left compared to the mWT. For the rat TM7 mutation, N7.39Y, the concentration-response curves for S(+) and R(-)METH were not shifted compared to the curves for rWT (Figure 7c, 7e). For the mouse TM7 mutation, Y7.39N, both S(+) and R(-) METH concentration response curves were shifted to the right compared to the corresponding curves for mWT TAAR1 (Figure 7d, 7f).

Rank order of potency

The rank order of potency for the rWT TAAR1 was R(-)METH < S(+)METH < S(+)AMPH < PEA < R(-)AMPH and the rank order of potency for the mWT TAAR1 was R(-)METH < R(-)AMPH < S(+)METH < PEA < S(+)AMPH (Table 1). For the rWT R(-)AMPH had the lowest EC_{50} of 34nM while for the mWT S(+) AMPH had the lowest EC_{50}, 85nM (Table 1). For the TM6 mutants the most potent of the compounds tested were again R(-)AMPH for the rTM6 with an EC_{50} of 214nM and S(+)AMPH for the mTM6 with an EC_{50} of just 4nM. The rank order of rTM6 was the same as that for rWT when the 95%CI s are taken into account. The actual EC_{50}s for the rTM6 are about an order of magnitude higher than for the corresponding rWT responses.

For rTM7 the most potent compound was S(+)AMPH with an EC_{50} of 14nM and for mTM7 PEA was the most potent with an EC_{50} of 59nM. For mTM6 the EC_{50} for each drug was significantly lower compared to the corresponding EC_{50}s of the mWT.

The rank order for the mWT and mTM6 were also the same, again when the 95%CIs are taken into account (Table 1). In contrast, the order of potency to the enantiomers of AMPH was reversed for both the rat and mouse TM7 mutants compared to the order of the wild type for both species. Surprisingly, the mouse TM7 mutant had an EC_{50} that was very significantly lower for the R(-) enantiomer of AMPH compared to the S(+) enantiomer. This was a reversal of potency stereoselectivity compared to the mWT.

Figure 1. Sequences of the transmembrane domains for rat, mouse, and human TAAR1 aligned to the human β_2 adrenergic receptor transmembrane domains. The amino acid sequences of the seven transmembrane domains of the receptors are shown without the connecting loops or terminal tails. Residues conserved across all

four receptors are highlighted in yellow. The sites selected for mutations in TM3, TM6 and TM7 are outlined in red.

Figure 1.

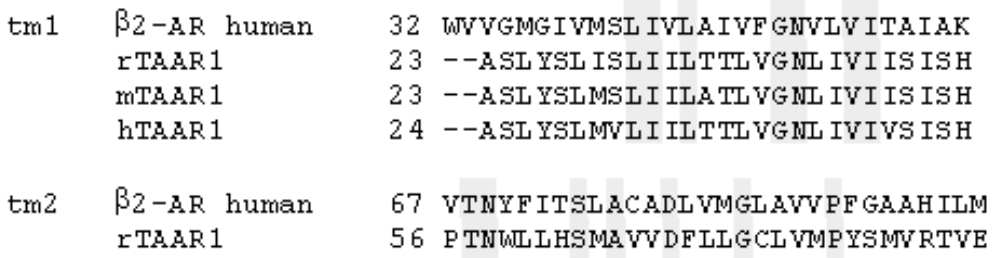

Figure 2. cAMP accumulation in response to β-phenylethylamine (PEA), AMPH, and METH for the rat and mouse wild type TAAR1The cAMP response curves are shown for

(a) rat wild type TAAR1 (rWT) in response to PEA (●) and to mouse wild type TAAR1 (mWT) in response to PEA (▲);

(b) rat wild type TAAR1 (rWT) in response to S(+)AMPH (●) and rWT in response to R(-)AMPH (O);

(c) mouse wild type TAAR1 (mWT) in response to S(+)AMPH (▲) and mWT in response to R(-)AMPH (△);

(d) rat wild type TAAR1 (rWT) in response to S(+)METH (●) and rWT in response to R(-)METH (O); and

(e) mouse wild type TAAR1 (mWT) in response to S(+)METH (▲) and mWT in response to R(-)METH (△).

Data are presented as a percentage of the maximal cAMP produced in response to PEA. Data shown are the mean ± S.E.M. from at least three experiments performed in duplicate. Concentrations of applied drug compounds along the X-axis are given in units of log M where M is molarity. Cells stably expressing the empty expression vector and selected by G418 produced no cAMP accumulation in response to drug treatments beyond the endogenous background level.

Figure 2.

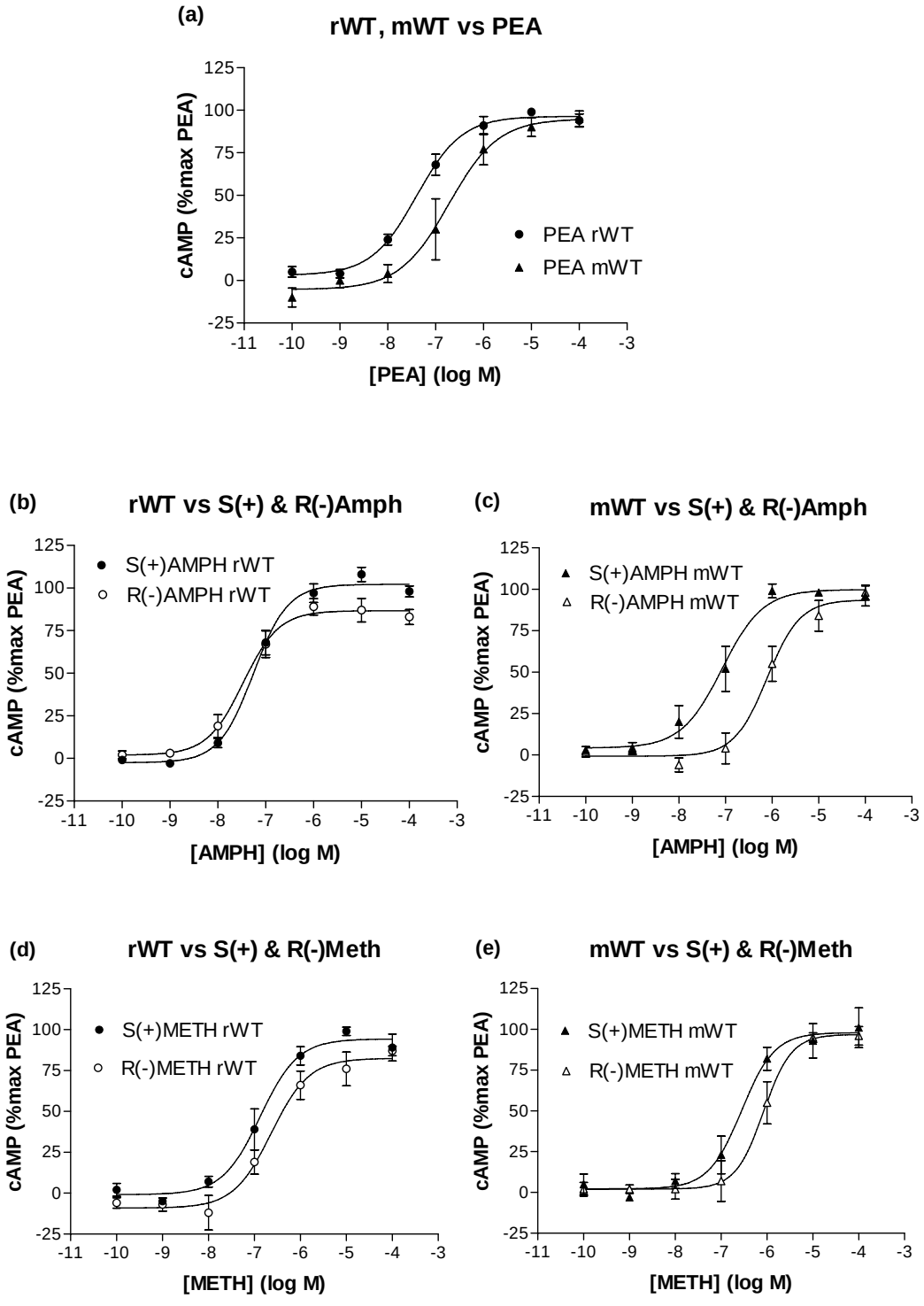
(a)
rWT, mWT vs PEA
cAMP (%max PEA)
[PEA] (log M)
PEA rWT
PEA mWT
(b)
rWT vs S(+) & R(-)Amph
S(+)AMPH rWT
R(-)AMPH rWT
[AMPH] (log M)
(c)
mWT vs S(+) & R(-)Amph
S(+)AMPH mWT
R(-)AMPH mWT
[AMPH] (log M)
(d)
rWT vs S(+) & R(-)Meth
S(+)METH rWT
R(-)METH rWT
[METH] (log M)
(e)
mWT vs S(+) & R(-)Meth
S(+)METH mWT
R(-)METH mWT
[METH] (log M)

Figure 3. Concentration-dependent stimulation of cAMP accumulation in response to PEA for rat and mouse wild type TAAR1 receptors and receptors with a mutation to TM6 or TM7. The cAMP response curves are for

(a) the wild type rat TAAR1 (rWT) (●) and rat TAAR1 TM6 mutation M6.55T (rTM6) (■);

(b) wild type mouse TAAR1 (mWT) (▲) and mouse TAAR1 TM6 mutation T6.55M (mTM6) (▼);

(c) rWT and rat TAAR1 transmembrane 7 mutation N7.39Y (rTM7) (□); and

(d) mWT and mouse TAAR1 transmembrane 7 mutation Y7.39N (mTM7) (▽), all vs. PEA.

Data are presented as a percentage of the maximal cAMP produced in response to PEA. Data shown are the mean ± S.E.M. from at least three experiments performed in duplicate. Concentrations of applied drug compounds along the X-axis are given in units of log M where M is molarity. Cells stably expressing the empty expression vector and selected by G418 produced no cAMP accumulation in response to drug treatments beyond the endogenous background level.

Figure 3.

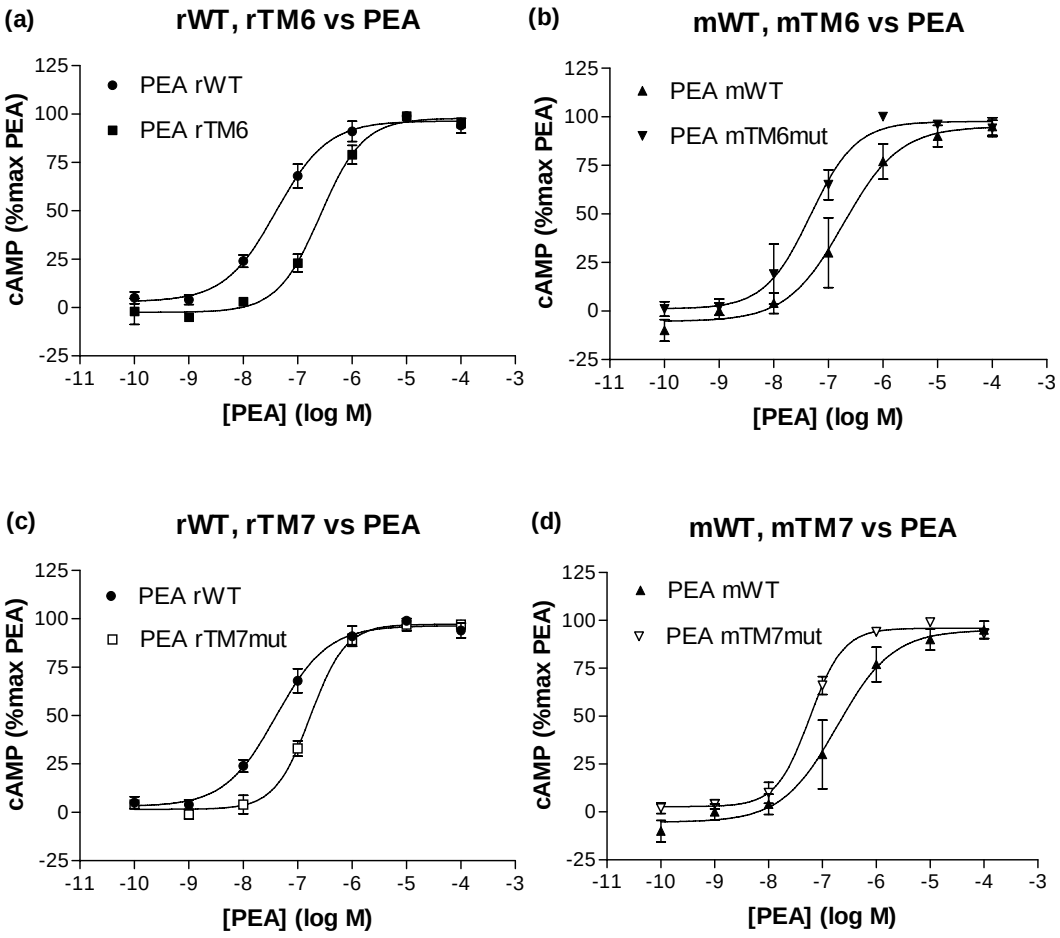
(a)
rWT, rTM6 vs PEA
PEA rWT
PEA rTM6
cAMP (%max PEA)
[PEA] (log M)
(b)
mWT, mTM6 vs PEA
PEA mWT
PEA mTM6mut
cAMP (%max PEA)
[PEA] (log M)
(c)
rWT, rTM7 vs PEA
PEA rWT
PEA rTM7mut
cAMP (%max PEA)
[PEA] (log M)
(d)
mWT, mTM7 vs PEA
PEA mWT
PEA mTM7mut
cAMP (%max PEA)
[PEA] (log M)

Figure 4. Rat and mouse TAAR1 cAMP response to amphetamine for wild type receptors and receptors with a mutation in TM6. The cAMP response curves are shown for

(a) rat TAAR1 with mutation to TM6 M6.55T (rTM6) in response to S(+)AMPH (■) and to rTM6 in response to R(-)AMPH (□);

(b) mouse TAAR1 with mutation to TM6 T6.55M (mTM6) in response to S(+)AMPH (▼) and mTM6 in response to R(-)AMPH (▽);

(c) rat wild type TAAR1 (rWT) in response to S(+)AMPH (●) and rTM6 M6.55T in response to S(+)AMPH (■);

(d) mouse wild type TAAR1 (mWT) in response to S(+)AMPH (▲) and mTM6 T6.55M in response to S(+)AMPH (▼);

(e) rWT in response to R(-)AMPH (O) and rTM6 M6.55T in response to R(-)AMPH (□); and

(f) mWT in response to R(-)AMPH (△) and mTM6 T6.55M in response to R(-)AMPH (▽).

Data are presented as a percentage of the maximal cAMP produced in response to PEA. Data shown are the mean ± S.E.M. from at least three experiments performed in duplicate. Concentrations of applied drug compounds along the X-axis are given in units of log M where M is molarity. Cells stably expressing the empty expression vector and selected by G418 produced no cAMP accumulation in response to drug treatments beyond the endogenous background level.

Figure 4.

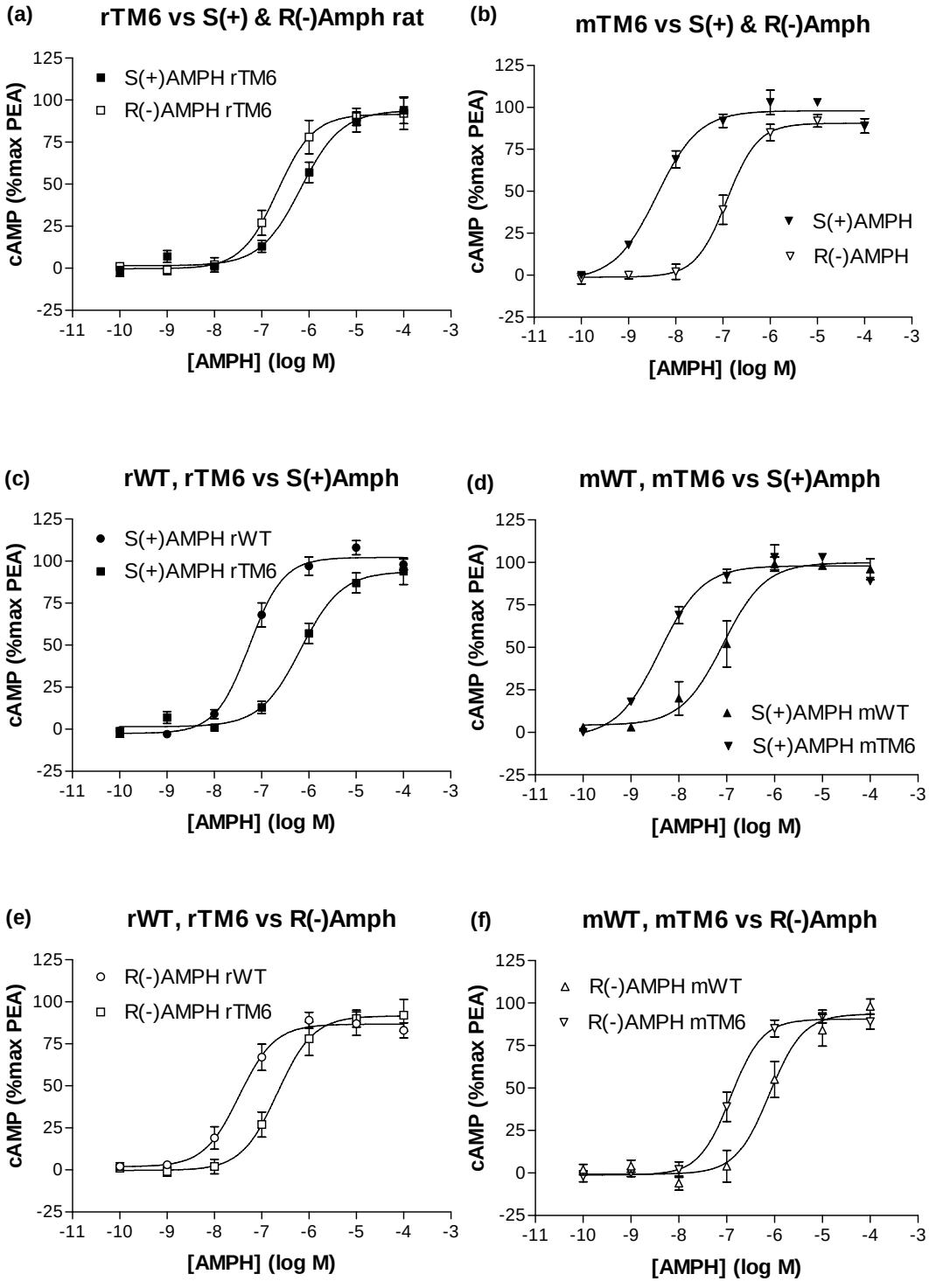
(a)
rTM6 vs S(+) & R(-)Amph rat
S(+)AMPH rTM6
R(-)AMPH rTM6
cAMP (%max PEA)
[AMPH] (log M)
(b)
mTM6 vs S(+) & R(-)Amph
S(+)AMPH
R(-)AMPH
cAMP (%max PEA)
[AMPH] (log M)
(c)
rWT, rTM6 vs S(+)Amph
S(+)AMPH rWT
S(+)AMPH rTM6
cAMP (%max PEA)
[AMPH] (log M)
(d)
mWT, mTM6 vs S(+)Amph
S(+)AMPH mWT
S(+)AMPH mTM6
cAMP (%max PEA)
[AMPH] (log M)
(e)
rWT, rTM6 vs R(-)Amph
R(-)AMPH rWT
R(-)AMPH rTM6
cAMP (%max PEA)
[AMPH] (log M)
(f)
mWT, mTM6 vs R(-)Amph
R(-)AMPH mWT
R(-)AMPH mTM6
cAMP (%max PEA)
[AMPH] (log M)

Figure 5. Rat and mouse TAAR1 cAMP accumulation response to methamphetamine for wild type receptors and for receptors with a mutation in TM6. Concentration response curves are shown for

(a) rat TAAR1 with mutation to TM6 M6.55T (rTM6) in response to S(+)METH (■), and R(-) METH (□);

(b) mouse TAAR1 with mutation to TM6 T6.55M (mTM6) in response to S(+)METH (▼) and to R(-)METH (▽);

(c) rat wild type TAAR1 (rWT) in response to S(+)METH (●) and rTM6 M6.55T in response to S(+)METH (■);

(d) mouse wild type TAAR1 (mWT) in response to S(+)METH (▲) and mTM6 T6.55M in response to S(+)METH (▼);

(e) rWT in response to R(-)METH (O) and rTM6 M6.55T in response to R(-)METH (□); and

(f) mWT in response to R(-)METH (△) and mTM6 T6.55M in response to R(-)METH (▽).

Data are presented as a percentage of the maximal cAMP produced in response to PEA. Data shown are the mean ± S.E.M. from at least three experiments performed in duplicate. Concentrations of applied drug compounds along the X-axis are given in units of log M where M is molarity. Cells stably expressing the empty expression vector and selected by G418 produced no cAMP accumulation in response to drug treatments beyond the endogenous background level.

Figure 5.

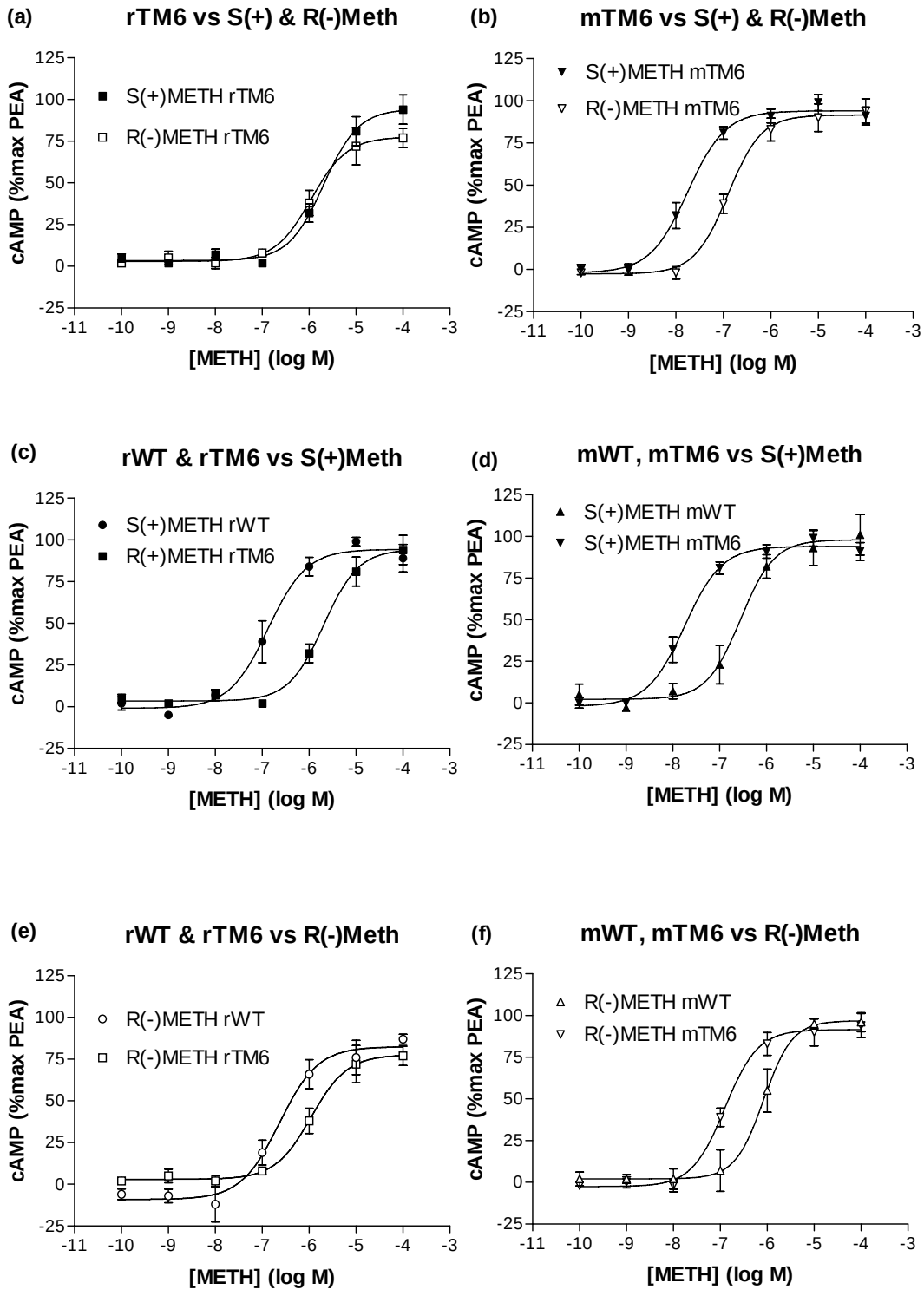
(a)
rTM6 vs S(+) & R(-)Meth
S(+)METH rTM6
R(-)METH rTM6
cAMP (%max PEA)
[METH] (log M)
(b)
mTM6 vs S(+) & R(-)Meth
S(+)METH mTM6
R(-)METH mTM6
cAMP (%max PEA)
[METH] (log M)
(c)
rWT & rTM6 vs S(+)Meth
S(+)METH rWT
R(+)METH rTM6
cAMP (%max PEA)
[METH] (log M)
(d)
mWT, mTM6 vs S(+)Meth
S(+)METH mWT
S(+)METH mTM6
cAMP (%max PEA)
[METH] (log M)
(e)
rWT & rTM6 vs R(-)Meth
R(-)METH rWT
R(-)METH rTM6
cAMP (%max PEA)
[METH] (log M)
(f)
mWT, mTM6 vs R(-)Meth
R(-)METH mWT
R(-)METH mTM6
cAMP (%max PEA)
[METH] (log M)

Figure 6. Rat and mouse TAAR1 cAMP response to amphetamine for wild type receptors and receptors with a mutation in TM7. The cAMP response curves are shown for

(a) rat TAAR1 with mutation to TM7 N7.39Y (rTM7) in response to S(+)AMPH (■) and to R(-)AMPH (□);

(b) mouse TAAR1 with mutation to TM7 Y7.39N (mTM7) in response to S(+)AMPH (▼) and mTM7 in response to R(-)AMPH (▽);

(c) rat wild type TAAR1 (rWT) in response to S(+)AMPH (●) and rTM7 N7.39Y in response to S(+)AMPH (■);

(d) mouse wild type TAAR1 (mWT) in response to S(+)AMPH (▲) and mTM7 Y7.39Y in response to S(+)AMPH (▼);

(e) rWT in response to R(-)AMPH (O) and rTM7 N7.39Y in response to R(-)AMPH (□); and

(f) mWT in response to R(-)AMPH (△) and mTM7 Y7.39N in response to R(-)AMPH (▽).

Data are presented as a percentage of the maximal cAMP produced in response to PEA. Data shown are the mean ± S.E.M. from at least three experiments performed in duplicate. Concentrations of applied drug compounds along the X-axis are given in units of log M where M is molarity. Cells stably expressing the empty expression vector and selected by G418 produced no cAMP accumulation in response to drug treatments beyond the endogenous background level.

Figure 6.

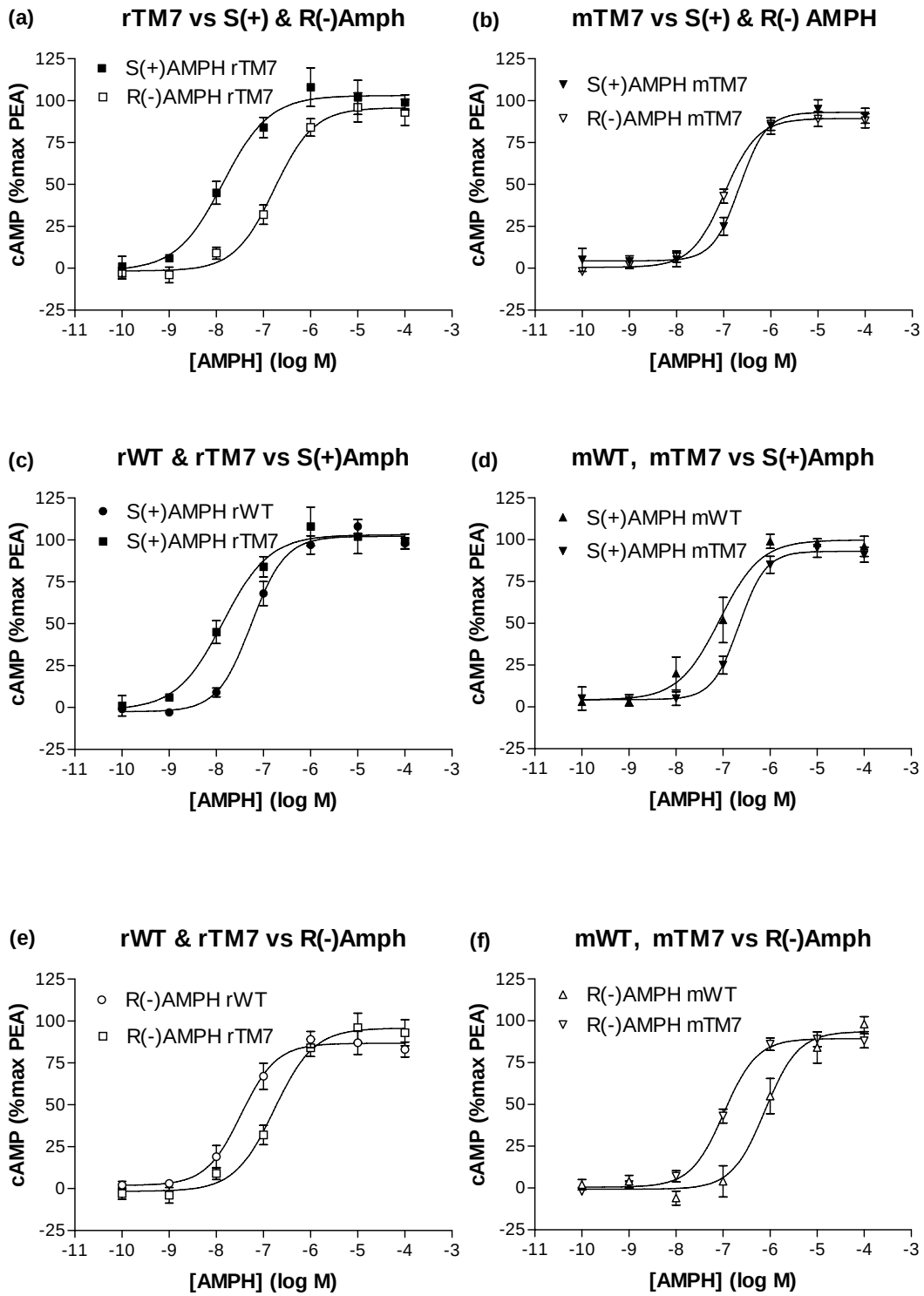
(a)
rTM7 vs S(+) & R(-)Amph
S(+)AMPH rTM7
R(-)AMPH rTM7
cAMP (%max PEA)
[AMPH] (log M)
(b)
mTM7 vs S(+) & R(-) AMPH
S(+)AMPH mTM7
R(-)AMPH mTM7
cAMP (%max PEA)
[AMPH] (log M)
(c)
rWT & rTM7 vs S(+)Amph
S(+)AMPH rWT
S(+)AMPH rTM7
cAMP (%max PEA)
[AMPH] (log M)
(d)
mWT, mTM7 vs S(+)Amph
S(+)AMPH mWT
S(+)AMPH mTM7
cAMP (%max PEA)
[AMPH] (log M)
(e)
rWT & rTM7 vs R(-)Amph
R(-)AMPH rWT
R(-)AMPH rTM7
cAMP (%max PEA)
[AMPH] (log M)
(f)
mWT, mTM7 vs R(-)Amph
R(-)AMPH mWT
R(-)AMPH mTM7
cAMP (%max PEA)
[AMPH] (log M)

Figure 7. Rat and mouse TAAR1 cAMP accumulation response to methamphetamine for wild type receptors and for receptors with a mutation in TM7. Concentration response curves are shown for

(a) rat TAAR1 with mutation to TM7 N7.39Y (rTM7) in response to S(+)METH (■), and R(-) METH (□);

(b) mouse TAAR1 with mutation to TM7 Y7.39N (mTM7) in response to S(+)METH (▼) and to R(-)METH (▽);

(c) rat wild type TAAR1 (rWT) in response to S(+)METH (●) and rTM7 N7.39Y in response to S(+)METH (■);

(d)) mouse wild type TAAR1 (mWT) in response to S(+)METH (▲) and mTM7 Y7.39N in response to S(+)METH (▼);

(e) rWT in response to R(-)METH (O) and rTM7 N7.39Y in response to R(-)METH (□); and

(f) mWT in response to R(-)METH (△) and mTM7 Y7.39N in response to R(-)METH (▽).

Data are presented as a percentage of the maximal cAMP produced in response to PEA. Data shown are the mean ± S.E.M. from at least three experiments performed in duplicate. Concentrations of applied drug compounds along the X-axis are given in units of log M where M is molarity. Cells stably expressing the empty expression vector and selected by G418 produced no cAMP accumulation in response to drug treatments beyond the endogenous background level.

Figure 7.

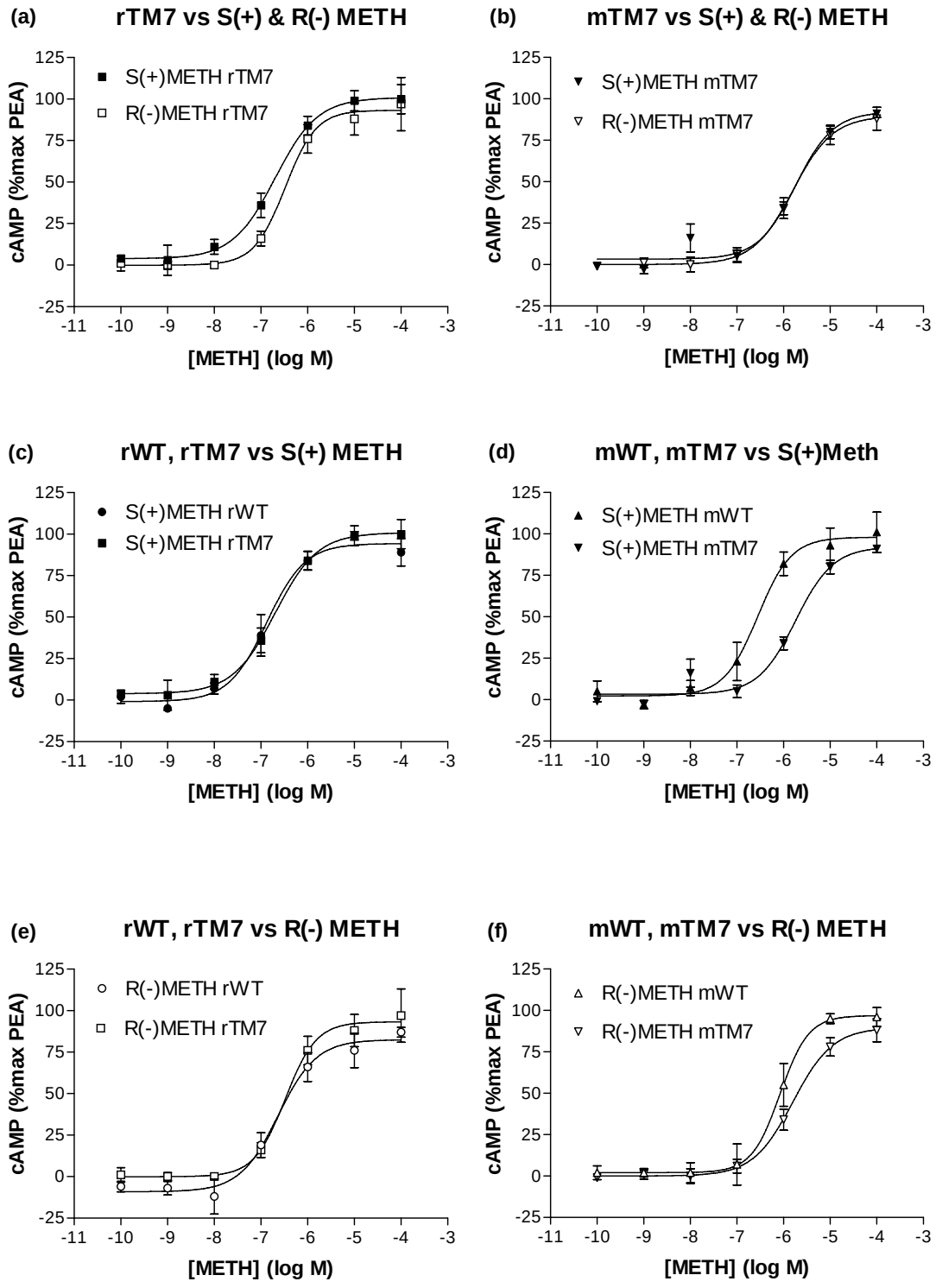
(a)
rTM7 vs S(+) & R(-) METH
S(+)METH rTM7
R(-)METH rTM7
cAMP (%max PEA)
[METH] (log M)
(b)
mTM7 vs S(+) & R(-) METH
S(+)METH mTM7
R(-)METH mTM7
cAMP (%max PEA)
[METH] (log M)
(c)
rWT, rTM7 vs S(+) METH
S(+)METH rWT
S(+)METH rTM7
cAMP (%max PEA)
[METH] (log M)
(d)
mWT, mTM7 vs S(+)Meth
S(+)METH mWT
S(+)METH mTM7
cAMP (%max PEA)
[METH] (log M)
(e)
rWT, rTM7 vs R(-) METH
R(-)METH rWT
R(-)METH rTM7
cAMP (%max PEA)
[METH] (log M)
(f)
mWT, mTM7 vs R(-) METH
R(-)METH mWT
R(-)METH mTM7
cAMP (%max PEA)
[METH] (log M)

Table 1.

Rank order of average EC_{50}[α] values for cAMP accumulation in HEK-293 cells stably expressing rTAAR1(rat WT), rat mutant M 6.55T (M268T) (rat TM6), rat mutant N7.39Y (N287Y) (rat TM7), or mTAAR1(mus WT), mouse TAAR1 mutant T6.55M (T268M) (mus TM6), or mouse mutant Y7.39Y (Y287N) (mus TM7) and exposed to the indicated monoamine compounds.

[α] The EC_{50} is measured from the concentration-response curves and is the concentration of the applied compound that results in a response equal to half of the saturated maximum response. *p* values relate to the comparison of values for enantiomeric pairs. Statistical significance is indicated as *, $p<0.05$; **, $p<0.01$; and ***, $p<0.001$.

Table 1.

	Rat WT				**Mus WT**			
Treatment	**EC_{50}**	**(95% CI)**	**Rank**	***p*-value**	**EC_{50}**	**(95% CI)**	**Rank**	***p*-value**
	(nM)		order		(nM)		order	
PEA	40.33	(24.6, 66.2)	2		189	(91.8, 389)	2	
S(+)AMPH	55.6	(30.6,101.3)	3	0.3243	84.6	(33, 217)	1	0.0393
R(-)AMPH	33.9	(19.5, 58.8)	1		785.5	(343, 1801)	4	*
S(+)METH	133.3	(59, 303)	4	0.443	278.9	(134, 580)	3	0.1908
R(-)METH	233.3	(91, 597)	5		843.3	(774, 918)	5	
	Rat TM6				**Mus TM6**			
Treatment	**EC_{50}**	**(95% CI)**	**Rank**	***p*-value**	**EC_{50}**	**(95% CI)**	**Rank**	***p*-value**
PEA	261.2	(161, 424)	2		47.3	(23, 97)	3	
S(+)AMPH	677.4	(359, 1279)	3	0.0349	3.98	(1.1, 14.3)	1	0.0385
R(-)AMPH	214.4	(182, 252)	1	*	121	(99.9,146.6)	4	*
S(+)METH	2044	(1100, 3777)	5	0.1736	17.81	(9.97, 31.8)	2	0.1069
R(-)METH	1109	(838, 1467)	4		125.5	(83.4, 188)	5	
	Rat TM7				**Mus TM7**			
Treatment	**EC_{50}**	**(95% CI)**	**Rank**	***p*-value**	**EC_{50}**	**(95% CI)**	**Rank**	***p*-value**
PEA	170.6	(127.4,228.3)	3		58.6	(40.6, 84.6)	1	
S(+)AMPH	13.9	(5.67, 34.1)	1	0.0258	218.8	(164, 292)	3	0.0004
R(-)AMPH	169.9	(86.5, 334)	2	*	104.5	(76.7,142.4)	2	***
S(+)METH	201.8	(156.8,259.7)	4	0.2463	1822	(370, 8979)	5	0.6597
R(-)METH	330.4	(197.8, 552)	5		1596	-13,041,953	4	

Table 2.

Efficacy [b] of trace amines, amphetamine, methamphetamine for cAMP accumulation in HEK-293 cells rTAAR1(rat WT), rat mutant M6.55T (M268T) (rat TM6), rat mutant N7.39Y (N287Y) (rat TM7), or mTAAR1(mus WT), mouse TAAR1 mutant T6.55M (T268M) (mus TM6), or mouse mutant Y7.39N (Y287N) (mus TM7) and exposed to the indicated monoamine compounds.

[b] The efficacy calculated here is the maximum saturated level of cAMP as a percent of PEA_{max} response of the concentration-response curves. The table entries are the calculated best-fit values of the top of the nonlinear sigmoidal curve used to model the dose response data. *p* values relate to the comparison of values for enantiomeric pairs. Statistical significance is indicated as *, $p<0.05$; **, $p<0.01$; and ***, $p<0.001$.

Table 2.

	Rat WT			**Mus WT**		
Treatment	**%PEA$_{max}$**	**(95% CI)**	***p* value**	**%PEA$_{max}$**	**(95% CI)**	***p* value**
PEA	96.44	(90.4, 102.5)		94.96	(83.3,106.6)	
S(+)AMPH	102.2	(93.1, 111.3)	0.0711	99.80	(85.6,114)	0.5025
R(-)AMPH	86.7	(80.4, 92.99)		93.58	(75.8,111.3)	
S(+)METH	94.33	(80.7, 107.9)	0.5142	98.01	(86.1,109.9)	0.9181
R(-)METH	82.48	(67.98,96.97)		96.87	(94.8,98.9)	
	Rat TM6			**Mus TM6**		
Treatment	**%PEA$_{max}$**	**(95% CI)**	***p* value**	**%PEA$_{max}$**	**(95% CI)**	***p* value**
PEA	97.83	(89.6, 106.0)		97.6	(88.1,107.1)	
S(+)AMPH	93.79	(82.1, 105.5)	0.8127	98.0	(85.9,110.1)	0.2421
R(-)AMPH	91.61	(89.1, 94.1)		90.55	(87.0,94.0)	
S(+)METH	94.31	(81.6, 107.0)	0.3560	94.04	(86.4,101.7)	0.8160
R(-)METH	77.59	(72.6, 82.6)		91.55	(84.3,98.8)	
	Rat TM7			**Mus TM7**		
Treatment	**%PEA$_{max}$**	**(95% CI)**	***p* value**	**%PEA$_{max}$**	**(95% CI)**	***p* value**
PEA	97.21	(92.3, 102.2)		95.94	(90.9,101.0)	
S(+)AMPH	103.1	(91.8, 114.3)	0.5243	93.05	(88.9,97.2)	0.9344
R(-)AMPH	95.77	(84.6, 106.9)		89.37	(84.1,94.6)	
S(+)METH	100.9	(96.8, 104.9)	0.5904	92.22	(59.6,124.8)	0.8868
R(-)METH	93.28	(85.1, 101.4)		89.61	(85.5,93.8)	

Discussion

Several key amino acids of the human β_2 adrenergic receptor associated with ligand binding have been identified using mutagenesis. This study investigated the stereoselective binding of amphetamines to TAAR1 receptors based on the assumption that the TAAR1 receptors conform to the classic GPCR structure that consists of seven helical transmembrane domains connected by extracellular and intracellular loops with an extracellular N-terminus and an intracellular C-terminus. Early mutagenesis studies demonstrated that the transmembrane domains and not the hydrophilic intra- and extracellular regions of the βARs are involved with ligand binding (Dixon et al., 1987). Mutagenesis studies that substituted for the conserved aspartate D3.32 (D113) on TM3 of the β_2AR demonstrated a greatly reduced response to known agonists. This aspartate is conserved across biogenic amine receptors including dopamine and serotonin receptors (Strader et al., 1988; Huang, 2003).

In this study, site directed mutagenesis of the conserved Asp in TM3 to an alanine, D3.32A (D102A), for both the rat and the mouse TAAR1 also resulted in a knockdown of cAMP response. This conserved aspartate site in TAAR1s most likely plays the same proposed ligand binding role as in other catecholamine receptors by forming a salt bridge between the amine of the ligand and the oxygen of the carboxylate of the aspartate side chain (Freddolino et al., 2004).

Mutations to TM7 of the rat and mouse TAAR1 receptors resulted in a reversal of stereoselectivity in both the potency and efficacy that were demonstrated by the wild

type receptors to enantiomers of amphetamine and methamphetamine. The TM7 site selected for mutation was homologous to the N7.39 (N312) of the β_2AR, which had been shown to be involved in ligand binding to aryloxyalkylamines (Suryanarayana and Kobilka, 1993). The rat and mouse sequences have different residues at the corresponding site. The mouse amino acid tyrosine was substituted into the rat sequence replacing asparagine, and conversely, the rat residue asparagine at this site replaced tyrosine in the mouse sequence. The response of the rat mutant (rTM7) with this substitution displayed a large separation of the S(+) and R(-)AMPH induced cAMP response curves which resembled the characteristic response of the mWT TAAR1 but was unlike the rWT TAAR1. Also, the response of the mouse TM7 mutant (mTM7), showed a reversal since the R(-) enantiomer of AMPH showed a lower EC_{50} (i.e. higher potency) than the S(+)AMPH. This response resembled that for the rWT and was unlike the mWT. These changes were due to shifts of the concentration response curves for the mutants compared to the wild type responses. Compared to the rWT, the rTM7 mutant EC_{50} for S(+)AMPH decreased and the EC_{50} for R(-)AMPH increased, thus creating the difference in potency and the stereoselectivity of the rTM7 mutant. This effect was reversed for the mouse TAAR1 TM7 mutant where the EC_{50} for S(+)AMPH was increased compared to the mWT while the EC_{50} for R(-)AMPH was decreased compared to the mWT, thus narrowing and actually reversing the stereoselectivity displayed by the wild type mouse TAAR1.

The stereoselectivity of efficacy to enantiomers to AMPH was demonstrated. S(+)AMPH was a full agonist while R(-)AMPH was a partial agonist at the rWT TAAR1. The term partial agonist is used to describe saturated responses less than

95% of the maximal activation due to a full agonist such as PEA for TAAR1s. For the mutants to the rat TM6 and TM7 the concentration response curves saturated for both enantiomers of AMPH. For rat TM7, but not TM6, R(-) AMPH became a full agonist with greater than a 95% response of the saturated maximum PEA level. For the mouse mutants mTM6 and mTM7, the 95% CIs for S(+)- and R(-)-AMPH overlap. Further, the 95% CI of S(+)- and R(-)-AMPH for both mTM6 and mTM7 overlap with the 95%CI for these isomers for the mWT TAAR1. These results suggest that there is no statistically significant difference in efficacy for the two isomers of AMPH at mTAAR1.

Mutations to TM6 were based on findings that a conserved asparagine, N6.55 (N293), of the hβ_2AR is known to have a role in binding epinephrine via hydrogen bonding to the alkyl hydroxyl group of epinephrine (Wieland et al., 1996; Swaminath et al., 2004). Examination of the sequence alignments showed that the rat and mouse TAAR1 had different residues at the site that corresponds to N6.55 (N293) of the hβ_2AR. The rat TAAR1 sequence has a methionine at site M6.55 (M268) and the mouse TAAR1 has a threonine, T6.55 (T268). Since the hβ_2AR TM6 site N6.55 (N293) has a known role in interacting with ligands at this site and since the rat and mouse residues at this site were different, these sites were targeted for site-directed mutagenesis in an attempt to reverse the stereoselectivity of the receptors. The methionine of the rat TAAR1 was changed to the threonine found in the mouse sequence, M6.55T (M268T). This mutation was also defined as rTM6. The threonine of the mouse sequence was changed to the methionine of the rat sequence, T6.55M (T268M). This was also defined as mTM6.

The rat and mouse TM6 mutations for TAAR1 had opposite effects on potency compared to their WT receptors. The rTM6 mutation, M6.55T (M268T), resulted in a decrease in potency, as shown by a shift to the right of the cAMP concentration-response curves for both S(+) and R(-) AMPH and for both S(+) and R(-)METH. On the other hand, the mouse TM6 mutation, T6.55M (T268M), had an increase in potency for both enantiomers of AMPH and METH compared to the mWT TAAR1 as evidenced by a shift to the left of the cAMP response curve. For example, the reduction in EC_{50} for (S+)AMPH for the mTM6 mutation was about 20-fold compared to the mWT TAAR1 response.

For the WT receptors the EC_{50} of the cAMP accumulation in response to S(+)AMPH was approximately the same for the rat (56nM) and mouse TAAR1 (85nM). The mouse TM6 mutant had about a 170 fold lower EC_{50} (4nM) compared to that for the rTM6 mutant (677nM) in response to S(+)AMPH. For the mTM6 the most potent drug applied was S(+)AMPH while for rTM6 it was R(-)AMPH. For the WT receptors the rat WT EC_{50} (34nM) was over twenty fold lower than for the mWT EC_{50} (785nM) for R(-)AMPH while for the TM6 mutants the EC_{50} for rTM6 (214nM) was about 2 fold greater than for the mTM6 EC_{50} (121nM) for R(-)AMPH.

These results suggest that the TM6 mutants affected the EC_{50}s differently for the rat and mouse, but the rank order of potency for the enantiomers of AMPH was not changed from that for the wild types. For the TM6 mutants, the response to both isomers of amphetamine was shifted from the WT in the same direction. For the rat TAAR1 the response of the TM6 mutant was shifted to the right compared to rWT for both S(+) and R(-) AMPH (Figure 4c, 4e) while for the mouse TAAR1 the TM6

response was shifted to the left from the WT response for both enantiomers of AMPH. These results show that the mutations to TM6 affected the potency.

These results also revealed that the mutation of a single amino acid likely involved in ligand binding at a GPCR can increase or decrease the EC_{50} of the second messenger response by an order of magnitude compared to the WT receptor. An example is the 18nM EC_{50} of the mTM6 for S(+)METH compared to the 279nM EC_{50} of the mWT. Based on this assay the EC_{50} for S(+)METH at the mouse WT TAAR1 was about 280nM. The mutation to TM6 of the mouse TAAR1 resulted in an EC_{50} to stimulation by S(+)AMPH of less than 4nM.

The combined results suggest that a single amino acid in TM7 is responsible for the species dependent stereoselectivity displayed by the rat and mouse TAAR1 receptors to the enantiomers of amphetamine. The mutation of just a single amino acid can cause the response of a GPCR to look like that of another species. Both TM6 and TM7 contain amino acids that affect the stimulated response of the receptors to ligand binding.

The function of TAAR1 and its endogenous ligand have not yet been identified. Here the wild type rat and mouse TAAR1 receptors have been potently stimuated by the psychostimulants AMPH and METH as well as by the endogenous trace amine PEA. It is interesting to speculate that the TAAR1 receptor could be potently activated *in vivo* by these psychostimulants and may contribute in some yet undetermined way to their effects. Future work with the hTAAR1 will be needed to explore this possible connection with the human response.

Chapter 4

Methamphetamine Activation of human Trace Amine-Associated Receptor 1 (hTAAR1)

Manuscript in Preparation

Abstract

Methamphetamine has been shown to activate the rat and mouse wild type (WT) trace amine-associated receptor 1 (TAAR1) *in vitro* (Bunzow et al., 2001). This work evaluated the *in vitro* response of WT hTAAR1 to the psychostimulants methamphetamine (METH) and amphetamine (AMPH). Due to difficulties in producing a stable cell line expressing the WT human TAAR1 (hTAAR1), a chimera TAAR1 consisting of the transmembrane domains with the human sequence and the rat sequence for the N and C terminal tails and third intracellular loop was constructed. The human chimera TAAR1 was shown to respond potently to these psychostimulants but this has not been demonstrated for the wild type hTAAR1. In this study, human embryonic kidney (HEK) 293 cells were transiently transfected with plasmids containing hTAAR1 and CRELuc, a luciferase reporter gene driven by a cAMP Response Element (CRE) promoter. The trace amine β phenylethylamine (PEA), both isomers of AMPH and METH, and the neurotransmitter dopamine (DA) were applied to HEK293 cells transiently transfected with hTAAR1. PEA and the amphetamines stimulated the expression of the CRE driven luciferase gene in a concentration-response fashion, but not in cells transfected with an empty vector. The dopamine-induced response was less potent compared to methamphetamine in stimulating CRE-driven transcription. These results imply that hTAAR1 is a novel target for methamphetamine and that methamphetamine stimulation of hTAAR1 activates downstream CRE-driven gene transcription *in vitro*.

Introduction

Methamphetamine abuse has reached epidemic proportions in many parts of the US (Research, 2005). There are no approved pharmacotherapies for methamphetamine abuse such as the use of methadone to treat heroin addiction. If some of methamphetamine's psychostimulative effects are mediated by hTAAR1 *in vivo* then this receptor may become a target for the development of novel therapeutics. The human trace amine-associated receptor 1 (hTAAR1) is a novel target for methamphetamine. Methamphetamine's psychostimulant capability is due to the increased release of the neurotransmitters dopamine and norepinephrine (NE) from presynaptic terminals. The known molecular mechanisms by which methamphetamine, amphetamine, and its congeners work include 1) uptake of amphetamine into the cell and the depletion of cytosolic DA by the reversal of the dopamine transporter (DAT), 2) inhibition of monoamine oxidase (MAO) B that normally breaks down biogenic amines, and 3) by acting as a substrate that displaces neurotransmitters (NT) from storage vesicles into the cytosol via the vesicular monoamine transporter 2 (VMAT2) (Sulzer et al., 2005) (Partilla et al., 2006). The DAT is a regulator of DA signaling so a modification of the redistribution of DAT from the cell surface plasma membrane of dopaminergic neurons would be expected to affect the duration and strength of DA signaling.

Trace amine receptors are G-protein coupled receptors (GPCRs) that are potently activated to stimulate cAMP accumulation in response to trace amines, neurotransmitters, and drugs including amphetamines (Borowsky et al., 2001; Bunzow et al., 2001; Lindemann et al., 2005). The mouse and rat TAAR1 can be

stably expressed in cell lines. Since hTAAR1 localizes primarily in the cytoplasm, presumably in vesicles, and has been difficult to express at the cell surface, a chimera was constructed. Borowsky et al. showed *in situ* hybridization histochemistry results that show TAAR1 from the mouse CNS localized in the cytoplasm (Borowsky et al., 2001) and Xie et al. showed cytoplasmic localization of TAAR1 in rhesus monkey dopaminergic neurons in the substantia nigra (Xie et al., 2007). The chimera was comprised of the seven transmembrane domains (7TM) from the human sequence and the N- and C- terminals as well as the third intracellular loop from the rat sequence. This human chimera TAAR1 (hCh TAAR1) was stably expressed and characterized along with the rat and mouse receptors as described in chapter 2 (Lindemann et al., 2005; Reese et al., 2007). The hCh TAAR1 is also potently activated by PEA and METH.

The physiological role for TAAR1 remains to be determined. TAAR1 was found in several regions of the rhesus monkey brain associated with monoaminergic neurons including the caudate nucleus, putamen, substantia nigra, nucleus accumbens, ventral tegmental area, raphe nucleus, and the amygdala (Xie et al., 2007). The localization of numerous TAARs, but not TAAR1, in rodent nasal epithelium was reported with results that suggest roles as odorant sensors (Liberles and Buck, 2006). A possible function for TAAR1 involves co-expression with DAT in dopaminergic neurons and modulation of the dopamine transporter. Work done with the Rhesus monkey TAAR1 expressed in HEK293 cells showed that co-expression with the human DAT increased the cAMP accumulation response of the monkey TAAR1 to methamphetamine (Miller et al., 2005; Xie and Miller, 2007).

However, it has not yet been demonstrated that methamphetamine activates the wild type human TAAR1 as well. The sequence homology between the rhesus monkey (*Macaca mulatto*) and the human TAAR1 is 96%.

This work explores whether methamphetamine induces hTAAR1 mediated transcription of a CRE-driven reporter gene. The general approach was to transiently transfect HEK293 cells with hTAAR1 along with CRELuc, a luciferase gene driven by a CRE promoter, and a β-Gal reporter gene, not driven by a CRE promoter. The reporter gene was used to normalize for expression and cell number. Transfected cells were then treated with METH, AMPH, and PEA, known agonists to the rat and mouse TAAR1. After incubation with varying concentrations of these drugs, cells were assayed for luminescence to quantify CRE-driven luciferase expression compared to non CRE-dependent beta-galactosidase expression in the cells.

Here I tested the hypothesis that methamphetamine activates hTAAR1 to increase cAMP accumulation which enables protein kinase A (PKA) second messenger signaling pathway. Chemiluminescence due to expression of the reporter gene CRELuc was expected to respond proportionally to the amount of hTAAR1 agonist applied. Increased cAMP causes PKA activation, separation, and translocation of the catalytic subunit to the nucleus to phosphorylate the cAMP response element (CRE) binding protein (CREB) at serine-133. Phosphorylated CREB binds as a dimer to the CRE of the promoter of target genes and also associates with CBP/P300 which assembles basal transcription factors to promote gene transcription (Gonzalez and Montminy, 1989; Mayr and Montminy, 2001). CREB has been implicated in long-term synaptic plasticity associated with both drug addiction (Carlezon et al., 2005;

Nestler and Carlezon, 2006) (McClung and Nestler, 2008) and mood and anxiety disorders (Nair and Vaidya, 2006; Zarate et al., 2006).

Here we report that PEA, METH, and AMPH concentration-dependently increased luminescence in HEK293 cells transiently transfected with hTAAR1, CRELuc, and β-gal, but not in cells transfected with the empty vector, CRELuc, and β-gal. These results suggest that METH along with PEA potently activate hTAAR1 mediated CRE-dependent transcription *in vitro*.

Methods and Materials

Tissue Culture and transient transfections

Wild type HEK293 cells were maintained at 37 ^{o}C in 5.1% CO_2 with Dulbeccos Modified Eagle's Medium (DMEM) (Invitrogen) supplemented with 10% fetal bovine serum and 1% PenStrep in 100mm dishes. When cells reached 80% confluency they were transfected with plasmids expressing 1) the hTAAR1 construct in pcDNA3.1TOPO, 2) CRELuc, a luciferase reporter gene driven by a CRE promoter, and 3) pCH110, a β-galactosidase gene used to normalize for expression and cell number. The DNA and Fugene 6 transfection reagent (Roche, Mannheim, Germany) were mixed in Opti-MEM (Invitrogen) or DMEM with no serum following the manufacturers directions. The maintainence medium was aspirated from the 100mm cell culture dish and replaced with the transfection solution. After cells were incubated at 37 ^{o}C in 5.1% CO_2 for five hours the transfection medium was removed and the cells were harvested with trypsin, pooled, then equally plated in 1ml aliquots

into 24 well plates with DMEM plus serum and incubated overnight. A single 100mm dish provided enough cells for plating two 24-well plates.

CRE Luciferase Assay

The following day drugs with a range of concentrations were mixed in DMEM with no serum or phenol red and added to the cells which were then incubated for an additional 18 hours. A shorter incubation time of 2 – 4 hours was attempted but there was little difference in response across a range of drug concentrations. Medium was aspirated from the wells and the cells were then lysed with Glo Lysis Buffer (Promega Corp., Madison, WI). The plates were put on a shaker for 20 – 30 minutes at room temperature to thoroughly lyse the cells. Then 50ul of lysate from each well of the 24-well plate was transferred into separate wells of a 96 well opaque white Optiplate-96 microplate (PerkinElmer, USA) and combined with 50ul of Steady Glo (Promega, Madison, WI) luciferase assay reagent containing a substrate for luciferase. A second 96- well plate was set up in parallel with each well containing 50ul of cell lysate and 50ul of Beta-Glo Assay System reagent (Promega, Madison, WI). The samples were covered to prevent exposure to light and incubated at room temperature for 30 minutes and then analyzed in a luminometer. The plates were read for chemiluminescence on the Fusion Universal Microplate Analyzer (Packard BioScience Company, Meriden, Connecticut).

Data analysis

Generation of the data involved averaging triplicate chemiluminescent readings for each drug and at each concentration taking the ratio of the CRE-luciferase average (S-Glo) to the beta galactosidase (B-Glo) average values. Background levels were determined from cells transfected with either hTAAR1 or EV, CRELuc, and β-gal but were mock treated in lieu of receiving any drug. Fold stimulation for each drug concentration was calculated by first normalizing the S-glo/B-glo ratio to the background ratio. Fold-increase data represented the ratio of the luciferase luminescence to the β-gal luminescence for a given concentration of applied drug relative to the ratio of luciferase to β-gal luminescence for the vehicle treated cells, which was defined to be equal to one. Data from replicated experiments were combined in an Excel spreadsheet (Microsoft Corp., Redmond WA) and the average values of the ratio of the S-Glo/B-Glo and the S.E.M. were calculated for each concentration of applied drug. The data was graphed using Prism data analysis software (Graph Pad Software Inc., San Diego, CA.). The concentration-response data was modeled using nonlinear regression sigmoidal curve fitting and plotted.

Results

Methamphetamine potently activated the wild type hTAAR1 receptor in a CRE-driven luciferase reporter assay. Both enantiomers of METH and AMPH activated hTAAR1 mediated CRE-promoter dependent transcription with approximately the same apparent potency in transiently transfected human embryonic kidney (HEK)-293 cells. The neurotransmitter dopamine stimulates this reporter system much less

potently than PEA, METH or AMPH. Cells transfected with the empty vector (EV) did not respond beyond the background level when exposed to either PEA or S(+)-METH across the entire range of applied concentrations (Figure 1). Both the EV-transfected as well as the hTAAR1- transfected cells were potently stimulated by exposure to 10μM forskolin (data not shown). At the higher applied concentrations, the S(+) isomer of METH potently stimulates CRE-driven expression nearly as efficaciously as PEA. A concentration-dependent response of hTAAR1 mediated, CRE-promoter driven expression showed that the response to S(+)-METH was not statistically different from PEA at the applied concentration of 100μM (Figure 2). DA, R(-)-METH, and both isomers of AMPH were less responsive than PEA in this assay. This result suggests that hTAAR1 may function as a detector of the TA PEA but not the neurotransmitter DA.

Generation of the data involved averaging triplicate chemiluminescent readings for each drug and at each concentration taking the ratio of the CRE-luciferase average to the beta galactosidase average values. Background levels were determined from cells transfected with either hTAAR1 or EV, CRELuc, and β-gal but were mock treated in lieu of receiving any drug. The ratio of CRE-dependent to non CRE-dependent luciferase based chemiluminescence (S-glo/B-glo) for the background was approximately 1 for all of the experiments.

The potencies of these compounds at hTAAR1 for this CRE-luciferase assay are similar to but lower compared to the potencies at the human-rat chimera TAAR1 based on the cAMP assay of Chapter 2. For example, the PEA EC_{50} for the CRE-luciferase assay was 1.12 uM while for the cAMP assay it was 0.38uM. For

S(+)METH the EC_{50} for the CRE-luciferase assay was 6.22 uM and 4.44 uM for the cAMP assay (Table 1). Apparent calculated EC_{50}s were used since the sigmoidal concentration-response curves for the CRE-luciferase assay were not saturated.

Figure 1.

Heterologously expressed wild type human TAAR1 mediates CRE-Luciferase expression in response to β-phenylethylamine, methamphetamine, and dopamine. The chemiluminescence of firefly luciferase driven by the CRE promoter is measured as fold-stimulation over background level, normalized to one, in HEK-293 cells transiently transfected with the hTAAR1 receptor in response to treatment by PEA, S(+)-METH, and DA. Cells transfected with the empty vector (EV), pcDNA3.1TOPO, were treated with PEA or S(+)-METH. Data shown are the mean +/- S.E.M. from at least four experiments performed in triplicate. Concentrations of applied drug compounds along the x-axis are given in units of log M, where M is the final molarity.

Figure 1

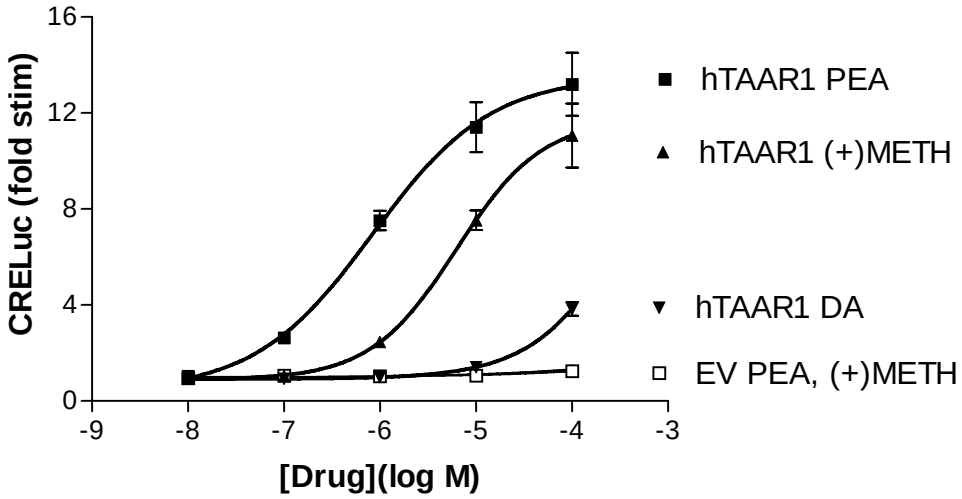
16
12
8
4
0
CRELuc (fold stim)
-9
-8
-7
-6
-5
-4
-3
[Drug](log M)
hTAAR1 PEA
hTAAR1 (+)METH
hTAAR1 DA
EV PEA, (+)METH

Figure 2.

hTAAR1 mediated CRE-luciferase expression in response to PEA, DA, and stereoisomers of METH and AMPH.

Heterologously expressed wild type human TAAR1 mediated CRE-luciferase expression in response to PEA, DA, and stereoisomers of METH and AMPH. Data shown are the measured chemiluminescence minus background level and are represented as a percent of maximum stimulation due to 10μM forskolin minus the background level and are the mean + S.E.M. from at least four experiments performed in triplicate. Concentrations of applied drug compounds along the x-axis are given in units of log M, where M is the final molarity.

Figure 2

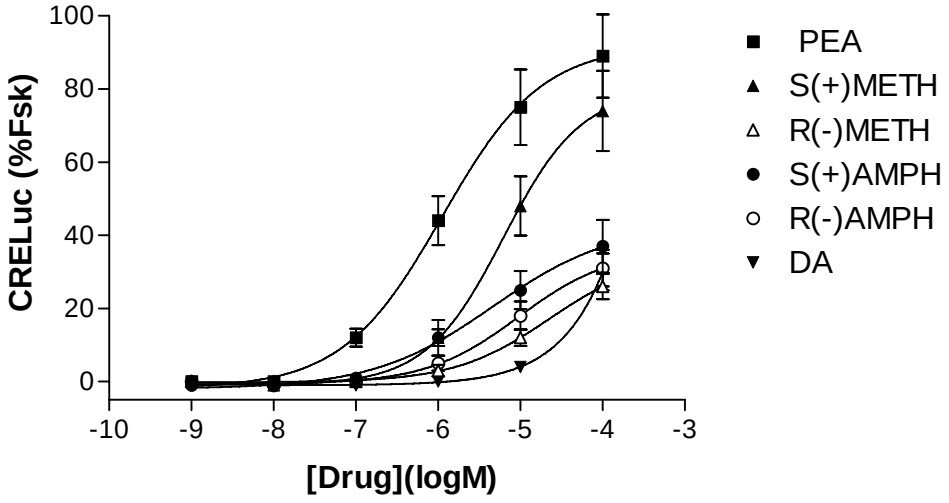
100
80
60
40
20
0
CRELuc (%Fsk)
-10
-9
-8
-7
-6
-5
-4
-3
[Drug](logM)
PEA
S(+)METH
R(-)METH
S(+)AMPH
R(-)AMPH
DA

Table 1. EC_{50}s of compounds that activate wild type human TAAR1 and human-rat chimera TAAR1

Average EC_{50}s (μM) for compounds at the hTAAR1 using the CRE Luc assay of chapter 4 and human-rat chimera TAAR1(hChTAAR1) using the cAMP assay of chapter 2.

Table 1.

compound	hChTAAR1	hTAAR1
PEA	0.38	1.12
S(+)METH	4.44	6.22
R(-)METH	9.83	22.35
S(+)AMPH	1.12	4.62
R(-)AMPH	3.09	9.50

Discussion

The results of this study show that methamphetamine potently activates human TAAR1- mediated, CRE-dependent transcription. Here, using a reporter assay, methamphetamine is shown for the first time to promote gene transcription mediated by the wild type human TAAR1 receptor. The trace amine *β*-phenylethylamine (PEA) and both enantiomers of methamphetamine and amphetamine activated CRE-driven luciferase expression in a concentration dependent manner while the neurotransmitter dopamine was a weak activator. Cells transfected with the empty vector showed no expression above background in response to these drugs even at the highest concentrations applied. PEA was even more potent than METH at stimulating hTAAR1 mediated transcription in this *in vitro* assay, suggesting a possible role for this endogenous ligand in mediating mood and alertness via this receptor. Previous *in vitro* assays have used measures of intracellular cAMP to evaluate the TAAR1 receptor (Borowsky et al., 2001; Bunzow et al., 2001; Wainscott et al., 2006). The assay in this study is more indirect since it measures the affects of cAMP response element dependent transcription. CREB activated by phosphorylation of serine 133 is required for recruiting CBP (Chrivia et al., 1993) which assembles transcription factors needed to initiate transcription. Other potential pathways can phosphorylate CREB in addition to the familiar PKA route. These include the MAP kinase pathway, NMDA receptor mediated calcium influx activation of CaMK, and phospholipase C (PLC) activation of PKC, all of which can regulate CREB (Shaw-Lutchman et al., 2003; Carlezon et al., 2005; Nair and Vaidya, 2006). Typically $G_{\alpha s}$ activates adenylyl cyclase (AC), $G_{\alpha i}$ inhibits AC, and $G_{\alpha q}$ activates phospholipase C (PLC).

While $G_{\alpha s}$ activates AC, the Gbg subunits can interact with PLC, G-protein activated inwardly rectifying K^+ (GIRK) channels, voltage sensitive calcium channels (VSCC), PI3 kinase and the MAPK pathways (Hur and Kim, 2002). The result is that downstream pathways of a GPCR can be complex and we cannot rule out these other downstream pathways as being consequences of hTAAR1.

Previous work has demonstrated that amphetamine given acutely to mice causes increased phosphorylation of CREB and this phosphorylation of CREB is associated with CRE-mediated transcription in regions of the brain associated with reward and mood such as the nucleus accumbens, ventral tegmental area, amygdala, and locus coeruleus (Shaw-Lutchman et al., 2003).

The curves of CRELuc fold stimulation above background did not saturate for the range of concentrations applied. However, concentrations of METH greater than 100μM could not be used due to toxicity effects. Above 100μM METH the CRE activation declined due to toxicity as evidenced by the decreasing expression of the control β-gal used to normalize the expression in the assay.

Previously it was reported that METH and AMPH as well as the trace amines PEA and p-tyramine activated the TAAR1 receptor for different mammalian species including the rat, mouse, and rhesus monkey. A chimera of the human and rat TAAR1 was also shown to be activated by exposure to METH. Other members of the TAAR family, excluding TAAR1, had been shown to be activated by numerous odorant molecules (Liberles and Buck, 2006). The unmodified hTAAR1 was previously reported to be stably expressed in CHO-K1 cells where the receptor activated the mobilization of internal calcium in response to known trace amines

agonists and neurotransmitters (Navarro et al., 2006). However, it has not yet been reported that METH activates the wild type hTAAR1. This study is the first to evaluate the non-chimeric hTAAR1 in response to methamphetamine.

The isomers of METH appear to be stable in solution. R(-)METH, the less physiologically active form, is excreted in the urine in the same form. The main metabolite of METH is AMPH and it is found to have no cross isomerization in assayed urine samples (Jirovsky et al., 2001).

Since the results of the current study show that hTAAR1 is activated *in vitro* by METH, hTAAR1 may represent a novel target by which methamphetamine mediates its effects in humans.

Future behavioral experiments could assess the contribution of TAAR1 in mediating some of METH's *in vivo* effects by using knockout and wild type mice exposed to S(+)METH.

The results presented here show that METH, along with PEA, potently activate hTAAR1 mediated CRE-dependent transcription *in vitro*. The plate-based assay described here could be used to evaluate the response of hTAAR1 to antagonist drugs with the potential to develop therapeutic treatments for methamphetamine addiction and abuse.

Chapter 5

Co-localization of the human Trace Amine-Associated Receptor 1 (hTAAR1) and the human Dopamine Transporter (hDAT)

Abstract

The trace amine-associated receptor 1 (TAAR1) is activated by trace amines (TA) and by the psychostimulants amphetamine (AMPH) and methamphetamine (METH). The dopamine transporter (DAT) is the primary regulator of released dopamine. It has been reported that AMPH causes a redistribution of cell surface DAT. Other groups have suggested that TAAR1 and DAT interact. This study was undertaken to see if hTAAR1 and DAT co-localize and to see if METH also causes internalization of DAT. Here, a GFP-human DAT fusion protein (hDAT-GFP) is expressed at the surface in untreated HEK293 cells and in the cytoplasm after treatment with phorbol 12-myristol 13-acetate (PMA). Evidence from confocal fluorescence microscope imaging shows that METH applied to cells stably expressing hDAT-GFP induced redistribution from the surface. Experiments also showed an example of hTAAR1 and DAT co-localization. Prior studies have shown the human TAAR1 (hTAAR1) to be localized primarily in the cytoplasm rather than in the cell surface plasma membrane. A motif, $R(X)_6LL$, required for exit from the endoplasmic reticulum (ER) for the majority of aminergic GPCRs, was found to be modified in the rat, mouse, and human TAAR1 sequences. This modification may account for the predominantly intracellular distribution of the hTAAR1.

Introduction

Endogenous trace amines acting at the trace amine-associated receptor may modify the ability of monoamine transporters to function by inducing redistribution of the transporters from the cell surface. The dopamine transporter (DAT) provides the principle mechanism for the regulation of the reuptake of extracellular dopamine (Giros et al., 1996). The monoamine transporters are targets for anti-depressant drugs. DAT is also the main target for AMPH and METH, both of which prevent DA uptake and induce DA to flow into the synaptic cleft (Koob and Bloom, 1988). AMPH as well as the TAs PEA and TYR induce DA efflux from dopaminergic neurons in rabbit striatal slices (Parker and Cubeddu, 1988). The phosphorylation of DAT causes internalization of transporters and inhibition of their activity. DAT phosphorylation in response to PKC activation by phorbol 12-myristate 13-acetate (PMA) inhibits DAT activity (Vaughan et al., 1997). Phosphorylation of the dopamine transporter by PKC activated by PMA results in internalization of the transporters (Daniels and Amara, 1999).

It was convincingly shown that AMPH causes internalization of human DAT stably expressed in HEK293 cells (Saunders et al., 2000). More recent findings have shown that a key element of AMPH's ability to induce DAT redistribution from the cell surface is the increase in intracellular AMPH (Kahlig et al., 2006). However, these authors did not identify the intracellular target that mediates the AMPH induced redistribution. Could it be TAAR1? TAAR1 is activated by endogenous TAs and by the abused psychostimulants AMPH and METH (Bunzow et al., 2001). Recently it was shown that DAT significantly enhanced TAAR1 signaling in HEK293 cells

stably expressing DAT and transiently transfected with rhesus monkey TAAR1 (rhTAAR1) (Xie et al., 2007). In this same article the authors demonstrate the co-expression of TAAR1 and DAT in rhesus monkey brain using confocal laser microscopy. This same group also provided evidence that, conversely, TAAR1 regulates the efflux of dopamine in response to METH (Xie and Miller, 2007).

Recently it was shown that the TA TYR causes a decrease in the spontaneous firing rate of dopaminergic neurons in wild type but not in TAAR1 knockout mice (Lindemann et al., 2007). This suggests that in wild type mice TAAR1 "decreases the firing rate" of dopaminergic neurons. In a recent article it was reported that PEA activation of TAAR1 inhibits uptake and induces efflux of [^{3}H]DA in tranfected cells, and in synaptosomes of both rhesus monkey and wild type mice but not in TAAR1 knockout mice (Xie and Miller, 2008). This suggests that PEA interaction with TAAR1 modulates transporter function.

TAAR1 resides primarily in the cytoplasm rather than at the cell surface plasma membrane. The reason for this localization is unknown. TAAR1 localization in the cytoplasm may be due to its retention in endosomes or it may be contained in synaptic vesicles. If TAAR1 is in synaptic vesicles, then upon merging with the plasma membrane TAAR1 would have a temporary presence at the surface during neurotransmitter release.

To investigate the possible interaction of TAAR1 with DAT, I used some of these same approaches in an attempt to replicate some of the reported findings. Here, I found evidence that METH, in addition to AMPH, and PMA used as a positive control, may cause internalization of DAT expressed in HEK293 cells. Results also

indicated some evidence of co-localization of hTAAR1 and hDAT in transfected HEK293 cells. And, finally, an endoplasmic reticulum exit motif was found to be missing, or at least modified in the rat, mouse, and human TAAR1.

Methods and Materials

Materials

S-(+)- and *R*-(–)-AMPH-sulfate and *S*-(+)-METH-HCl were purchased from Sigma-Aldrich (St. Louis, MO). Plasmid constructs containing the GFP-hDAT sequence were provided as a gift from Spencer Watts, PhD., University of Pittsburgh, Pittsburgh, PA. The primary hTAAR1 antibody was rat anti-HA and the secondary antibody was Fab-Cy3 anti-rat.

Cell culture

HEK293 cells stably expressing hDAT-GFP, a protein that expresses the human dopamine transporter fused to an enhanced green fluorescent protein at the N-terminus, were maintained in Dulbecco's Modified Eagle's medium (DMEM), GIBCO-Invitrogen (Grand Island, NY) with 10% fetal bovine serum (FBS) and 1% Pennstrep and 0.8% G418. The expression vector for HA-tagged hTAAR1used in transient transfections was pcDNA3.1/V5/His-TOPO (Invitrogen, Carlsbad, CA). Cells were maintained at 37 ^{o}C in humidified air with 5.1% CO_2.

Transfections

The establishment of a stably expressing hDAT-GFP cell line followed the same procedure as previously outlined in chapter 3. The construction of the hDAT-GFP plasmid was described previously by Daniels and Amara. Briefly, hDAT cDNA was inserted between the *Kpn*I and *Xba*I sites of the expression vector pEGFP-C1 (Clontech). Transient transfection of hTAAR1 into HEK293 cells stably expressing hDAT-GFP was performed using FUGENE HD Transfection Reagent according to the manufacturers directions. The reagent, the DNA, and the diluent Optimem were allowed to come to room temperature. The ratio of Fugene HD reagent (μl) to DNA (μg) was 4:2 in 100μl of diluent. The Fugene HD transfection reagent was added directly to the diluted DNA and the mixture was vortexed for 1 to 2 seconds, then the mixture was incubated for 15 minutes at room temperature in a tissue culture hood. The transfection complex was then added to cells growing on coverslips in 25μl volumes per well in a 24 well plate. The plate was swirled gently to mix the transfection complex throughout the media and then incubated overnight for approximately 18 hours prior to treatment with drugs.

Drug treatment

Cells were treated with drug for one hour at 37 ^{o}C. Drug treatment was stopped by aspiration of media and cells were rinsed 1X in Phosphate Buffered Saline (PBS). Drugs were applied at a final concentration of 10μM with the exception of phorbol 12-myristol 13-acetate, PMA, which was applied at a final concentration of 100nM.

The PMA was a gift from Robert Shapiro, PhD., Oregon Health and Science University, Portland, OR.

Immunofluorescent antibody staining and confocal microscopy

After drug treatment the transfected HEK293 cells were fixed in Hanks balanced salt solution (HBSS) pH7.4 with 3% paraformaldehyde at room temperature and incubated for 15 minutes in the dark. Cells were washed 3X in Tris Buffered Saline (TBS) washing buffer with 0.1%Triton X-100 for permeabilization. Cells were pre-blocked in TBS plus fish gelatin and 1:10 hen block for 20 minutes. Cells were washed 3X in 1X TBS. Rat anti-HA primary antibody diluted 1:500 in TBS plus blocking solution was added and cells were incubated for 45 minutes at room temperature. The primary antibody was removed and cells were washed 3X in TBS 1X. Cells were blocked again as described above and incubated for 5 minutes, then washed 3X in TBS. Secondary antibody, Fab-Cy3 anti-rat diluted at 1:500 in blocking solution was added and incubated for 30 minutes in the dark. Cells were washed 3X in TBS 1X plus 0.1% TritonX-100. Coverslips with stained cells were dipped in H2O, the excess water was wicked off, and the coverslips were mounted onto glass slides in Molwiol (Sigma/Aldrich, Milwaukee, WI) that was pre-warmed to 37 ^{o}C. Slides were labeled, dried overnight in the dark at room temperature, then stored in the dark at 4 ^{o}C until imaging with a laser scanning confocal microscope. Confocal microscopy was performed using an Olympus Fluoview 300 scanning head mounted on a BX51 microscope stand with a 60x1.4NA oil immersion objective. A green HeNe 543nm

laser was used for excitement of Cy3 fluoresence and a blue 488nm Ar laser was used to excite GFP.

Results and Discussion

In an effort to explain the predominantly cytoplasmic location of the TAAR1s, a search of the literature was made to determine what motifs represent a retention signal and to see if the TAAR1s contained such a motif. The $GABA_{B1}$ receptor is a GPCR that requires dimerization to the $GABA_{B2}$ receptor in order to be expressed at the cell surface (Marshall et al., 1999). The RSRR sequence near the end of the $GABA_{B1}$ C-Terminus (figure 1) constitutes a retention motif that prevents protein trafficking from the endoplasmic reticulum (ER) (Margeta-Mitrovic et al., 2000). The C-terminus tails of the two receptor subtypes coil together which blocks the retention site on $GABA_{B1}$. The blockage of the retention site allows the release sites to direct transport to the cell surface.

In addition, the α_{1D}-AR remains located intracellularly unless it heterodimerizes with α_{1B}-AR (Uberti et al., 2003). It was found that the conserved sequence $F(X)_6LL$ represents an ER exit motif that enables transport to the cell surface (Duvernay et al., 2004). This reference included a table of GPCRs that contain this conserved exit motif. The α- and β-AR receptors were listed as well as the dopamine and 5HT receptors. The motif FXXXFXXXF was also identified as an ER exit motif for the dopamine D1 receptor (Bermak et al., 2001). Inspection of the dopamine receptors D1-D5 revealed that they all have this same additional exit motif. Interestingly, the

D1 and D5 motifs align and the D2-D4 motifs align but the D1 and D5 motifs are offset by one amino acid to the left compared to the D2-D4 sequences.

Both of the exit motifs for D1 and D2, i.e. $F(X)_6LL$ and FXXXFXXXF, are included in the sequences shown in Figure 1. The sequences include the TM7 domain and the initial segment of each C-terminus. The sequences are aligned to hβ2AR which has only the $F(X)_6LL$ exit motif.

The next logical question was to ask if the TAAR1s had either this same $F(X)_6LL$ exit motif which is common to the majority of the adrenergic receptors or the FXXXFXXXF exit motif of the D1 and D2 receptors. The rat, mouse, and human TAAR1 TM7 sequences were aligned to the hβ2AR sequence (Figure 1). The residues that are conserved in TM7 across most of the aminergic GPCRs are indicated by bold type. Inspection revealed that the TAAR1s have modified versions of the $F(X)_6LL$ exit motif but the FXXXFXXXF motif is absent from the TAAR1 sequences. The rat sequence $F(X)_6VL$ has a valine in place of a leucine. The mouse has a $F(X)_6VLL$ and the hTAAR1 has a $F(X)_7L$ motif with just a single leucine. Here I speculate that the extra distance between the F and the L and the single L rather than a double may render the modified exit TAAR1 motifs inactive or less effective with the result of significantly reduced cell surface expression. An alternative explanation could be that, *in vivo*, TAAR1 dimerizes and manages to be trafficked but its unknown traveling partner was not expressed in the *in vitro* studies that employed HEK293 cells.

Future studies should include mutagenesis of the hTAAR1 exit motif to match that of the hβ2AR. The hypothesis is that surface expression would be significantly

enhanced. This effort would help determine if the native hTAAR1 exit motif is functional or not and would explain the cytoplasmic localization if the hypothesis were shown to be true.

An HEK293 cell line stably expressing a GFP labeled hDAT was established in an effort to provide a vehicle to investigate possible co-localization and interactions between hDAT and hTAAR1 and to explore the effects of METH on the cell location of the DAT. Cells stably expressing hDAT-GFP fusion protein were grown on cover slips and treated with phorbol 12-myristate 13-acetate (PMA) 100nM or no drug and incubated for one hour. The cells were rinsed, fixed in paraformaldehyde, rinsed and mounted on glass slides prior to imaging with a confocal microscope. For controls with no applied drug the hDAT was expressed at the cell surface as expected (figure 2a).

The phorbol ester PMA was previously demonstrated to cause internalization of the DA transporter from the plasma membrane (Daniels and Amara, 1999). The same approach was taken here in order to demonstrate the ability to detect DAT internalization. In this study, exposure to PMA caused DAT internalization (Figure 2b) similar to the results shown by Daniels and Amara. The fluorescence appears as intracellular puncta with little or no cell surface fluorescence. The cells in Figures 2a and 2b were grown and plated in the same 24-well tissue culture dish and experienced the same environmental conditions except for the drug treatment difference.

In prior studies using confocal microscopy it was shown that AMPH applied to cells expressing DAT caused the internalization of the transporters from the cell

surface (Saunders et al., 2000). There are also reports that the activity of the DAT was reduced in response to METH (Saunders et al., 2000) (Baucum et al., 2004).

I wanted to know if METH would cause the same internalization of DAT that had previously been shown for AMPH.

METH 10μM was applied to cells expressing the hDAT-GFP. For cells exposed to METH and incubated for 30 minutes DAT-GFP remained primarily at the surface (Figure 3a). The prominent bright spot in one of the cells may be protein still in the ER or Golgi structure. After exposeure to METH for 2 hours there was some evidence of internalization (Figure 3b). The cell in the lower right portion of figure 3b shows the most evidence of internalization while the other cells still exhibited surface location.

The next question was whether DAT and TAAR1 co-localize. That would be expected if one protein mediates the effects of the other as proposed by Xie and Miller (Xie and Miller, 2007; Xie et al., 2007). HA-tagged hTAAR1 was transiently transfected into HEK293 cells stably expressing hDAT-GFP. Cells were treated with drugs then fixed and prepared for antibody staining. Since the transfection efficiency was not very good for this experiment, relatively few hTAAR1 expressing cells were found that exhibited Cy3 fluorescence. Cells with GFP fluorescence are shown in the top panel of Figure 4. The center panel shows cells expressing the HA-tagged wild type hTAAR1 in the same field of view.

These cells were treated with PMA. Due to the poor transfection efficiency of the hTAAR1 in this experiment it was not possible to demonstrate hTAAR1 localization for cells with no drug. These drug treatment experiments would need to be duplicated

with improved transfection efficiency to generate enough co-transfected cells to permit valid statistical analysis.

The bottom panel is the result of merging to first two. The yellow areas indicate sites of hDAT-GFP and hTAAR1 co-localization. Upon close examination the DAT and hTAAR1 appear to be intracellular with some possible surface sites as well.

In summary, DAT cell surface expression was redistributed to the cytoplasm upon treatment with PMA. Preliminary evidence of DAT internalization was also shown in response to METH. Some evidence was shown suggesting co-localization of hDAT and hTAAR1.

Figure 1. Endoplasmic reticulum exit and retention motifs

(a) Amino acid sequences of the TM7 and initial section of the C-Terminus of human dopamine receptors D1 and D2, and the rat, mouse, and human TAAR1 aligned to the human β2AR. The transmembrane seven domains are indicated by a line over each sequence and are based on the recently determined crystal structure of the β2AR (Rasmussen et al., 2007). Highly conserved residues across the aminergic GPCRs are indicated by bold type. The ER exit motifs are underlined and also highlighted in yellow.

(b) Amino acid sequences of the C-Terminus ends of the GABA B1 and GABA B2 receptors. The putative TM7 for GABA B1 is indicated by a line over the sequence. The ER exit motifs are underlined and highlighted in yellow. The ER retention motif for GABA B1 is underlined in red.

Figure 1.
(a)

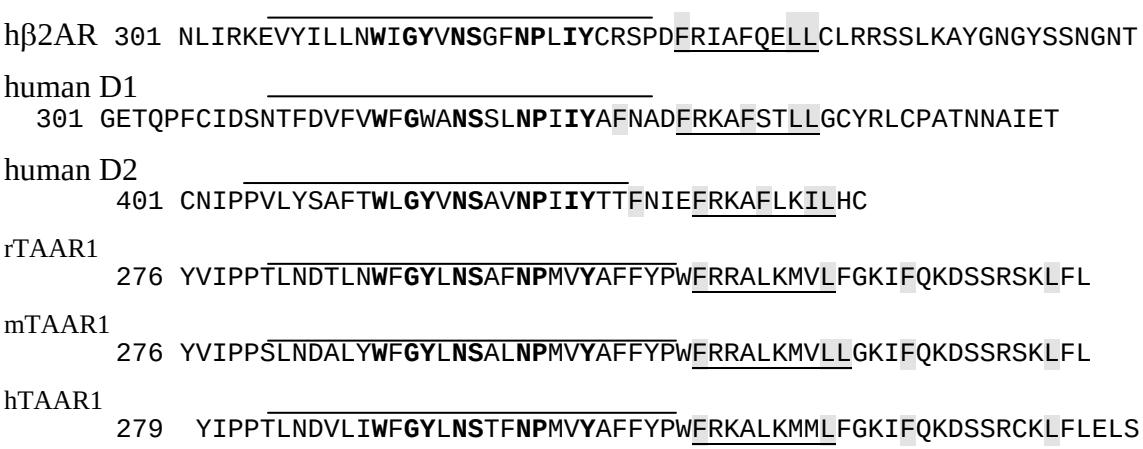
hβ2AR 301 NLIRKEVYILLNWIGYVNSGFNPLIYCRSPDFRIAFQELLCLRRSSLKAYGNGYSSNGNT
human D1
301 GETQPFCIDSNTFDVFVWFGWANSSLNPIIYAFNADFRKAFSTLLGCYRLCPATNNAIET
human D2
401 CNIPPVLYSAFTWLGYVNSAVNPIIYTTFNIEFRKAFLKILHC
rTAAR1
276 YVIPPTLNDTLNWFGYLNSAFNPMVYAFFYPWFRRALKMVLFGKIFQKDSSRSKLFL
mTAAR1
276 YVIPPSLNDALYWFGYLNSALNPMVYAFFYPWFRRALKMVLLGKIFQKDSSRSKLFL
hTAAR1
279 YIPPTLNDVLIWFGYLNSTFNPMVYAFFYPWFRKALKMMLFGKIFQKDSSRCKLFLELS

(b)

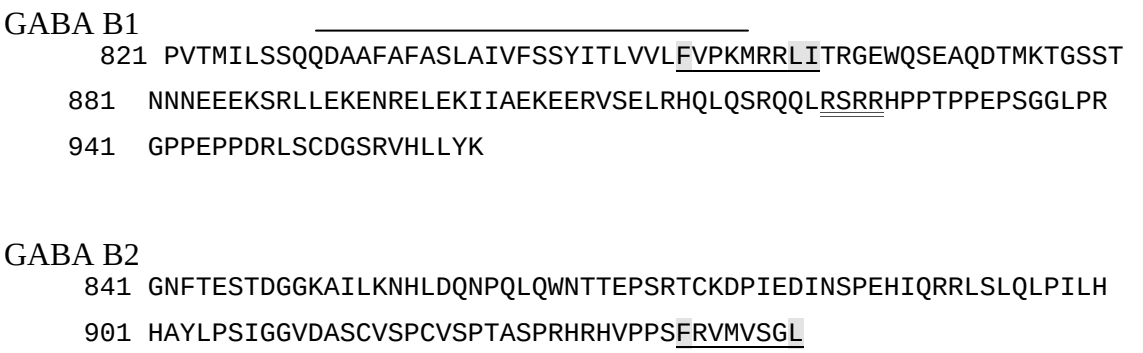
GABA B1
821 PVTMILSSQQDAAFAFASLAIVFSSYITLVVLFVPKMRRLITRGEWQSEAQDTMKTGSST
881 NNNEEEKSRLLEKENRELEKIIAEKEERVSELRHQLQSRQQLRSRRHPPTPPEPSGGLPR
941 GPPEPPDRLSCDGSRVHLLYK
GABA B2
841 GNFTESTDGGKAILKNHLDQNPQLQWNTTEPSRTCKDPIEDINSPEHIQRRLSLQLPILH
901 HAYLPSIGGVDASCVSPCVSPTASPRHRHVPPSFRVMVSGL

Figure 2. Confocal microscope images of hDAT-GFP in HEK293 cells.

HEK293 cells stably expressing hDAT-GFP were treated and incubated, then washed, fixed, and mounted onto slides.

(a) Cells treated with vehicle only, no drugs, or

(b) cells treated with PMA 100nM then incubated for 1 hour at 37C.

Figure 2.

(a)

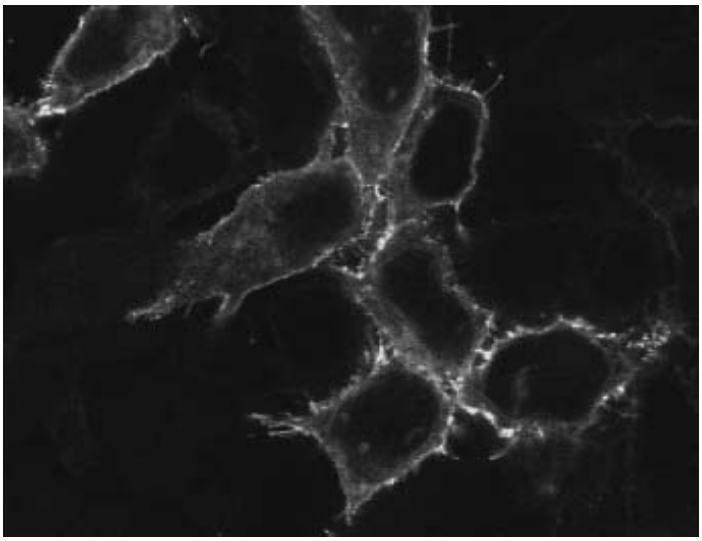

(b)

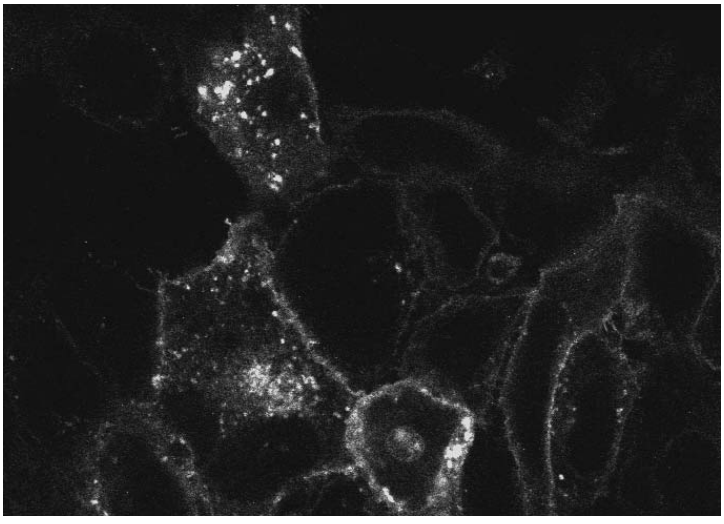

Figure 3. Confocal microscope images of METH treated HEK293 cells stably expressing hDAT-GFP.

(a) Cells treated with METH 10μM for ½ hour at 37 ^{o}C and

(b) cells treated with METH 10μM for 2 hours.

Figure 3.

(a)

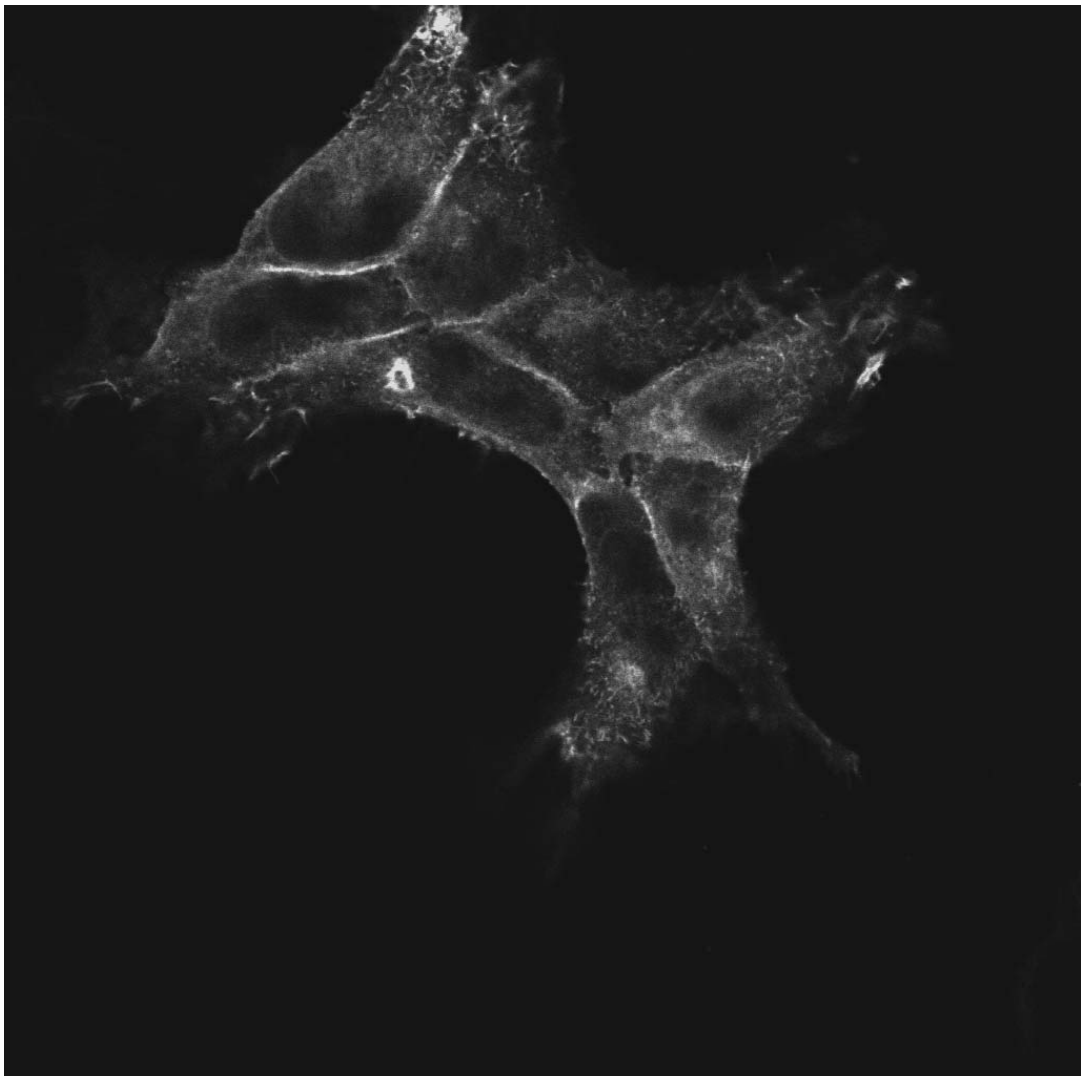

Figure 3.

(b)

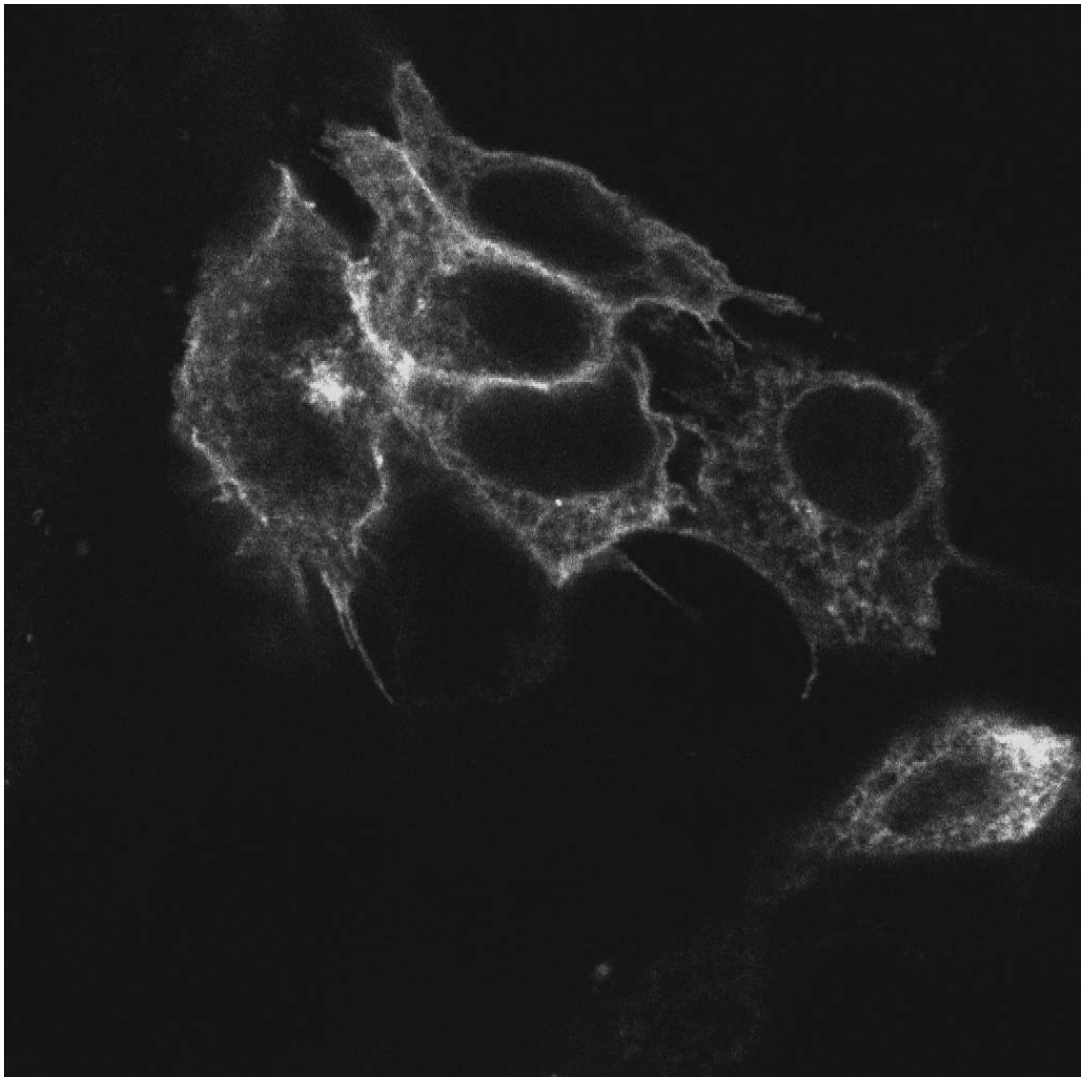

Figure 4. Confocal microscope images of PMA-treated HEK293 cells stably expressing hDAT-GFP and transiently co-expressing hTAAR1.

Cells were treated with PMA 100nM for 1 hour at 37C. Cells were then fixed in paraformaldehyde, then washed 3x in TBS plus 0.1%TritonX-100, blocked in TBS plus fishgelatin and henblock, washed, then incubated with primary antibody r α HA, incubated, washed, blocked and again washed 3x, incubated with secondary Ab, Fab-cy3 α rat for 30 to 60 minutes, washed 3x, and mounted on glass cover slides, dried and stored in dark until imaged.

Top panel: GFP tagged dopamine transporter, hDAT-GPF (green).

Center panel: hTAAR1 cy3 (red).

Bottom panel: Merged images, co-localization of hDAT-GFP and hTAAR1 (yellow).

Figure 4

Chapter 6 Summary and Conclusions

Since the discovery of the trace amine-associated receptors in 2001 and subsequent investigations at different laboratories, some major questions remain about these GPCRs. Significantly, the biological function of TAAR1 in the mammalian brain remains to be ascertained along with the determination of the downstream targets of TAAR1. Even though *in vitro* pharmacological characterizations of some of the TAARs have been performed and many agonists are known, the *in vivo* ligands for TAAR1 remain to be identified and these may differ across species and, furthermore, could potentially differ in different brain regions of the same species. Whether naturally mutated alleles of TAAR1 or other members of the TAAR family occur in patients who have been diagnosed with mental disorders or in people who are prone to abuse psychostimulants such as methamphetamine are questions related to human health that have yet to be answered. Questions also remain about whether amphetamine or methamphetamine activates TAAR1 *in vivo* and, if so, does the activation occur at phsysiologically revelant concentrations. And finally, does TAAR1 mediate some of the effects of these drugs *in vivo,* especially in humans? Below is a summary review of my research followed by an integration of my findings with reports from related literature.

Species-dependent stereoselectivity of TAAR1 (Chapter 2)

After the work by Bunzow et al. (2001) showed that the rat TAAR1 was activated by trace amines and psychostimulants, I wanted to characterize the mouse and human TAAR1s using trace amines and amphetamine along with some of its congeners and

to compare the response of these species to that for the rat. Some unexpected results were

found from the characterization of the concentration-dependent response of cAMP accumulation to these drugs. The trace amine PEA was a full agonist in all three species. All three species had similar cAMP concentration response curves to PEA indicating that PEA was equipotent at rat-, mouse-, and the human chimera-TAAR1 (hChTAAR1). In sharp contrast to PEA, however, the trace amine TYR had distinctly species-dependent characteristics. The potency of TYR was greatest in rat. The EC_{50} of the rTAAR1 cAMP concentration-response to TYR was about an order of magnitude lower than the EC_{50} of the mouse TAAR1 and the human chimera TAAR1 EC_{50} was even higher.

In addition to a striking difference in potencies for TYR, the efficacies were also different for each species. TYR was a full agonist at the rat TAAR1 but only a partial agonist at the hChTAAR1 with the mouse efficacy closer to that of the human than to the rat. These results suggest that PEA may be an endogenous ligand for TAAR1 *in vivo* and that TYR may also be an *in vivo* TAAR1 ligand, especially in the rat.

When the cAMP response curves were generated for the enantiomers of AMPH and its congeners, differences in response to the isomers of the compounds became apparent in each species. An unexpected and surprisingly large difference between species for enantiomeric stereoselectivity was revealed. The rat TAAR1 has about the same EC_{50} for both the S(+) and R(-) isomers of AMPH. However, rat TAAR1 has a much lower efficacy for the R(-) isomer compared to the S(+)isomer. The stereoselectivity of the mouse TAAR1 to the enantiomers of AMPH was quite

different from that of the rat. For mTAAR1, the EC_{50} of R(-)AMPH was over an order of magnitude higher than for S(+)AMPH indicating a much lower potency for the R(-) isomer. The efficacies for both S(+) and R(-)AMPH were nearly the same at mTAAR1 and both enantiomers were partial agonists. The potency stereoselectivity of the hChTAAR1 had characteristics similar to that of the mouse while its efficacy stereoselectivity was more like that of the rat.

In summary, the findings of this work, described in Chapter 2, showed that amphetamine and methamphetamine are potent agonists of TAAR1 and display concentration dependent pharmacological profiles as well as species-dependent stereoselectivity. It was clearly shown that the trace amines PEA and TYR activate TAAR1 receptors *in vitro* which suggests the possibility that these may be the endogenous TAAR1 ligands *in vivo*. That the EC_{50} for TAAR1 activation by S(+)METH in humans is below concentrations found in some addicts suggests that TAAR1 may mediate some of the effects of methamphetamine *in vivo*.

Determination of stereoselectivity by site-directed mutagenesis (Chapter 3)

A site directed mutagenesis approach was used to determine the features of the TAAR1 receptors that are responsible for the major stereoselectivity differences between the rat and the mouse. The substitution of aspargine at amino acid 287 in TM7 of the rat sequence by tyrosine, N7.39Y, which is at the same position in the mouse sequence caused the pharmacological profile of the rat mutant TAAR1 to isomers of AMPH and METH to look like that of the wild type mouse. Briefly, both isomers of AMPH had the same efficacy but the EC_{50} of S(+)AMPH was about an

order of magnitude lower compared to R(-)AMPH. Similar results were found for METH. Conversely, mutation of the mouse TM7 sequence by replacing the tyrosine at amino acid 287 with asparagine, Y7.39N, as found at the corresponding site in the rat sequence, caused the profile of the mouse TM7 mutant to resemble that of the rat wild type TAAR1. Here, for the mouse TM7 mutant, both isomers produced about the same EC_{50}. However the efficacies were also about the same, as opposed to the lower efficacy seen for R(-)AMPH vs. S(+)AMPH as seen on the wild type rat. The stereoselectivity, and its reversal in the mutants, are likely due to steric hindrance of the methyl group attached to the alpha carbon of the amphetamines with the hydroxyphenyl of tyrosine.

In summary this study revealed that a single amino acid difference in TM7 between the two species is responsible for the species dependent stereoselectivity to isomers of AMPH and METH.

METH activation of wild type hTAAR1 (Chapter 4)

Due to the difficulty of stably expressing the wild type hTAAR1, a chimera of the human and rat TAAR1 was used in the first study. To evaluate the response of the wild-type hTAAR1 to METH, a reporter assay using transiently transfected wild type hTAAR1 was employed. The wild type hTAAR1 was shown to mediate cAMP dependent CRE-luciferase expression *in vitro*. PEA was more potent than METH which was more potent than DA at inducing CRE-luciferase expression. These *in vitro* findings support the interpretation that hTAAR1 is a likely target for METH *in vivo*. Furthermore, hTAAR1 may mediate METH induced cAMP accumulation and

CRE-promoter dependent transcription *in vivo*. Future animal studies would be needed to confirm TAAR1 agonist induced transcription *in vivo*.

Co-localization of hTAAR1 and hDAT (Chapter 5)

This study was undertaken to establish evidence that supports the hypothesis that hTAAR1 is involved in regulating the function of the dopamine transporter. The focus of this study was to see if the two proteins co-localize and if METH causes the internalization of DAT.

A GFP-human DAT fusion protein, stably expressed in HEK293 cells, was redistributed from the surface of cells in response to the PKC activator PMA with similar results to earlier published findings. Evidence from fluorescence confocal microscopy suggests that METH induces redistribution of DAT from the cell surface *in vitro*. Co-transfection experiments provided evidence of hTAAR1 co-localization with hDAT.

Additional experiments replicating these results are needed. Finally, it was observed that the endoplasmic reticulum exit motifs in the C-terminus of the wild type rat, mouse, and human TAAR1s are modified from that of most aminergic GPCRs. Further mutagenesis experiments and immunofluorescent imaging studies could help evaluate if this modification accounts for the predominantly intracellular distribution of TAAR1. Future localization studies in neurons would help determine if the lack of transport of TAAR1 to the cell surface is an artifact of expressing the receptors in HEK293 cells. Transient transfections of mouse neurons could be

performed using nucleofection techniques such as those available using a nucleofector kit (Amaxa Biosystems, Cologne, Germany).

Relevant findings reported in the literature

There are a number of reports that suggest an association of the TAAR1 receptor in mediating some of the effects of psychostimulant drugs of abuse as well as being involved in mood disorders. First of all, it has been established that TAAR1 is activated by AMPH and METH as well as by the trace amines PEA and TYR. It is well accepted that the dopamine transporter regulates extracellular dopamine concentrations by the re-uptake of the neurotransmitter from the synaptic cleft. It is also well accepted that methamphetamine and amphetamine act at the dopamine transporter where they release dopamine into the synapse resulting in extended exposure of dopamine receptors to their endogenous ligand. Increased DA release is thought to be responsible for the rewarding effects of the drug. Amphetamine is known to cause the internalization of DAT. In my research I demonstrated that methamphetamine might also cause internalization of DAT.

Psychiatric and mood disorders have also been linked to trace amines and the trace amine-associated receptors. Amphetamine has been used to induce manic symptoms in bipolar disorder patients and in healthy control subjects (Anand et al., 2000). There is also evidence of the involvement of the trace amine PEA in mood disorders. For example low levels of PEA have been found in depressed patients (Sabelli and Mosnaim, 1974) and increased levels of PEA have been associated with the manic phase of bipolar disorder (Linnoila et al., 1983). TAARs have been

associated with schizophrenia although this is somewhat controversial based on conflicting reports possibly due to genetic differences in the isolated populations used in the studies.

TAAR1 has been found in the limbic regions of the brain. Using the rhesus monkey TAAR1 stably expressed in HEK293 cells, Miller et al. have indicated that there is an interaction of DAT with TAAR1. In cells co-expressed with TAAR1 and DAT it was shown that TAAR1 reduces DA uptake and this reduction was inhibited by both PKA and PKC inhibitors (Xie and Miller, 2007).

Integration of my research findings with accounts from the literature

Taking into account all of these separate findings and integrating them with my own research, I propose a mechanism to explain the possible physiological function of TAAR1 and how it may be involved with the trace amine PEA, and possibly TYR, as well as its association with DAT and DA. Some suggestions for future experiments to test the hypothesis follow the description of the proposed model (Figure 1).

In healthy individuals, PEA may act as an endogenous amphetamine to stimulate alertness and elevate mood. Extracellular PEA could act like AMPH to activate TAAR1, though it is not known if PEA exists in the synaptic cleft. PEA may possibly be present if it were released at the same time that DA is released upon activation of dopaminergic neurons. If TAAR1 normally occurs in the plasma membrane of the synaptic vesicles, then TAAR1 may be inserted at the cell surface upon fusion of synaptic vesicles during neurotransmitter release. The PEA activation of TAAR1 would increase cAMP and PKA activity. It is hypothesized that the $\beta\gamma$ subunit that is

released when the α_s subunit is activated could activate phospholipase C (PLC). However, it has been observed that the $\beta\gamma$ subunit released from $G\alpha_s$ does not signal much. This may be due to lower concentrations of $\beta\gamma$ resulting from $G\alpha_s$ activation compared to higher concentrations of $\beta\gamma$ due to activation of $G\alpha_i$ or $G\alpha_o$ (Sunahara et al., 1996). Since some GPCRs couple to more than one G protein subtype (Wong, 2003), it remains a possibility that TAAR1 may activate parallel signaling pathways. An alternative source for $\beta\gamma$ subunits to activate PLC could be from a $G\alpha_q$ or $G\alpha_{i/o}$ family of GPCRs. PLC in turn cleaves phosphatidylinositol 4,5-bisphosphate (PIP_2) to form diacylglycerol (DAG) and inositol 1,4,5-triphosphate (IP_3). The IP_3 interacts with Ca^{+2} channels on the surface of the endoplasmic reticulum, which releases Ca^{+2} from ER stores. Protein kinase C (PKC) binds Ca^{+2} and is recruited to the cell surface plasma membrane. At the cytosolic side of the plasma membrane PKC binds to and is activated by DAG. Activated PKC subsequently phosphorylates the dopamine transporter. Phosphorylation of the C-terminus tail would target DAT for internalization to endosomes likely mediated by clathrin-dependent endocytosis (Torres et al., 2001). This would decrease the quantity of transporters at the cell surface and thus increase sensitivity of the DA receptors to released DA (since the neurotransmitter would be able to stay in the synapse longer).

This model agrees with findings in the literature that AMPH induces internalization of DAT and with my findings reported in chapter 5 that suggest METH may also induce DAT internalization. In the case of psychostimulant abuse, METH or AMPH would take the place of PEA in the model description. This is also

consistent with the idea that TAAR1 is a novel target of methamphetamine and amphetamine.

In a recent study it was reported that AMPH induced locomotor function of TAAR1 knockout mice was increased compared to the response of wild type mice (Lindemann et al., 2007). In addition, they reported a 2½ fold increase in dopamine, noradrenaline, and serotonin release, in response to AMPH, in TAAR1 knockout mice compared to wild type mice. These results are similar to the increase in DA and NE release reported in a study of another TAAR1 KO mouse (Wolinsky et al., 2007). These findings of increased DA release and increased locomoter effects in the TAAR1 KO are reconciled with the proposed model as follows. The increased DA release of the TAAR1 KO may be due to reduced DAT internalization. With more DAT (or NET or SERT) remaining at the cell surface, more neurotransmitters can be reverse exchanged upon application of AMPH. The increased DA release would also explain the increased locomotor activity of the KO vs WT. The WT TAAR1 cells would undergo DAT internalization as described in the model. With fewer surface transporters, less DA would be reverse exchanged resulting in less DA release compared to levels in the KO mice.

The model also is consistent with findings of lower levels of PEA in patients with depression. PEA levels that are less than normal would diminish DAT removal thus increasing DA uptake, resulting in depressed mood. For the case of higher levels of PEA reported in mania, the model also applies in that increased PEA would reduce levels of the DAT and thus increase DA signaling.

In summary, the proposed model suggests that the function of TAAR1 is to regulate aminergic transporter control of monoamine neurotransmitter signaling, i.e. it is a regulator of the regulator. This model is a potential solution to one of the major remaining questions about TAARs, which is the determination of its biological function in the mammalian brain.

Future directions and conclusions

Future experiments to test the above speculative model could include the co-expression of DAT and TAAR1 in cells subsequently treated with PEA, METH, AMPH, PMA, or vehicle followed by immunoblotting to look for DAT and phosphorylated DAT proteins. Primary tissue culture experiments could also be done using neurons instead of HEK293 cells to make the assay more physiological. Additional co-localization experiments should also be done. Due to the lack of a binding assay, renewed efforts to find or synthesize a specific antagonist to the TAAR1 receptor and to develop a binding assay would be well worth pursuing.

If TAAR1 is confirmed as a target of amphetamine and methamphetamine *in vivo* and shown to regulate transporter function, then developing novel human TAAR1-selective agonists and antagonists could ultimately lead to successful pharmacotherapies for METH addiction and overdose as well as contribute to a better understanding of the etiology of several mental disorders leading to improved treatments for mood disorders such as depression and bipolar disorder.

Figure 1. Physiological roles of TAAR1 – a new model

Figure 1.

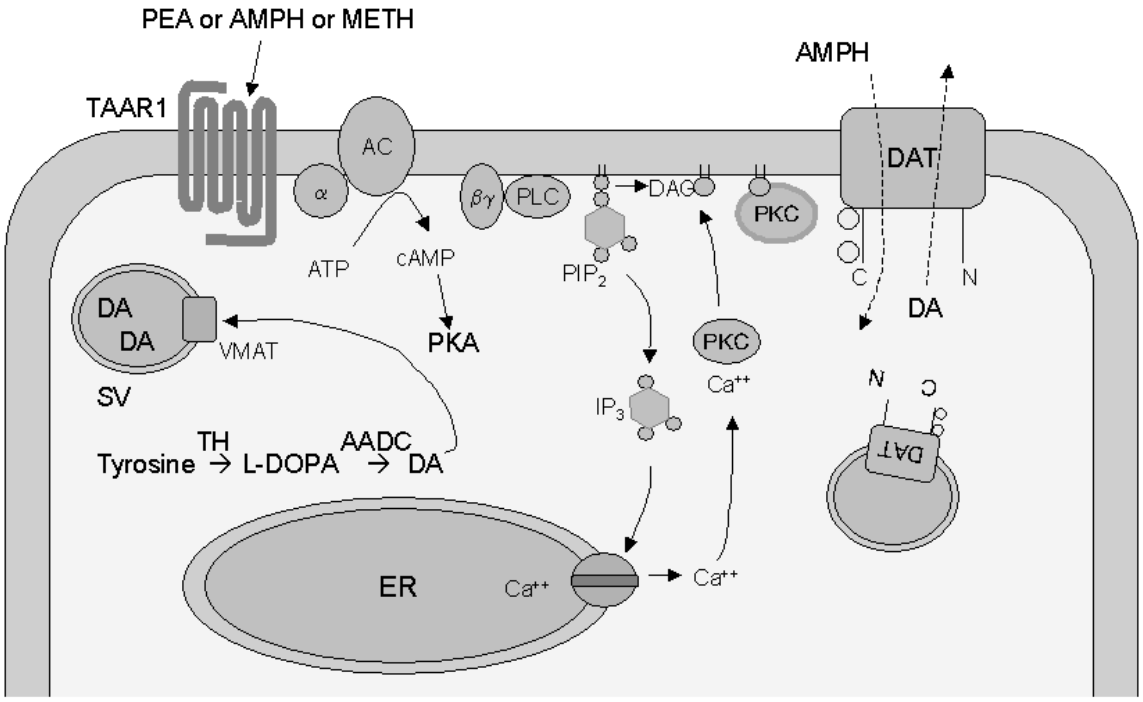
PEA or AMPH or METH
TAAR1
AC
α
βγ
PLC
DAG
PKC
AMPH
DAT
ATP
cAMP
PIP2
C
N
DA
DA
DA
VMAT
SV
PKA
PKC
Ca++
IP3
N
C
DAT
Tyrosine → TH → L-DOPA → AADC → DA
ER
Ca++
Ca++

Bibliography

Abou Jamra R, Sircar I, Becker T, Freudenberg-Hua Y, Ohlraun S, Freudenberg J, Brockschmidt F, Schulze TG, Gross M, Spira F, Deschner M, Schmal C, Maier W, Propping P, Rietschel M, Cichon S, Nothen MM and Schumacher J (2005) A family-based and case-control association study of trace amine receptor genes on chromosome 6q23 in bipolar affective disorder. *Mol Psychiatry* **10**:618-620.

Anand A, Verhoeff P, Seneca N, Zoghbi SS, Seibyl JP, Charney DS and Innis RB (2000) Brain SPECT imaging of amphetamine-induced dopamine release in euthymic bipolar disorder patients. *Am J Psychiatry* **157**:1108-1114.

Anglin MD, Burke C, Perrochet B, Stamper E and Dawud-Noursi S (2000) History of the methamphetamine problem. *J Psychoactive Drugs* **32**:137-141.

Angrist BM, Shopsin B and Gershon S (1971) Comparative psychotomimetic effects of stereoisomers of amphetamine. *Nature* **234**:152-153.

Axelrod J and Saavedra JM (1977) Octopamine. *Nature* **265**:501-504.

Baker GB, Bornstein RA, Rouget AC, Ashton SE, van Muyden JC and Coutts RT (1991) Phenylethylaminergic mechanisms in attention-deficit disorder. *Biol Psychiatry* **29**:15-22.

Ballesteros JA, Shi L and Javitch JA (2001) Structural mimicry in G protein-coupled receptors: implications of the high-resolution structure of rhodopsin for structure-function analysis of rhodopsin-like receptors. *Mol Pharmacol* **60**:1-19.

Ballesteros JAaWH (1995) Integrated methods for the construction of three-dimensional models and computational probing of structure-function relations in G protein-coupled receptors. *Methods Neurosci* **25**:366-428.

Baselt R (2002) *Disposition of Toxic Drugs and Chemicals in Man*. Chemical Toxicology Institute, Foster City, CA, London.

Baucum AJ, 2nd, Rau KS, Riddle EL, Hanson GR and Fleckenstein AE (2004) Methamphetamine increases dopamine transporter higher molecular weight complex formation via a dopamine- and hyperthermia-associated mechanism. *J Neurosci* **24**:3436-3443.

Baud P, Arbilla S, Cantrill RC, Scatton B and Langer SZ (1985) Trace amines inhibit the electrically evoked release of [3H]acetylcholine from slices of rat striatum in the presence of pargyline: similarities between beta-phenylethylamine and amphetamine. *J Pharmacol Exp Ther* **235**:220-229.

Bermak JC, Li M, Bullock C and Zhou QY (2001) Regulation of transport of the dopamine D1 receptor by a new membrane-associated ER protein. *Nat Cell Biol* **3**:492-498.

Berry MD (2004) Mammalian central nervous system trace amines. Pharmacologic amphetamines, physiologic neuromodulators. *J Neurochem* **90**:257-271.

Borowsky B, Adham N, Jones KA, Raddatz R, Artymyshyn R, Ogozalek KL, Durkin MM, Lakhlani PP, Bonini JA, Pathirana S, Boyle N, Pu X, Kouranova E, Lichtblau H, Ochoa FY, Branchek TA and Gerald C (2001) Trace amines: identification of a family of mammalian G protein-coupled receptors. *Proc Natl Acad Sci U S A* **98**:8966-8971.

Boulton AA (1976) Identification, distribution, metabolism, and function of meta and para tyramine, phenylethylamine and tryptamine in brain. *Adv Biochem Psychopharmacol* **15**:57-67.

Bradley C (1937) The behavior of children receiving benzedrine. *American Journal of Psychiatry* **94**:577-585.

Branchek TA and Blackburn TP (2003) Trace amine receptors as targets for novel therapeutics: legend, myth and fact. *Curr Opin Pharmacol* **3**:90-97.

Bronstein I, Edwards B and Voyta JC (1989) 1,2-dioxetanes: novel chemiluminescent enzyme substrates. Applications to immunoassays. *J Biolumin Chemilumin* **4**:99-111.

Bunney BS, Walters JR, Kuhar MJ, Roth RH and Aghajanian GK (1975) D & L amphetamine stereoisomers: comparative potencies in affecting the firing of central dopaminergic and noradrenergic neurons. *Psychopharmacol Commun* **1**:177-190.

Bunzow JR, Sonders MS, Arttamangkul S, Harrison LM, Zhang G, Quigley DI, Darland T, Suchland KL, Pasumamula S, Kennedy JL, Olson SB, Magenis RE, Amara SG and Grandy DK (2001) Amphetamine, 3,4-methylenedioxymethamphetamine, lysergic acid diethylamide, and metabolites of the catecholamine neurotransmitters are agonists of a rat trace amine receptor. *Mol Pharmacol* **60**:1181-1188.

Carlezon WA, Jr., Duman RS and Nestler EJ (2005) The many faces of CREB. *Trends Neurosci* **28**:436-445.

Carter SM, Reveley MA, Sandler M, Dewhurst J, Little BC, Hayworth J and Priest RG (1980) Decreased urinary output of conjugated tyramine is associated with lifetime vulnerability to depressive illness. *Psychiatry Res* **3**:13-21.

Cho AK SD (1994) *Amphetamine and its Analogs*. Academic Press, Inc., San Diego.

Chrivia JC, Kwok RP, Lamb N, Hagiwara M, Montminy MR and Goodman RH (1993) Phosphorylated CREB binds specifically to the nuclear protein CBP. *Nature* **365**:855-859.

Cornea-Hebert V, Watkins KC, Roth BL, Kroeze WK, Gaudreau P, Leclerc N and Descarries L (2002) Similar ultrastructural distribution of the 5-HT(2A) serotonin receptor and microtubule-associated protein MAP1A in cortical dendrites of adult rat. *Neuroscience* **113**:23-35.

Dabrowska J and Brylinski M (2006) Stereoselectivity of 8-OH-DPAT toward the serotonin 5-HT1A receptor: biochemical and molecular modeling study. *Biochem Pharmacol* **72**:498-511.

D'Andrea G GF, Leone M, Perini F, Farruggio A, Bussone G (2006) Abnormal platelet trace amine profiles in migraine with and without aura. *Cephalalgia* **26**:968-972.

D'Andrea G, Terrazzino S, Leon A, Fortin D, Perini F, Granella F and Bussone G (2004) Elevated levels of circulating trace amines in primary headaches. *Neurology* **62**:1701-1705.

Daniels GM and Amara SG (1999) Regulated trafficking of the human dopamine transporter. Clathrin-mediated internalization and lysosomal degradation in response to phorbol esters. *J Biol Chem* **274**:35794-35801.

Davis BA and Boulton AA (1994) The trace amines and their acidic metabolites in depression--an overview. *Prog Neuropsychopharmacol Biol Psychiatry* **18**:17-45.

Derlet RW, Rice P, Horowitz BZ and Lord RV (1989) Amphetamine toxicity: experience with 127 cases. *J Emerg Med* **7**:157-161.

Dixon RA, Sigal IS, Rands E, Register RB, Candelore MR, Blake AD and Strader CD (1987) Ligand binding to the beta-adrenergic receptor involves its rhodopsin-like core. *Nature* **326**:73-77.

Drummer O, Odell, M (2001) *The Forensic Pharmacology of Drugs of Abuse*. Oxford University Press, New York.

Duan J, Martinez M, Sanders AR, Hou C, Saitou N, Kitano T, Mowry BJ, Crowe RR, Silverman JM, Levinson DF and Gejman PV (2004) Polymorphisms in the trace amine receptor 4 (TRAR4) gene on chromosome 6q23.2 are associated with susceptibility to schizophrenia. *Am J Hum Genet* **75**:624-638.

Durden DA and Davis BA (1993) Determination of regional distributions of phenylethylamine and meta- and para-tyramine in rat brain regions and presence in human and dog plasma by an ultra-sensitive negative chemical ion gas chromatography-mass spectrometric (NCI-GC-MS) method. *Neurochem Res* **18**:995-1002.

Durden DA, Philips SR and Boulton AA (1973) Identification and distribution of beta-phenylethylamine in the rat. *Can J Biochem* **51**:995-1002.

Duvernay MT, Zhou F and Wu G (2004) A conserved motif for the transport of G protein-coupled receptors from the endoplasmic reticulum to the cell surface. *J Biol Chem* **279**:30741-30750.

Eshleman AJ, Carmolli M, Cumbay M, Martens CR, Neve KA and Janowsky A (1999) Characteristics of drug interactions with recombinant biogenic amine transporters expressed in the same cell type. *J Pharmacol Exp Ther* **289**:877-885.

Freddolino PL, Kalani MY, Vaidehi N, Floriano WB, Hall SE, Trabanino RJ, Kam VW and Goddard WA, 3rd (2004) Predicted 3D structure for the human beta 2 adrenergic receptor and its binding site for agonists and antagonists. *Proc Natl Acad Sci U S A* **101**:2736-2741.

Geracitano R, Federici M, Bernardi G and Mercuri NB (2006) On the effects of psychostimulants, antidepressants, and the antiparkinsonian drug levodopa on dopamine neurons. *Ann N Y Acad Sci* **1074**:320-329.

Giros B, Jaber M, Jones SR, Wightman RM and Caron MG (1996) Hyperlocomotion and indifference to cocaine and amphetamine in mice lacking the dopamine transporter. *Nature* **379**:606-612.

Giros B, Wang YM, Suter S, McLeskey SB, Pifl C and Caron MG (1994) Delineation of discrete domains for substrate, cocaine, and tricyclic antidepressant interactions using chimeric dopamine-norepinephrine transporters. *J Biol Chem* **269**:15985-15988.

Gonzalez GA and Montminy MR (1989) Cyclic AMP stimulates somatostatin gene transcription by phosphorylation of CREB at serine 133. *Cell* **59**:675-680.

Grandy DK (2007) Trace amine-associated receptor 1-Family archetype or iconoclast? *Pharmacol Ther* **116**:355-390.

Griffith JD, Cavanaugh J, Held J and Oates JA (1972) Dextroamphetamine. Evaluation of psychomimetic properties in man. *Arch Gen Psychiatry* **26**:97-100.

Grohmann L, Blenau W, Erber J, Ebert PR, Strunker T and Baumann A (2003) Molecular and functional characterization of an octopamine receptor from honeybee (Apis mellifera) brain. *J Neurochem* **86**:725-735.

Guan XM, Peroutka SJ and Kobilka BK (1992) Identification of a single amino acid residue responsible for the binding of a class of beta-adrenergic receptor antagonists to 5-hydroxytryptamine1A receptors. *Mol Pharmacol* **41**:695-698.

Hanyaloglu AC and von Zastrow M (2008) Regulation of GPCRs by endocytic membrane trafficking and its potential implications. *Annu Rev Pharmacol Toxicol* **48**:537-568.

Holschneider DP, Chen K, Seif I and Shih JC (2001) Biochemical, behavioral, physiologic, and neurodevelopmental changes in mice deficient in monoamine oxidase A or B. *Brain Res Bull* **56**:453-462.

Hopkins AL and Groom CR (2002) The druggable genome. *Nat Rev Drug Discov* **1**:727-730.

Huang ES (2003) Construction of a sequence motif characteristic of aminergic G protein-coupled receptors. *Protein Sci* **12**:1360-1367.

Hur EM and Kim KT (2002) G protein-coupled receptor signalling and cross-talk: achieving rapidity and specificity. *Cell Signal* **14**:397-405.

Janssen PA, Leysen JE, Megens AA and Awouters FH (1999) Does phenylethylamine act as an endogenous amphetamine in some patients? *Int J Neuropsychopharmacol* **2**:229-240.

Jeng W, Ramkissoon, A, Parman, T, Wells, PC (2006) Prostaglandin H synthase-catalyzed bioactivation of amphetamines to free radical intermediates that cause CNS regional DNA oxidation and nerve terminal degenderation. *Faseb J* **20**:638-650.

Kahlig KM, Javitch JA and Galli A (2004) Amphetamine regulation of dopamine transport. Combined measurements of transporter currents and transporter imaging support the endocytosis of an active carrier. *J Biol Chem* **279**:8966-8975.

Kahlig KM, Lute BJ, Wei Y, Loland CJ, Gether U, Javitch JA and Galli A (2006) Regulation of dopamine transporter trafficking by intracellular amphetamine. *Mol Pharmacol* **70**:542-548.

Kaminskas LM, Irvine RJ, Callaghan PD, White JM and Kirkbride P (2002) The contribution of the metabolite p-hydroxyamphetamine to the central actions of p-methoxyamphetamine. *Psychopharmacology (Berl)* **160**:155-160.

Kanamori T, Tsujikawa K, Ohmae Y, Iwata YT, Inoue H, Kishi T, Nakahama T and Inouye Y (2005) A study of the metabolism of methamphetamine and 4-bromo-2,5-dimethoxyphenethylamine (2C-B) in isolated rat hepatocytes. *Forensic Sci Int* **148**:131-137.

Kenakin TP and Morgan PH (1989) Theoretical effects of single and multiple transducer receptor coupling proteins on estimates of the relative potency of agonists. *Mol Pharmacol* **35**:214-222.

Koob GF and Bloom FE (1988) Cellular and molecular mechanisms of drug dependence. *Science* **242**:715-723.

Kramer JC, Fischman VS and Littlefield DC (1967) Amphetamine abuse. Pattern and effects of high doses taken intravenously. *Jama* **201**:305-309.

Kratochwil NA, Malherbe P, Lindemann L, Ebeling M, Hoener MC, Muhlemann A, Porter RH, Stahl M and Gerber PR (2005) An automated system for the analysis of G protein-coupled receptor transmembrane binding pockets: alignment, receptor-based pharmacophores, and their application. *J Chem Inf Model* **45**:1324-1336.

Kristiansen K (2004) Molecular mechanisms of ligand binding, signaling, and regulation within the superfamily of G-protein-coupled receptors: molecular modeling and mutagenesis approaches to receptor structure and function. *Pharmacol Ther* **103**:21-80.

Kusaga A (2002) [Decreased beta-phenylethylamine in urine of children with attention deficit hyperactivity disorder and autistic disorder]. *No To Hattatsu* **34**:243-248.

Kusaga A, Yamashita Y, Koeda T, Hiratani M, Kaneko M, Yamada S and Matsuishi T (2002) Increased urine phenylethylamine after methylphenidate treatment in children with ADHD. *Ann Neurol* **52**:372-374.

Law MY and Moody DE (2000) Urinary excretion of 4-hydroxyamphetamine and amphetamine in male and female Sprague-Dawley and Dark Agouti rats following multiple doses of amphetamine. *Toxicol Lett* **117**:139-144.

Leitz FH and Stefano FJ (1971) The effect of tyramine, amphetamine and metaraminol on the metabolic disposition of 3 H-norepinephrine released from the adrenergic neuron. *J Pharmacol Exp Ther* **178**:464-473.

Lewin AH (2006) Receptors of mammalian trace amines. *Aaps J* **8**:E138-145.

Liang NY and Rutledge CO (1982) Comparison of the release of [3H]dopamine from isolated corpus striatum by amphetamine, fenfluramine and unlabelled dopamine. *Biochem Pharmacol* **31**:983-992.

Liberles SD and Buck LB (2006) A second class of chemosensory receptors in the olfactory epithelium. *Nature* **442**:645-650.

Lindemann L, Ebeling M, Kratochwil NA, Bunzow JR, Grandy DK and Hoener MC (2005) Trace amine-associated receptors form structurally and functionally distinct subfamilies of novel G protein-coupled receptors. *Genomics* **85**:372-385.

Lindemann L, Meyer CA, Jeanneau K, Bradaia A, Ozmen L, Bluethmann H, Bettler B, Wettstein JG, Borroni E, Moreau JL and Hoener MC (2007) Trace Amine-Associated Receptor 1 (TAAR1) Modulates Dopaminergic Activity. *J Pharmacol Exp Ther*.

Linnoila M, Karoum F, Cutler NR and Potter WZ (1983) Temporal association between depression-dependent dyskinesias and high urinary phenylethylamine output. *Biol Psychiatry* **18**:513-516.

Logan BK, Fligner CL and Haddix T (1998) Cause and manner of death in fatalities involving methamphetamine. *J Forensic Sci* **43**:28-34.

Madras BK, Miller GM and Fischman AJ (2005) The dopamine transporter and attention-deficit/hyperactivity disorder. *Biol Psychiatry* **57**:1397-1409.

Margeta-Mitrovic M, Jan YN and Jan LY (2000) A trafficking checkpoint controls GABA(B) receptor heterodimerization. *Neuron* **27**:97-106.

Marshall FH, Jones KA, Kaupmann K and Bettler B (1999) GABAB receptors - the first 7TM heterodimers. *Trends Pharmacol Sci* **20**:396-399.

Mayr B and Montminy M (2001) Transcriptional regulation by the phosphorylation-dependent factor CREB. *Nat Rev Mol Cell Biol* **2**:599-609.

McClung CA and Nestler EJ (2008) Neuroplasticity mediated by altered gene expression. *Neuropsychopharmacology* **33**:3-17.

Mendelson J, Uemura N, Harris D, Nath RP, Fernandez E, Jacob P, 3rd, Everhart ET and Jones RT (2006) Human pharmacology of the methamphetamine stereoisomers. *Clin Pharmacol Ther* **80**:403-420.

Merikangas KR, Stevens DE, Merikangas JR, Katz CB, Glover V, Cooper T and Sandler M (1995) Tyramine conjugation deficit in migraine, tension-type headache, and depression. *Biol Psychiatry* **38**:730-736.

Metzger RR, Haughey HM, Wilkins DG, Gibb JW, Hanson GR and Fleckenstein AE (2000) Methamphetamine-induced rapid decrease in dopamine transporter function: role of dopamine and hyperthermia. *J Pharmacol Exp Ther* **295**:1077-1085.

Miller GM, Verrico CD, Jassen A, Konar M, Yang H, Panas H, Bahn M, Johnson R and Madras BK (2005) Primate trace amine receptor 1 modulation by the dopamine transporter. *J Pharmacol Exp Ther* **313**:983-994.

Millichap JG and Yee MM (2003) The diet factor in pediatric and adolescent migraine. *Pediatr Neurol* **28**:9-15.

Nair A and Vaidya VA (2006) Cyclic AMP response element binding protein and brain-derived neurotrophic factor: molecules that modulate our mood? *J Biosci* **31**:423-434.

Navarro HA, Gilmour BP and Lewin AH (2006) A rapid functional assay for the human trace amine-associated receptor 1 based on the mobilization of internal calcium. *J Biomol Screen* **11**:688-693.

Nestler EJ and Carlezon WA, Jr. (2006) The mesolimbic dopamine reward circuit in depression. *Biol Psychiatry* **59**:1151-1159.

Olson KR and Eglen RM (2007) Beta galactosidase complementation: a cell-based luminescent assay platform for drug discovery. *Assay Drug Dev Technol* **5**:137-144.

Pae CU, Yu HS, Amann D, Kim JJ, Lee CU, Lee SJ, Jun TY, Lee C, Paik IH, Patkar AA and Lerer B (2008) Association of the trace amine associated receptor 6 (TAAR6) gene with schizophrenia and bipolar disorder in a Korean case control sample. *J Psychiatr Res* **42**:35-40.

Palczewski K, Kumasaka T, Hori T, Behnke CA, Motoshima H, Fox BA, Le Trong I, Teller DC, Okada T, Stenkamp RE, Yamamoto M and Miyano M (2000) Crystal structure of rhodopsin: A G protein-coupled receptor. *Science* **289**:739-745.

Parker EM and Cubeddu LX (1988) Comparative effects of amphetamine, phenylethylamine and related drugs on dopamine efflux, dopamine uptake and mazindol binding. *J Pharmacol Exp Ther* **245**:199-210.

Partilla JS, Dempsey AG, Nagpal AS, Blough BE, Baumann MH and Rothman RB (2006) Interaction of amphetamines and related compounds at the vesicular monoamine transporter. *J Pharmacol Exp Ther* **319**:237-246.

Paulos MA and Tessel RE (1982) Excretion of beta-phenethylamine is elevated in humans after profound stress. *Science* **215**:1127-1129.

Peters FT, Samyn N, Wahl M, Kraemer T, De Boeck G and Maurer HH (2003) Concentrations and ratios of amphetamine, methamphetamine, MDA, MDMA, and MDEA enantiomers determined in plasma samples from clinical toxicology

and driving under the influence of drugs cases by GC-NICI-MS. *J Anal Toxicol* **27**:552-559.
Philips SR, Durden DA and Boulton AA (1974a) Identification and distribution of p-tyramine in the rat. *Can J Biochem* **52**:366-373.
Philips SR, Durden DA and Boulton AA (1974b) Identification and distribution of tryptamine in the rat. *Can J Biochem* **52**:447-451.
Premont RT, Gainetdinov RR and Caron MG (2001) Following the trace of elusive amines. *Proc Natl Acad Sci U S A* **98**:9474-9475.
Prinzmetal M, Bloomberg W (1935) The use of benzedrine for the treatment of narcolepsy. *Journal of the American Medical Association* **105**:2051-2054.
Rasmussen SG, Choi HJ, Rosenbaum DM, Kobilka TS, Thian FS, Edwards PC, Burghammer M, Ratnala VR, Sanishvili R, Fischetti RF, Schertler GF, Weis WI and Kobilka BK (2007) Crystal structure of the human beta2 adrenergic G-protein-coupled receptor. *Nature* **450**:383-387.
Reese EA, Bunzow JR, Arttamangkul S, Sonders MS and Grandy DK (2007) Trace amine-associated receptor 1 displays species-dependent stereoselectivity for isomers of methamphetamine, amphetamine, and para-hydroxyamphetamine. *J Pharmacol Exp Ther* **321**:178-186.
Research IWD (2005) The meth epidemic In America: Two Surveys of US Counties, in pp 1-11.
Riviere GJ, Gentry WB and Owens SM (2000) Disposition of methamphetamine and its metabolite amphetamine in brain and other tissues in rats after intravenous administration. *J Pharmacol Exp Ther* **292**:1042-1047.
Roeder T (1999) Octopamine in invertebrates. *Prog Neurobiol* **59**:533-561.
Roeder T (2005) Tyramine and octopamine: ruling behavior and metabolism. *Annu Rev Entomol* **50**:447-477.
Rosenbaum DM, Cherezov V, Hanson MA, Rasmussen SG, Thian FS, Kobilka TS, Choi HJ, Yao XJ, Weis WI, Stevens RC and Kobilka BK (2007) GPCR engineering yields high-resolution structural insights into beta2-adrenergic receptor function. *Science* **318**:1266-1273.
Rothman RB and Baumann MH (2006) Therapeutic potential of monoamine transporter substrates. *Curr Top Med Chem* **6**:1845-1859.
Rothman RB, Baumann MH, Dersch CM, Romero DV, Rice KC, Carroll FI and Partilla JS (2001) Amphetamine-type central nervous system stimulants release norepinephrine more potently than they release dopamine and serotonin. *Synapse* **39**:32-41.
Rutledge CO (1970) The mechanisms by which amphetamine inhibits oxidative deamination of norepinephrine in brain. *J Pharmacol Exp Ther* **171**:188-195.
Saavedra JM, Brownstein MJ, Carpenter DO and Axelrod J (1974a) Octopamine: presence in single neurons of Aplysia suggests neurotransmitter function. *Science* **185**:364-365.
Saavedra JM, Coyle JT and Axelrod J (1974b) Developmental characteristics of phenylethanolamine and octopamine in the rat brain. *J Neurochem* **23**:511-515.
Sabelli H (2002) Treatment of Mood Disorders: Phenylethylamine Deficit and Replacement in Depressive Illness, in *Natural medications for psychiatric*

disorders; considering the alternatives (Rosenbaum DMaJF ed), Lippincott Williams & Wilkins, Philadelphia.
Sabelli H, Fink P, Fawcett J and Tom C (1996) Sustained antidepressant effect of PEA replacement. *J Neuropsychiatry Clin Neurosci* **8**:168-171.
Sabelli HC and Mosnaim AD (1974) Phenylethylamine hypothesis of affective behavior. *Am J Psychiatry* **131**:695-699.
Sandler M and Reynolds GP (1976) Does phenylethylamine cause schizophrenia? *Lancet* **1**:70-71.
Sandler M, Ruthven CR, Goodwin BL, Reynolds GP, Rao VA and Coppen A (1979) Deficient production of tyramine and octopamine in cases of depression. *Nature* **278**:357-358.
Saunders C, Ferrer JV, Shi L, Chen J, Merrill G, Lamb ME, Leeb-Lundberg LM, Carvelli L, Javitch JA and Galli A (2000) Amphetamine-induced loss of human dopamine transporter activity: an internalization-dependent and cocaine-sensitive mechanism. *Proc Natl Acad Sci U S A* **97**:6850-6855.
Scanlan TS, Suchland KL, Hart ME, Chiellini G, Huang Y, Kruzich PJ, Frascarelli S, Crossley DA, Bunzow JR, Ronca-Testoni S, Lin ET, Hatton D, Zucchi R and Grandy DK (2004) 3-Iodothyronamine is an endogenous and rapid-acting derivative of thyroid hormone. *Nat Med* **10**:638-642.
Schmitz Y, Lee CJ, Schmauss C, Gonon F and Sulzer D (2001) Amphetamine distorts stimulation-dependent dopamine overflow: effects on D2 autoreceptors, transporters, and synaptic vesicle stores. *J Neurosci* **21**:5916-5924.
Seeman P and Madras BK (1998) Anti-hyperactivity medication: methylphenidate and amphetamine. *Mol Psychiatry* **3**:386-396.
Segal DS (1975) Behavioral characterization of d- and l-amphetamine: neurochemical implications. *Science* **190**:475-477.
Shaw-Lutchman TZ, Impey S, Storm D and Nestler EJ (2003) Regulation of CRE-mediated transcription in mouse brain by amphetamine. *Synapse* **48**:10-17.
Shirkande S, O'Reilly R, Davis B, Durden D and Malcom D (1995) Plasma phenylethylamine levels of schizophrenic patients. *Can J Psychiatry* **40**:221.
Smith RC and Davis JM (1977) Comparative effects of d-amphetamine, l-amphetamine, and methylphenidate on mood in man. *Psychopharmacology (Berl)* **53**:1-12.
Strader CD, Sigal IS, Candelore MR, Rands E, Hill WS and Dixon RA (1988) Conserved aspartic acid residues 79 and 113 of the beta-adrenergic receptor have different roles in receptor function. *J Biol Chem* **263**:10267-10271.
Strader CD, Sigal IS and Dixon RA (1989) Structural basis of beta-adrenergic receptor function. *Faseb J* **3**:1825-1832.
Strader CD, Sigal IS, Register RB, Candelore MR, Rands E and Dixon RA (1987) Identification of residues required for ligand binding to the beta-adrenergic receptor. *Proc Natl Acad Sci U S A* **84**:4384-4388.
Sulzer D, Chen TK, Lau YY, Kristensen H, Rayport S and Ewing A (1995) Amphetamine redistributes dopamine from synaptic vesicles to the cytosol and promotes reverse transport. *J Neurosci* **15**:4102-4108.
Sulzer D, Sonders MS, Poulsen NW and Galli A (2005) Mechanisms of neurotransmitter release by amphetamines: A review. *Prog Neurobiol* **75**:406-433.

Sunahara RK, Dessauer CW and Gilman AG (1996) Complexity and diversity of mammalian adenylyl cyclases. *Annu Rev Pharmacol Toxicol* **36**:461-480.

Suryanarayana S and Kobilka BK (1993) Amino acid substitutions at position 312 in the seventh hydrophobic segment of the beta 2-adrenergic receptor modify ligand-binding specificity. *Mol Pharmacol* **44**:111-114.

Swaminath G, Deupi X, Lee TW, Zhu W, Thian FS, Kobilka TS and Kobilka B (2005) Probing the beta2 adrenoceptor binding site with catechol reveals differences in binding and activation by agonists and partial agonists. *J Biol Chem* **280**:22165-22171.

Swaminath G, Xiang Y, Lee TW, Steenhuis J, Parnot C and Kobilka BK (2004) Sequential binding of agonists to the beta2 adrenoceptor. Kinetic evidence for intermediate conformational states. *J Biol Chem* **279**:686-691.

Tan ES, Groban ES, Jacobson MP and Scanlan TS (2008) Toward deciphering the code to aminergic g protein-coupled receptor drug design. *Chem Biol* **15**:343-353.

Torres GE, Yao WD, Mohn AR, Quan H, Kim KM, Levey AI, Staudinger J and Caron MG (2001) Functional interaction between monoamine plasma membrane transporters and the synaptic PDZ domain-containing protein PICK1. *Neuron* **30**:121-134.

Uberti MA, Hall RA and Minneman KP (2003) Subtype-specific dimerization of alpha 1-adrenoceptors: effects on receptor expression and pharmacological properties. *Mol Pharmacol* **64**:1379-1390.

Van Kammen DP and Murphy DL (1975) Attenuation of the euphoriant and activating effects of d- and l-amphetamine by lithium carbonate treatment. *Psychopharmacologia* **44**:215-224.

Vaughan RA, Huff RA, Uhl GR and Kuhar MJ (1997) Protein kinase C-mediated phosphorylation and functional regulation of dopamine transporters in striatal synaptosomes. *J Biol Chem* **272**:15541-15546.

Venken T, Claes S, Sluijs S, Paterson AD, van Duijn C, Adolfsson R, Del-Favero J and Van Broeckhoven C (2005) Genomewide scan for affective disorder susceptibility Loci in families of a northern Swedish isolated population. *Am J Hum Genet* **76**:237-248.

Vladimirov V, Thiselton DL, Kuo PH, McClay J, Fanous A, Wormley B, Vittum J, Ribble R, Moher B, van den Oord E, O'Neill FA, Walsh D, Kendler KS and Riley BP (2007) A region of 35 kb containing the trace amine associate receptor 6 (TAAR6) gene is associated with schizophrenia in the Irish study of high-density schizophrenia families. *Mol Psychiatry* **12**:842-853.

Wainscott DB, Little SP, Yin T, Tu Y, Rocco VP, He JX and Nelson DL (2006) Pharmacologic Characterization of the Cloned Human Trace Amine-Associated Receptor1 (TAAR1) and Evidence for Species Differences with the Rat TAAR1. *J Pharmacol Exp Ther*.

Wieland K, Zuurmond HM, Krasel C, Ijzerman AP and Lohse MJ (1996) Involvement of Asn-293 in stereospecific agonist recognition and in activation of the beta 2-adrenergic receptor. *Proc Natl Acad Sci U S A* **93**:9276-9281.

Wolinsky TD, Swanson CJ, Smith KE, Zhong H, Borowsky B, Seeman P, Branchek T and Gerald CP (2007) The Trace Amine 1 receptor knockout mouse: an animal model with relevance to schizophrenia. *Genes Brain Behav* **6**:628-639.

Wong SK (2003) G protein selectivity is regulated by multiple intracellular regions of GPCRs. *Neurosignals* **12**:1-12.

Xie Z and Miller G (2008) {beta}-Phenylethylamine Alters Monoamine Transporter Function via Trace Amine-Associated Receptor 1: Implication for Modulatory Roles of Trace Amines in Brain. *J Pharmacol Exp Ther*.

Xie Z and Miller GM (2007) Trace amine-associated receptor 1 is a modulator of the dopamine transporter. *J Pharmacol Exp Ther* **321**:128-136.

Xie Z, Westmoreland SV, Bahn ME, Chen GL, Yang H, Vallender EJ, Yao WD, Madras BK and Miller GM (2007) Rhesus monkey trace amine-associated receptor 1 signaling: enhancement by monoamine transporters and attenuation by the D2 autoreceptor in vitro. *J Pharmacol Exp Ther* **321**:116-127.

Yang HY and Neff NH (1974) The monoamine oxidases of brain: selective inhibition with drugs and the consequences for the metabolism of the biogenic amines. *J Pharmacol Exp Ther* **189**:733-740.

Yoshimoto S, Kaku H, Shimogawa S, Watanabe A, Nakagawara M and Takahashi R (1987) Urinary trace amine excretion and platelet monoamine oxidase activity in schizophrenia. *Psychiatry Res* **21**:229-236.

Young SN, Davis BA and Gauthier S (1982) Precursors and metabolites of phenylethylamine, m and p-tyramine and tryptamine in human lumbar and cisternal cerebrospinal fluid. *J Neurol Neurosurg Psychiatry* **45**:633-639.

Zarate CA, Jr., Singh J and Manji HK (2006) Cellular plasticity cascades: targets for the development of novel therapeutics for bipolar disorder. *Biol Psychiatry* **59**:1006-1020.

Zhou G, Miura Y, Shoji H, Yamada S and Matsuishi T (2001) Platelet monoamine oxidase B and plasma beta-phenylethylamine in Parkinson's disease. *J Neurol Neurosurg Psychiatry* **70**:229-231.

Zhou G, Shoji H, Yamada S and Matsuishi T (1997) Decreased beta-phenylethylamine in CSF in Parkinson's disease. *J Neurol Neurosurg Psychiatry* **63**:754-758.